# Characterization of the MYST histone acetyltransferase MYS-2 in *Caenorhabditis elegans*

Inaugural-Dissertation

zur

Erlangung des Doktorgrades

Dr. rer. nat.

der Fakultät für

Biologie

an der

Universität Duisburg-Essen

vorgelegt von

**Martin Müller**

aus Berlin

Essen, Februar 2013

Die der vorliegenden Arbeit zugrunde liegenden Experimente wurden in der Abteilung für Genetik der Universität Duisburg- Essen durchgeführt.

1. Gutachter: Prof'in Dr. A. Ehrenhofer-Murray
2. Gutachter: Prof. Dr. H. Meyer
3. Gutachter:

Vorsitzender des Prüfungsausschusses: Prof'in Dr. A. Vortkamp

Tag der mündlichen Prüfung: 05. Juni 2013

## Abstract

Members of the MYST family of histone acetyltransferases (HATs) are found in eukaryotes from yeast to human. They covalently attach acetyl groups to lysine residues of the core histones as well as of other proteins. With this function, they affect the structure of chromatin and influence elementary cellular processes like transcription, DNA replication and DNA repair. Global acetylation of lysine 16 on histone H4 (H4K16Ac) has been found to be dependent on the conserved homologues Sas2 (*Saccharomyces cerevisiae*), dMOF (*Drosophila melanogaster*) and hMOF (*Homo sapiens*) in their respective species, and they are components of multi-protein complexes. Their acetylation activity is regulated by additional complex subunits. Dosage compensation in flies is mediated by dMOF, and as part of the MSL complex, it acetylates H4K16 on male X chromosomes, leading to increased X-linked transcription.

MYS-2 is a histone acetyltransferase of the MYST family from the model organism *Caenorhabditis elegans*. Little is known about MYS-2 function, though it has been reported to influence cell identity and to mediate inheritance of RNA interference. Here, we report that MYS-2 is ubiquitously expressed in worms, and that it has an essential function in the worm and influences early embryogenesis. MYS-2 was found to be expressed throughout development in germ cells and somatic tissues, including the first stages of embryogenesis. The main portion of MYS-2 was found in nuclei, where it colocalized with DNA. Furthermore, the absence of MYS-2 was lethal. MYS-2-depleted animals were rescued to wild-type phenotype by a maternal contribution of *mys-2* gene products, and incomplete rescue with residual levels of *mys-2* gene products caused severe developmental defects. Growth rate, general morphology and particularly the vulva, the somatic gonad and germ cell nuclei were affected. These findings are consistent with reported effects of other chromatin modifiers in *C. elegans*, for instances the HAT CBP-1 or the histone deacetylases HDA-1. In contrast to reports on the close homologues Sas2, dMOF and hMOF, a significant impact on global levels of H4K16Ac was not observed. In an interactor screen, a number of candidates were found that include a potential subunit of a MYS-2 containing HAT complex and histone H3 as a potential acetylation substrate. In summary, our data suggest a function for MYS-2 in early embryogenesis, presumably in the regulation of global transcription in a chromatin-dependent manner.

## Zusammenfassung

Mitglieder aus der MYST Familie der Histonacetyltransferasen (HATs) finden sich in Eukaryoten von der Bäckerhefe bis zum Menschen. Sie binden Acetylgruppen kovalent an Lysine von Histonen sowie anderen Proteinen. Mit dieser Funktion verändern sie die Struktur von Chromatin und beeinflussen so elementare zelluläre Prozesse wie Transkription, DNA-Replikation und DNA-Reparatur. Genomweite Acetylierung des Lysin 16 von Histon H4 (H4K16Ac) wird von den konservierten Homologen Sas2 (*Saccharomyces cerevisiae*), dMOF (*Drosophila melanogaster*) und hMOF (*Homo sapiens*) in ihren jeweiligen Spezies durchgeführt, und diese Homologen sind Untereinheiten von Multiproteinkomplexen. Ihre Acetylierungsaktivität ist durch zusätzliche Untereinheiten der Komplexe reguliert. Dosiskompensation in Fliegen wird von dMOF vermittelt, das als Untereinheit des MSL Komplexes H4K16 an männlichen Chromosomen acetyliert, was zu erhöhter Transkription am X-Chromosom führt.

MYS-2 ist eine Histonacetyltransferase der MYST Familie aus dem Modellorganismus *Caenorhabditis elegans*. Nur wenig ist bisher über die Funktion von MYS-2 bekannt. Es wurde jedoch berichtet, dass MYS-2 die Zellidentität beeinflusst und die Vererbung von RNA-Interferenz vermittelt. In dieser Arbeit wurde gezeigt, dass MYS-2 ubiquitär exprimiert ist, dass es eine essentielle Funktion hat, und dass es die und frühe Embryogenese beeinflusst. MYS-2 war während der kompletten Entwicklung in Keimbahnzellen und somatischem Gewebe exprimiert einschließlich der ersten Stadien der Embryogenese. Der Großteil von MYS-2 wurde in Zellkernen gefunden, wo es mit der DNA kolokalisierte. Darüber hinaus war das Fehlen von MYS-2 letal. Tiere, in denen MYS-2 depletiert war, wurden durch maternale Versorgung mit *mys-2* Genprodukten vollständig vor der Letalität gerettet, wohingegen unvollständige Versorgung mit geringen Mengen von *mys-2* Genprodukten schwere Entwicklungsschäden verursachte. Die Wachstumsrate, allgemeine Morphologie und im speziellen die Vulva, die somatische Gonade und Keimbahnzellkerne waren betroffen. Diese Ergebnisse sind konsistent mit berichteten Effekten anderer Chromatinmodifikatoren in *C. elegans*, wie zum Beispiel der HAT CBP-1 oder der Histondeacetylase HDA-1. Im Gegensatz zu Berichten über die nahen Homologen Sas2, dMOF und hMOF, wurde kein signifikanter Effekt auf die globale Menge an H4K16Ac beobachtet. In einem Screen nach Interaktoren wurde eine Reihe von Kandidaten gefunden, unter denen sich eine mögliche Untereinheit eines potentiellen MYS-2 enthaltenden Komplexes, sowie Histon H3 als potentielles Acetylierungssubstrat befinden. Zusammengefasst lassen unsere Daten vermuten, dass MYS-

2 eine Funktion in der frühen Embryogenese hat, wahrscheinlich durch die chromatinbasierte Regulation globaler Transkription.

# Table of contents

# List of Tables



# List of Figures

# Abbreviations

| | |
|---|---|
| 5-FOA | 5-Fluoroorotic Acid |
| Ac | Acetylation |
| bp | base pair(s) |
| Clr | clear phenotype |
| DAPI | 4',6-diamidino-2-phenylindole |
| DCC | dosage compensation complex |
| DIC | differential interference contrast microscopy |
| Dpy | dumpy phenotype |
| dsRNA | double-stranded ribonucleic acid |
| *g* | gravitational acceleration |
| Gb | giga base pairs |
| GFP | green fluorescence protein |
| HAT | histone acetyltransferase |
| HDAC | histone deacetylase |
| *HML* | homothallic mating left |
| *HMR* | homothallic mating right |
| HMT | histone methyltransferases |
| HOX | homeobox |
| IP | immunoprecipitation |
| IPTG | isopropyl β-D-1-thiogalactopyranoside |
| kb | kilo base pairs |
| kDa | kilo Dalton |
| LB | Luria-Bertani |
| Lva | larval arrest |
| *MAT* | mating type locus |
| Mb | mega base pairs |
| MCS | multiple cloning site |
| MES | maternal effect sterile |
| MLE | male less |
| MOF | males-absent on the first |
| MRE | MSL recognition elements |
| MSL | male-specific lethal |

| | |
|---|---|
| Mut | mutant phenotype |
| MYST | family of histone acetyltransferases (MOZ, Ybf2/Sas3, Sas2 and Tip60) |
| NGM | Nematode Growth Medium |
| NSL | non-specific lethal |
| NTD | N-terminal domain |
| OD | optical density |
| ORF | open reading frame |
| PFGE | pulsed field gel electrophoresis |
| Pvl | protruding vulva phenotype |
| RNAi | RNA interference |
| rpm | rounds per minute |
| Rup | ruptured phenotype |
| SAS-I | HAT complex (Sas2, Sas4, Sas5) |
| Sas2 | something about silencing |
| SDS | sodium dodecyl sulfate |
| SDS-PAGE | sodium dodecyl sulfate polyacrylamide gel electrophoresis |
| Sir | silent information regulator |
| siRNA | small inferring ribonucleic acid |
| Slg | slow growing phenotype |
| Sma | small phenotype |
| synMuv | synthetic Multivulvae |
| Unc | uncoordinated phenotype |
| wt | wild-type |
| Xist | X-inactive specific transcript |
| YAC | yeast artificial chromosome |
| YM | yeast minimal medium |
| YPD | yeast peptone dextrose medium |

Worm genes were named according to nomenclature of *Caenorhabditis elegans* genome database (Wormbase), e.g. *mys-2* – gene, MYS-2 – Protein, *mys-2*(ok2429) – mutant allele.

All of the bases and amino acids refer to the predicted gene- or protein models as proposed by Wormbase, release WS234, 02.12.2012.

Yeast genes were named according to nomenclature conventions of *Saccharomyces cereviseae* genome database (SGD). Amino acids were given in the single-letter code, for instance K – lysine.

# 1. Introduction

## 1.1. Epigenetics - from DNA to chromatin

All living species and some viruses encode the blueprint of their structure in a large, polymeric molecule, the deoxyribonucleic acid (DNA). The genetic information is distributed along the DNA molecule in discrete regions, the genes. While it is still hard to define the word "gene", it is common sense that genes are transcribed to give rise to the ultimate products in form of proteins or non-coding RNAs (Pesole 2008). The sum of an organism's genetic information is the genome. *Caenorhabditis elegans* was the first multicellular organism whose genome was completely sequenced (Consortium 1998). Its genome is comparatively compact, about 25 % are coding exons, in contrast to only 1.5 % estimated for the human genome (Lander et al. 2001). 26041 coding sequences (20537 of them are protein-coding genes) are distributed over approximately 100 Mb (Wormbase, WS234 release). Surprisingly, the number of genes predicted for the human genome is similar, but they are distributed over more than 3 Gb (Naidoo et al. 2011). Another striking difference between the worm's genome and the genome of most other eukaryotes is the fact that a significant number (3632) of genes are organized in operons, a feature that is very common in bacteria, but not in other eukaryotes.

One of the main differences between pro- and eukaryotes is the way in which they organize their genome. While prokaryotes mostly have one circular chromosome embedded in the cytoplasm, eukaryotes organize their genome in the nucleus, separated into several linear chromosomes. The eukaryote's DNA is associated to a variety of proteins, mostly histones, and together they build a highly dynamic nucleoprotein complex, the chromatin. Not only does chromatin help in organizing the chromosomes during cell division, but it also permits a far more complex network of genetic regulation, arguably one of the key features enabling development of multicellular organisms.

The term epigenetics was initially used for the study of heritable changes of gene expression or phenotypes that are not based on changes in DNA sequence. The research results of the last decades revealed that especially changes in chromatin structure are responsible for epigenetic effects. Furthermore, genetic investigations cannot be undertaken without consideration of chromatin biology, because DNA and associated protein form a functional entity, the chromatin. Although chromatin biology not only studies epigenetic effects, both terms are used as synonyms nowadays.

## 1.2. Chromatin structure

The basic repeating unit of chromatin is the nucleosome. 147 bp of DNA are wrapped around the core particle consisting of a tetramer with two copies each of histones H3 and H4, and two heterodimers of histones H2A and H2B. The linker histone H1 associates with nucleosomes at the entry and exit site of the DNA, stabilizing the nucleosome and higher-order chromatin structure. The core histone-free linker DNA connects the nucleosomes, and its length varies among species and tissues. Repeats of nucleosomes and linker DNA form the 10 nm fibre, also referred to as 'beads on a string' (Figure 1e). The next organizational level is a helical 30 nm fibre (Figure 1d), where each turn consists of 6-11 nucleosomes. The structure of this fibre is still under debate. The solenoid model describes a well-ordered, one-start helical structure, where each nucleosome interacts with its sixth neighbour (Finch and Klug 1976). In contrast, a second model proposes a two-start fibre, where the DNA zigzags back and forth between two stacks of nucleosome cores (Schalch et al. 2005). However, evidence for both models mainly derives from *in vitro* data. The transition from the open and accessible 10 nm fibre to the more compact 30 nm fibre was widely assumed to correspond to active and repressive chromatin states, but recent data suggests that this does not reflect the *in vivo* situation in interphase nuclei (Fussner et al. 2012).

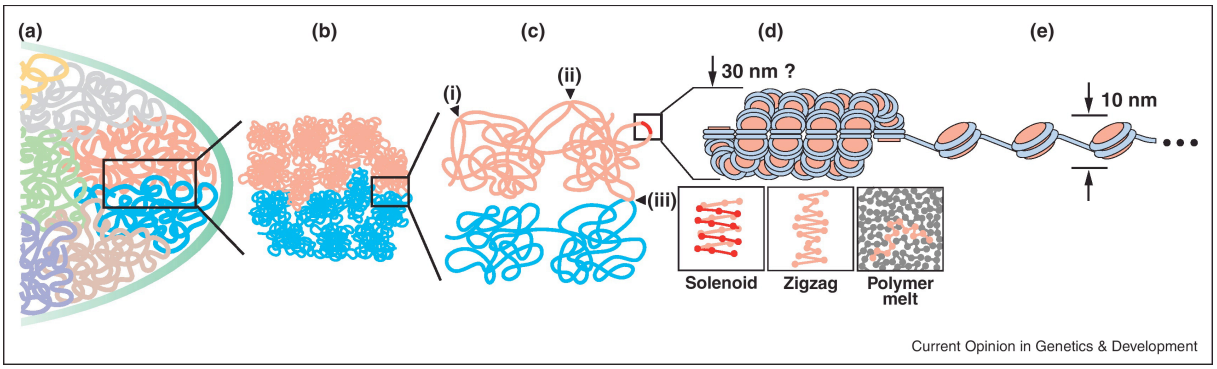


**Figure 1: Chromatin structure in the mammalian nucleus** **(a)** Chromosomes are organized in chromosome territories. **(b)** Chromosome territories are comprised of fractal globules, and fractal globules from adjacent chromosome territories can interdigitate. **(c)** Chromatin fibres interact **(i)** within a fractal globule (frequent), **(ii)** between fractal globules of the same chromosome territory (rare), or **(iii)** between adjacent chromosome territories (very rare). **(d)** Chromatin may form a 30 nm fibre with a solenoid zigzag, or polymer melt organization (see text). **(e)** Chromatin is resolved as a 10 nm 'beads on a string' fibre consisting of nucleosomes (Figure and legend taken from Hubner et al. 2012).

Approaches using different microscopy techniques revealed the presence of the 10 nm structure for both active and inactive chromatin. Instead of the 30 nm structure, those *in vivo* studies rather propose a highly disordered, interdigitated state like a "polymer-melt" (Maeshima et al. 2010). In this "polymer-melt", nucleosomes not neighbouring each other on

the DNA strand interact with each other, building chromatin regions that may share the same transcriptional state. Furthermore, a fractal globule model is proposed, where chromatin organizes into distinct domains, that are more or less compacted depending on their transcriptional state (Dekker 2008)(Figure 1b/c). These fractal globules ultimately associate on the chromosome level to form chromosome territories (Lieberman-Aiden et al. 2009) (Figure 1a).

In general, two different states of chromatin are distinguished, the open and transcriptionally active euchromatin and the closed and transcriptionally inactive heterochromatin. The terms were introduced in 1928 by the botanist Emil Heitz. He defined heterochromatin as staining intensively and remaining compacted during the cell cycle, while euchromatin stains lightly and disappears during telophase. The perhaps most prominent example for heterochromatin was already observed more than hundred years ago. In 1908, Pasquale Baccarini reported dark stained bodies in interphase nuclei of plants, which he named chromocenters. Chromocenters are territories in the nucleus where centromeric regions of the chromosomes accumulate and remain transcriptionally silent throughout the cell cycle. Actively transcribed genes are reversibly silenced when moved to telomeric regions, a phenomenon also referred to as telomere position effect (TPE) (Aparicio et al. 1991). Even whole chromosomes can be silenced by heterochromatinization. For example, on one of the female X chromosomes in mammals, a large non-coding RNA (X-inactive specific transcript, Xist) associates with the X chromosome from which it is expressed, inducing a series of subsequent chromatin modifications that finally lead to a complete silencing of nearly all of the genes on that chromosome (Kohlmaier et al. 2004).

While these examples seem to be features of chromosomal regions, the formation of heterochromatin can also be directed by sequence elements, as it is the case at centromeres with numerous repetitive sequence elements. Another example for silencing of repetitive elements is transgenes that are introduced into *C. elegans*. They generally form large, repetitive, extrachromosomal arrays that are specifically silenced in the germline of worms (Kelly et al. 1997; Kelly and Fire 1998).

While telomeres and centromeres are the most prominent examples for constitutive chromatin, heterochromatin can also convert to euchromatin and *vice versa*, also referred to as facultative heterochromatin. In the case of the X inactivation in female mammals or germline silencing, the formation of heterochromatin depends on the sex or the tissue, respectively. Other factors influencing the formation of heterochromatin can be the developmental stage or a distinct point in the cell cycle. For instance, the HOX genes in *Drosophila melanogaster*

control development and are regulated by proteins of the Polycomb and the Trithorax group via changes in chromatin structure (Schuettengruber et al. 2007), and the cyclin E gene is silenced in G1 phase in every round of the cell cycle by HP1 (Nielsen et al. 2001). The distinction between eu- and heterochromatin, as well as the terms themselves, have grown historically and might implicate very static conditions. However, especially the latter examples show that these are in most cases no static conditions, but instead, transitions are fluent, occur frequently and can be transient.

The two different chromatin states are mainly defined by the composition of chromatin. The incorporation of histone variants, non-coding RNAs and post-translational modifications on histones play a key role in defining chromatin states.

## 1.3. Chromatin modifications

Histones are highly conserved in structure among eukaryotic species. The core histones of the worm share at least 80 % amino acid sequence identity with the human histones. The amino acid sequences of *C. elegans* H3 (CeHIS3) and H4 (CeHIS4) are even 97 % and 98 % identical to the human histones H3 and H4, respectively (Vanfleteren et al. 1986; Vanfleteren et al. 1987a; Vanfleteren et al. 1987b; Vanfleteren et al. 1987c; Vanfleteren et al. 1989)(Figure 2).

Amino acid residues can be reversibly modified post-translationally, including acetylation and methylation of lysines (K), acetylation of arginines (R), phosphorylation of serines (S) and threonines (T), ubiquitylation and sumoylation of lysines, as well as ribosylation and others. Similar to other eukaryotes, heterochromatin in *C. elegans* is usually enriched for repressive histone marks like the trimethylation of lysine 27 on histone H3 (H3K27Me3) or di- and trimethylation of lysine 9 on histone H3 (H3K9Me2/3), whereas euchromatin is usually enriched for active histone marks like acetylation marks on H3 and H4, as well as H3K4Me2/3 and H3K36Me3 (Gerstein et al. 2010; Liu et al. 2011).

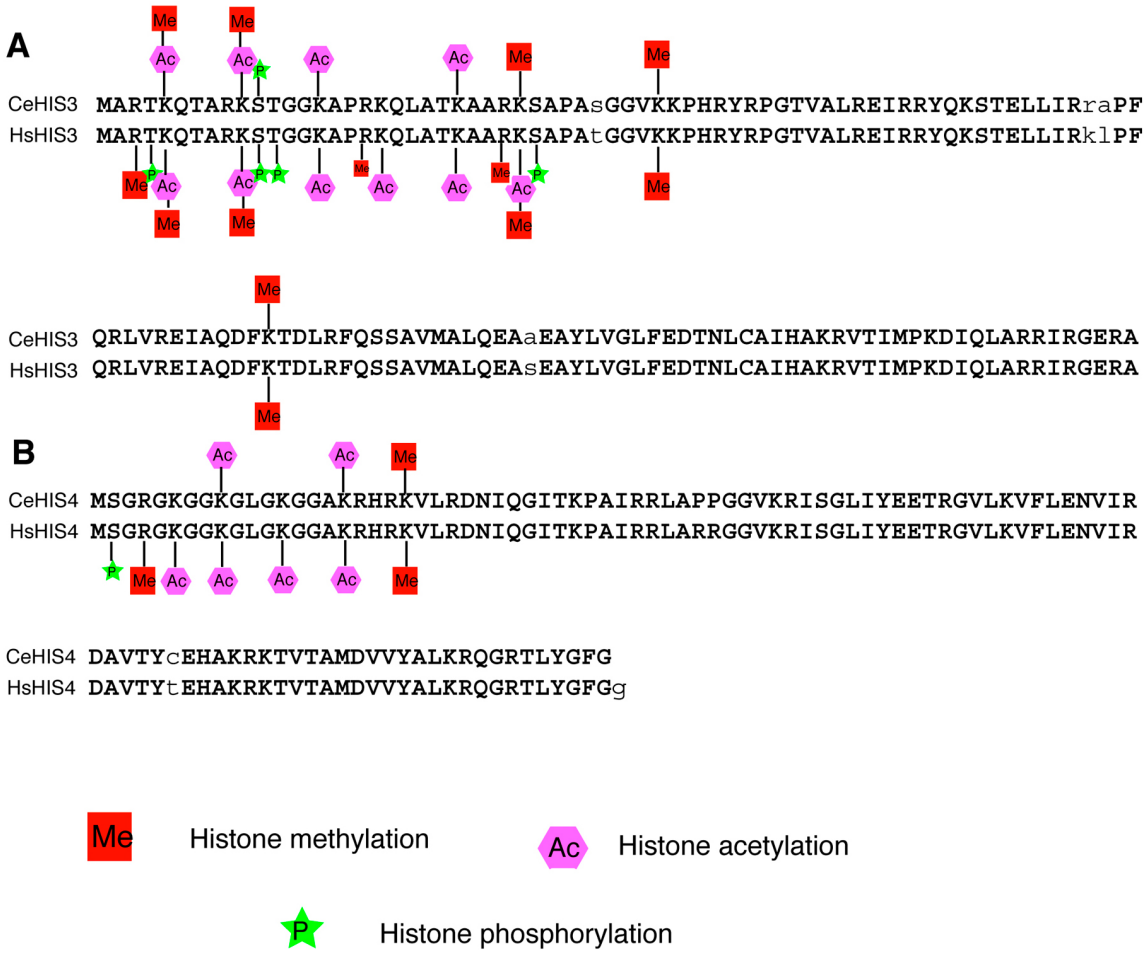


**Figure 2: Histone alignment and histone modifications** **(A)** Alignment of *C. elegans* histone H3 (CeHIS3) and *Homo sapiens* histone H3 (HsHIS3) with the characterized histone modifications marked **(B)** Alignment of *C. elegans* histone H4 (CeHIS4) and *Homo sapiens* histone H4 (HsHIS4) with the characterized histone modifications marked (Figure and legend taken from Cui and Han)

However, these are by far not the only differences between eu- and heterochromatin. The incorporation of histone variants like H2A.Z and H3.3 (both at active chromatin) or CENP-A (at heterochromatic centromeres), the association of additional factors like heterochromatin protein HP1 and non-coding dsRNAs (both at repressive heterochromatin) or transcription factors and remodelling complexes (both at active chromatin) (Wenzel et al. 2011), widens the list of regulating factors, suggesting a highly complex network that coordinates elementary processes like transcription, replication and recombination in eukaryotic genomes.

## 1.4. Histone acetylation

Acetylation of histones is one of the most abundant post-translational modifications and occurs on lysine residues. An acetyl group is enzymatically transferred from acetyl-coenzyme

A (acetyl-CoA) to the ε-amino group of the lysine, thereby neutralizing the basic character of the positively charged lysine residue. The positions of histone modifications are almost as strongly conserved among species as the histone sequences themselves (Figure 2), indicating their relevance in elementary processes. Acetylated residues mainly occur in the N-terminal domain (NTD) of histones, which protrudes from the globular core of nucleosomes (Luger et al. 1997). However, there is also evidence for acetylated lysines within the globular domain, for instance H3K56Ac (Xu et al. 2005) or H3K79Ac (Bheda et al. 2012), both characterized in *S. cerevisiae*. Examples of histone acetylation in the NTD are numerous. Histone H4 alone can be acetylated on four residues of its NTD, K5, K8, K12 and K16.

The biochemical or biophysical effects caused by the acetylation of lysine residues are not yet understood in detail. While it is likely that the removal of one or more positive charges at the exposed NTD influences the interaction between the nucleosome and DNA or between two nucleosomes, leading to changes in chromatin architecture, experimental evidence for such a mechanism so far has only been obtained for H4K16Ac (Shogren-Knaak et al. 2006). Additionally, histone modifications are reported to establish a platform for the binding of additional factors, as for instance bromodomains are known to bind specifically to acetylated residues (Filippakopoulos and Knapp 2012).

The biological consequences of histone acetylation are much better investigated. Acetylation is generally associated with open and active chromatin (Marushige 1976), but also plays a role in DNA metabolism and DNA repair (Celic et al. 2006).

## 1.5. Histone acetyltransferases

Acetylation at lysine residues is catalyzed by histone acetyltransferases (HATs), while deacetylation is carried out by histone deacetylases (HDACs). HATs can be grouped into at least five different families, based on their homology, particularly in the catalytic domain. The HAT1 family is named after its founding member Histone Acetyltransferase 1. Gcn5/PCAF is named after its founding member Gcn5 in yeast and its human ortholog PCAF. The MYST family is named after its founding members MOZ (human), Ybf2/Sas3 (yeast), Sas2 (yeast) and Tip60 (human). p300/CBP is named for the two human paralogs p300 and CBP. Rtt109 is named for its initial identification as a yeast regulator of Ty1 transposition gene product 109 (Yuan and Marmorstein 2013). The Rtt109 family is fungal-specific, and p300/CBP is metazoan-specific. Gcn5/PCAF, MYST and HAT1 have homologs from yeast to humans.

While all HATs catalyze the same reaction, as described in 1.4, the way they transfer the acetyl group to the lysine residue differs. How the HATs bind their substrate at the molecular

level is largely unknown. However, *in vitro* studies have revealed structures of the binding of the human HAT1 HAT domain to acetyl-CoA and to a histone H4 peptide centred around K12 (Wu et al. 2012a). Furthermore, the structures of the binding of *Tetrahymena* Gcn5 HAT domain to CoA and several cognate substrate peptides including histone H3 (centred around K14), histone H4 (centred around K8) and p53 (centred around K320) were reported (Rojas et al. 1999; Clements and Marmorstein 2003; Poux and Marmorstein 2003). While lysine acetylation was first discovered on histones (Allfrey et al. 1964), there are numerous non-histone proteins being acetylated by HATs. For this reason a change in nomenclature from HATs to KATs (lysine (K) acetyltransferases) has been initiated (Allis et al. 2007). One of the most prominent acetylated non-histone proteins acetylated by HATs is the tumour suppressor protein p53. The human MOF, a member of the MYST family of HATs, specifically acetylates p53 within its DNA-binding domain at K120, thereby regulating apoptosis (Sykes et al. 2006). Furthermore, at least some HATs are able to autoacetylate, as was recently reported for the human MOF at its K274 residue, which decreases its ability to bind to nucleosomes (Lu et al. 2011).

HATs are often found to be part of a multisubunit complex *in vivo*, and some HATs are members of several complexes. For instance, yeast Gcn5 is reported to be part of the SAGA and the Ada complex (Grant et al. 1997). The only essential Hat in yeast Esa1 was identified as the catalytic subunit of NuA4, and it was also found to be part of a sub-complex, Piccolo NuA4 that can act independently (Allard et al. 1999; Boudreault et al. 2003). Moreover, those complexes are often well conserved among species. For instance, NuA4 contains the Esa1 homologue Tip60 in flies and humans (Squatrito et al. 2006). The complexes regulate substrate specificity by recruiting the HATs to their target sites.

## 1.6. The MYST family of histone acetyltransferases

The members of the MYST family of HATs are characterized by the presence of the conserved catalytic MYST domain. The MYST domain contains a $C_2HC$ zinc finger (only missing in Esa1) and an acetyl-CoA binding site that is homologous to the canonical acetyl-CoA binding site of the Gcn5/PCAF family. Additional domains, such as chromodomains, PHD and zinc fingers, vary among the family members (Yang 2004; Sapountzi and Cote 2011). These additional domains mediate the binding properties; Chromodomains and PHD domains can bind to methylated histones, while zinc fingers are a DNA binding motif (Musselman and Kutateladze 2009; Eissenberg 2012; Razin et al. 2012)

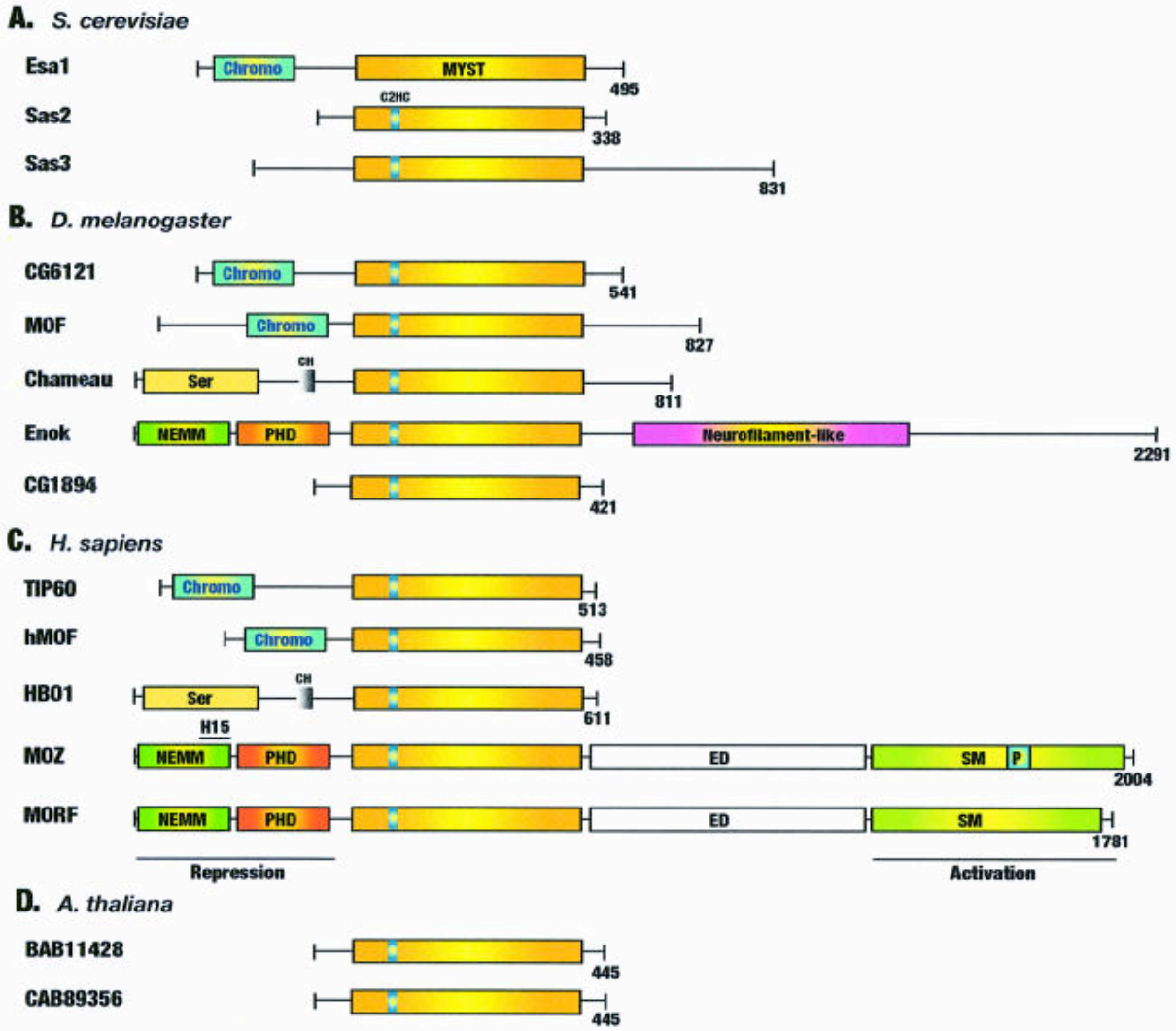


**Figure 3: Domain organization of MYST proteins** from *S.cerevisiae* (**A**), *Drosophila* (**B**), human (**C**) and *A.thaliana* (**D**). Chromo, chromodomain; Ser, serine-rich domain; CH, cysteine/histidine-rich motif; H15, linker histones H1- and H5-like domain; NEMM, N-terminal part of Enok, MOZ or MORF; PHD, PHD zinc finger; ED, glutamate/aspartate-rich region; SM, serine/methionine-rich domain. The SM domain of MOZ has an insertion of a proline/glutamine-stretch (labeled P). Bars below the N-terminal and SM domains of MORF denote its transcriptional repression and activation domains, respectively. Numbers on the right correspond to the total residues that each protein has (Figure and legend taken from Yang 2004).

The following sections will provide a closer look at Sas2 in yeast as one of the founding members of this family, and at MOF, its homolog in flies and humans.

### 1.6.1. The MYST HAT Sas2 in *Saccharomyces cerevisiae*

Sas2 (something about silencing) in yeast was, together with Sas3, first identified in a screen for enhancers of epigenetic silencing defects caused by the deletion of the silencing factor *SIR1* (Reifsnyder et al. 1996). Furthermore, it was identified as a suppressor of silencing defects at the yeast *HMR*-E silencer. Remarkably, opposing effects of the *SAS2* deletion were observed at the silent mating-type locus *HML* (Ehrenhofer-Murray et al. 1997). Sas2 thus

plays in role in transcriptional regulation in the context of silencing. Sas2 was later found to be part of a HAT complex, where it interacts with Sas4 and Sas5 to form the SAS-I complex that mediates silencing at *HML, HMR* and the telomeres (Meijsing and Ehrenhofer-Murray 2001; Osada et al. 2001). Furthermore, it was shown to interact with the chromatin assembly factor CAF-I as well as Asf1, and performs acetylation of H4K16, possibly in cooperation with replication-dependent and independent chromatin assembly (Meijsing and Ehrenhofer-Murray 2001).

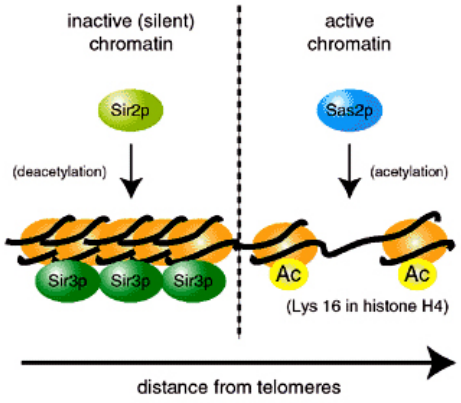


**Figure 4: Model of the region-dependent regulation of the interaction between Sir3p and H4 through the reversible acetylation of H4−Lys16 by Sas2p and Sir2p (Figure taken from Kimura et al. 2002)**

Further studies provided deeper insight into the role of Sas2 in transcriptional regulation. Sas2 contributes significantly to genome-wide acetylation of H4K16, and its activity antagonizes the HDAC Sir2 at telomeric regions. The loss of Sas2 results in global H4K16 hypoacetylation (Kimura et al. 2002; Suka et al. 2002). This allows the spreading of SIR-mediated heterochromatin at telomeres. In wild-type cells this is opposed by the SAS-mediated maintenance of euchromatin in more telomere-distal regions. The boundary between active and repressive chromatin is additionally regulated by Rpd3 (HDAC) that competes with Sir2 for the acetylated H4K16 substrate (Ehrentraut et al. 2010). Despite its role in transcriptional regulation, Sas2-dependent H4K16Ac has recently been shown not to be a consequence of transcription or histone exchange, but to be incorporated in a DNA replication dependent manner (Heise et al. 2012).

### 1.6.2. MOF in *Drosophila melanogaster*

*Drosophila* MOF (dMOF) is the closest homologue to Sas2 from *S. cerevisiae,* and it is required for male X hyperacetylation in flies. In species where the sexes differ in the number or composition of their sex chromosomes, the dosage of X-linked gene products has to be adjusted by a mechanism referred to as dosage compensation. In *Drosophila,* this is achieved

by a twofold enhancement of transcription on the single male X-chromosome to match the expression level of the two female X-chromosomes. Several msl (male-specific lethal) genes have been identified and their proteins locate specifically to the X-chromosome in male somatic nuclei. As a consequence, early on, a MSL complex was postulated to exist that functions via histone modification to regulate expression on the male X-chromosome, since it is significantly enriched for MSL-dependent H4K16Ac (Kelley and Kuroda 1995). The identification of MOF (males-absent on the first), a HAT homolog to Sas2, filled that missing link (Hilfiker et al. 1997).

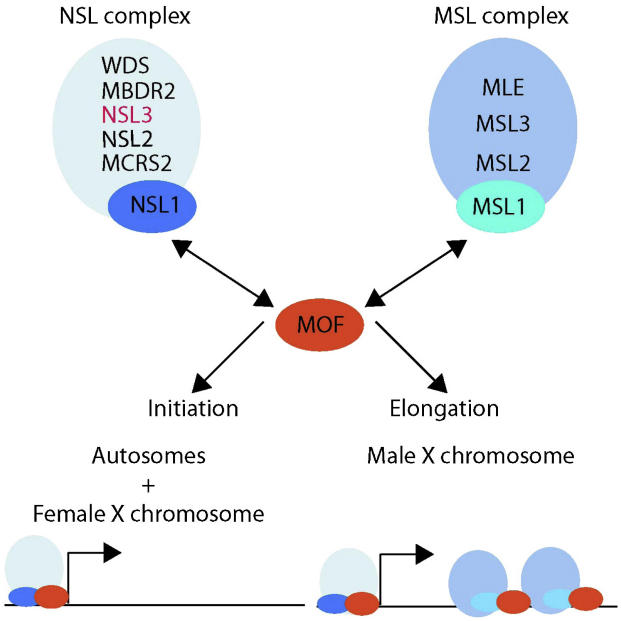


**Figure 5: Model of two distinct MOF-containing complexes in *Drosophila melanogaster*,** the MSL complex targets MOF to gene bodies on the male X chromosome where it regulates transcriptional elongation, the NSL complex targets MOF to active promoters on autosomes and female X chromosomes where it regulates transcriptional initiation (Figure taken from Raja et al. 2010)

The MSL complex responsible for dosage compensation in male flies consists of at least five subunits: MOF, MLE (maleless), MSL-1, MSL-2 and MSL-3, as well as the two non-coding RNAs roX1 and roX2 that are bound by the chromodomain of MOF (Gu et al. 1998; Kelley et al. 1999). MOF specifically acetylates H4K16 and is the catalytic subunit responsible for the MSL HAT activity (Akhtar and Becker 2000; Smith et al. 2000). The MSL complex covers the male X chromosome along its entire length, where it assembles at MSL recognition elements (MRE) and spreads from there into flanking regions on the male X chromosome (Alekseyenko et al. 2008). In particular, MSL is enriched at gene bodies with a peak towards the 3' end. 90 % of those genes are actively transcribed, linking the MOF-mediated H4K16Ac to transcriptional elongation (Kind et al. 2008).

Interestingly, MOF is also localized to sites outside the male X-chromosome in an MSL-independent manner (Kind et al. 2008). A second MOF-containing complex has been identified, the NSL (non-specific lethal) complex, which is composed of NSL1, NSL2, NSL3, MCRS2, MBDR2 and WDS (Raja et al. 2010)(Figure 5). In the context of that complex, MOF is recruited to the autosomes both in males and females. It is enriched at promoter regions of housekeeping genes, implicating a function in transcriptional initiation (Lam et al. 2012).

### 1.6.3. MOF (MYST1) in *Homo sapiens*

The human MOF (hMOF or MYST1) was first isolated three years after its *Drosophila* homolog dMOF (Neal et al. 2000). It contains the family-specific MYST domain including the $C_2HC$ zinc finger region, which is required for *in vitro* activity. A knockdown of hMOF with siRNA resulted in severely decreased acetylation of H4K16 *in vivo*, while acetylation of other lysine residues (H3K14, H3K23, H4K12) remained unaffected. Furthermore, an interaction between hMOF and hMSL3 (homolog to dMSL3) was reported (Taipale et al. 2005). Shortly after these findings, a human MSL complex was identified, containing human homologs to *Drosophila* MSL subunits: hMOF, hMSL1, hMSL2 and hMSL3 (Figure 6). An interaction of hMOF with MSL1v1 was also observed in this study. MSL1v1 only shares similarity with hMSL in a 15 to 20 amino acid region of the C terminus, but this region is responsible for hMOF binding (Smith et al. 2005). Additionally, hMOF was co-immunoaffinity purified with an MLL1-WDR5 complex (Dou et al. 2005). The *MLL1* (mixed lineage leukemia-1) gene, which is linked to several acute and myelogenous leukemias, is a key regulatory factor controlling the expression of homeobox (*Hox*) genes (Milne et al. 2002) and one of the founding members of the SET1 family of histone methyltransferases (HMT). The complex purified by Dou et al. showed a robust MLL1-mediated histone methyltransferase activity that can affect mono-, di-, and trimethylation of H3K4 and a MOF-mediated histone acetyltransferase activity that is specific for H4K16. In a later study that addressed the regulation of MOF in the context of two distinct complexes, remarkable differences in substrate specificity were revealed. While both complexes showed indistinguishable activity on H4K16, the MOF-MSL1v1 acetylated additional non-histone substrates. The complex (containing MLL1-WDR5) was exclusively required for the acetylation of the transcription factor p53 at K120 as well as for optimal transcriptional activation of p53 target genes (Li et al. 2009)(Figure 6).

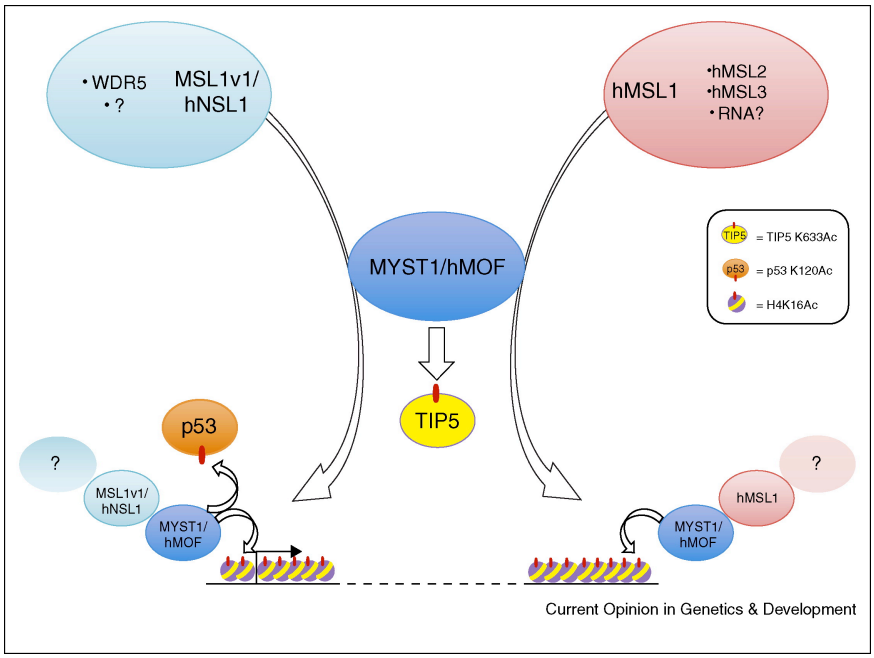


**Figure 6: Different roles for the mammalian acetyltransferase MYST1/hMOF.** hMOF resides in at least two different complexes in mammalian cells. When recruited in a complex with MSL1v1/hNSL1, hMOF is responsible for the acetylation of both p53 K120 and H4K16 at the 5′ end of target loci. If MYST1 is instead recruited to the mammalian MSL complex via an interaction with hMSL1, the protein specifically acetylates H4K16 at the 3′ end of target loci. hMOF also acetylates the Tip5 component of the NoRC chromatin remodeling complex, but the regulation of specificity for this substrate is as yet unknown (Figure taken from Laverty et al. 2010)

Taken together, these findings show the existence of at least two distinct, MOF-containing complexes that are highly (MSL) or partially (NSL) conserved from flies to human. They further implicate that the molecular function of MOF is also conserved, although the biological context might have changed throughout evolution. The *Drosophila* MSL adopted the dosage compensation mechanism described above, while in humans dosage compensation is achieved by inactivation of one female X chromosome.

## 1.7. Chromatin modifications in *Caenorhabditis elegans*

The nematode *C. elegans* has been used as a model organism for nearly four decades now (Brenner 1974). It is a comparably simple metazoan but has a nervous system. It is small and transparent, can be stored for long periods of time and is easy to grow in bulk populations on a bacterial diet, making it an excellent model to study development. A large set of genetic tools has been developed over the years, and with the sequencing of its complete genome (1998), it perhaps is the best-studied metazoan to date and used as a model in many research fields related to genetics and molecular biology. At the same time, the knowledge about its wild ecology is surprisingly small.

However, there are limitations to the genetic possibilities of *C. elegans*. It was until recently not possible to manipulate endogenous loci in a targeted manner, which hampers the introduction of targeted mutations, the knockout of genes or the use of affinity tags at endogenous loci. Protein biochemistry is further complicated. Neither are there established cell lines, nor is it possible to isolate specific tissues at large scale. For this reason, researchers are restricted to working with the whole proteome when trying to isolate proteins. These may be some of the factors why *C. elegans* is not as popular as yeast, flies or mammalian cells in the field of chromatin biology. Performing a PubMed (January 2013) search and combining the query "chromatin" with either "*Saccharomyces cerevisiae*" or "*Drosophila melanogaster*" leads to 4718 and 2207 results, respectively. The same search with "*Caenorhabditis elegans*" gave only 521 results, indicating that chromatin work in the worm is lagging behind.

Nonetheless, progress had been made in the investigation of chromatin modifications in *C. elegans*. Several mechanisms had been well characterized first using genetics and were subsequently linked to chromatin modifications. One example is the differentiation of vulval cells throughout development. The synMuv genes fall into three classes of genes (synMuv A, B and C) that act redundantly for vulval cell fate specification. If two genes of different classes are inactivated simultaneously, ectopic EGF/RTK/Ras signalling is initiated, resulting in the formation of ectopic vulvae (synthetic Multivulvae). The synMuv genes were found to encode chromatin associated factors, including homologues to mammalian class I histone deacetylases (HDA-1), histone methyltransferases (MET-1, MET-2) and homologues of the evolutionarily conserved NuRD/Mi-2 nucleosome remodelling and HDAC complex (LET-418/Mi-2, LIN-53/RbAp48, MEP-1 and HDA1/HDAC-1)(Sternberg and Horvitz 1991; Lu and Horvitz 1998; Dufourcq et al. 2002; Ceol and Horvitz 2004; Cui et al. 2006a; Cui et al. 2006b; Andersen and Horvitz 2007).

Another fascinating topic is the maintenance of cellular identity in a developing multicellular organism. MES-4 (maternal effect sterile, homolog to the yeast H3K36 methyltransferase Set2) has been shown to transmit memory of gene expression from one generation of germ cells to the next by maintaining methylation of H3K36 of germline-expressed loci in embryos (Rechtsteiner et al. 2010). Chromatin regulators are further involved in the maintenance of somatic cell fate. The synMuv genes antagonize germline fate in somatic cells. In their absence germline-specific genes are ectopically expressed in the soma (Petrella et al. 2011). Interestingly, MES-4 is required for somatic cells to acquire germ cell fate in the absence of synMuv activity (Wang et al. 2005). Repetitive sequences are silenced in the *C. elegans* germline (Kelly et al. 1997; Kelly and Fire 1998). It has been shown, that these silenced

arrays acquire heterochromatic marks (H3K9me3 and H3K27me3) and are preferentially located at the nuclear envelope through interaction with nuclear lamina components. In differentiated tissues, transgenes become decompacted and occupy specific subnuclear positions upon activation of gene expression, indicating the existence of nuclear compartments similar to mammalian nuclei (Towbin et al. 2010)

Dosage compensation in worms has been studied extensively. The two X chromosomes in the hermaphrodite are downregulated by half to match the expression levels of the single male X. This downregulation is accomplished by the dosage compensation complex (DCC), which consists of ten subunits. SDC-1, SDC-2, SDC-3, DPY-21 and DPY-30 are exclusive to DCC, the other five subunits (DPY-26, DPY-27, DPY-28, MIX-1, CAPG-1) are related to subunits of the two condensin complexes in worms. The Condensin I complex only differs in one subunit (SMC-4 instead of DPY-27) and controls meiotic crossover. Condensin II shares MIX-1 with the DCC. It is the prime condensin complex responsible for mitotic and meiotic chromosome compaction and resolution. The DCC covers both X chromosomes in hermaphrodites and is not assembled in males. However, the DCC compensates most, but not all genes on X and it does not always achieve a precise twofold repression. Strikingly, DCC binding to the promoter or body of a gene is neither necessary nor sufficient to dosage-compensate that gene. These findings indicate that it acts over a long range to achieve dosage compensation, possibly by altering higher-order chromosome structure to control the interaction between dispersed regulatory elements that modulate gene expression (Meyer 2010).

The worm differs in some very basic aspects from yeast, flies and mammals. Besides having operons, it furthermore has no specially restricted centromeres, but instead carries holocentric chromosomes that are attached on their entire length by microtubules during cell division. Nevertheless, the list of conserved chromatin modifiers that are characterized in worms is growing, and future information obtained from studies in *C. elegans* will assist in a better understanding of the fundamental mechanisms involved in epigenetic regulation during the metazoan development.

### 1.7.1. Histone (de)acetylation in *Caenorhabditis elegans*

The histone deacetylase HDA-1 is homologous to RPD3 in yeast and flies. In the worm, it causes defects in vulval development and gonadogenesis when mutated, linking histone acetylation to the regulation of Ras signalling responsible for vulval development (Dufourcq et al. 2002). Furthermore, later studies showed that HDA-1 regulates a variety of extracellular matrix genes (especially collagen genes) and is involved in cell migration and axon

pathfinding (Whetstine et al. 2005; Zinovyeva et al. 2006). In combination with the linker histone HIS-24, the HDAC SIR-2.1 (sirtuin family, homolog to human SIRT1) was reported to propagate repressive chromatin at subtelomeric regions (Wirth et al. 2009). SIR-2.1 can also promote longevity via the activation of DAF-16 (Berdichevsky et al. 2006).

Dosage compensation in worms has also been linked to histone deacetylation. The two X chromosomes of hermaphrodites are downregulated by half, thereby matching expression levels of the single male X and the autosomes. The hermaphrodite X chromosomes are depleted for H4K16Ac in a DCC-dependent manner. This DCC-dependency is reported to be mediated by SIR-2.1, which is proposed to be the H4K16 HDAC (Wells et al. 2012). Another aspect of dosage compensation is the equalization of expression levels between the autosomal and the X-linked genes. A male worm has only one X chromosome that, in contrast to male flies, is not targeted by sex-specific dosage compensation. Since this would result in halved gene dosage of X-linked genes, a corresponding mechanism was hypothesized that upregulates the X chromosomes regardless of the sex. While this results in equal gene dosage in males, the two hermaphrodite X chromosomes are additionally regulated by the sex-specific dosage compensation described above. Recent analysis of RNA-Seq data supports this hypothesis, which is also referred to as “Ohno’s hypothesis”. It showed that average expression levels are equal between autosomal and X-linked genes in worms, flies and humans, although the underlying mechanism remains unclear (Deng et al. 2011).

In *C. elegans,* there exist four predicted histone acetyltransferases of the MYST family, MYS-1, MYS-2, MYS-3 (LSY-12) and MYS-4. MYS-1 is most homologous to TIP60 in human and flies and to Esa1 in yeast. MYS-2 encodes the homolog to Sas2, dMOF and hMOF, while MYS-3 and MYS-4 are homologues to enok in flies and MYST3 in humans, and have weaker homology to the yeast MYST HATs (Sanjuan and Marin 2001). MYS-1 has been found to be a synMuv C gene and is involved in transcriptional regulation during foregut development (Ceol and Horvitz 2004; Updike and Mango 2006). LSY-12 (laterally symmetric (defective in lateral asymmetry), formerly known as MYS-3) works in a complex together with LSY-13 and LIN-49 to regulate the expression of genes responsible for neuronal laterality (O'Meara et al. 2010). MYS-4 was mentioned in a study to be likely required for regulating gene expression in multiple tissues, including vulval synMuv regulation (Ceol and Horvitz 2004; Cui et al. 2006b). MYS-2 is the subject of this study and will be further discussed in the next section.

### 1.7.2. The histone acetyltransferase MYS-2 from *Caenorhabditis elegans*

The aim of this study was to characterize the putative MYST HAT MYS-2 from *C. elegans*. It is the closest homolog to Sas2 in yeast, which had been studied extensively in our group and was found, as a part of the SAS-I complex, to be responsible for the majority of H4K16Ac in gene bodies and to be involved in several aspects of transcriptional regulation, including silencing of the mating-type loci *HML* and *HMR*, as well as cryptic transcription (Ehrenhofer-Murray et al. 1997; Meijsing and Ehrenhofer-Murray 2001; Heise et al. 2012). Furthermore, MYS-2 is homologous to MOF in flies and human, which are both reported to be part of conserved complexes, the NSL and MSL complexes (described in sections 1.6.2 and 1.6.3). Both are the prime H4K16 acetyltransferases.

When this study was initiated, MYS-2 still had its generic gene name derived from sequencing: K03D10.3. To our knowledge, it has only been mentioned twice so far in the scientific literature, which is surprising, given the fact that its homologs are quite "popular". It was tested in a candidate RNAi screen that was designed to identify new synMuv genes. In a synMuv class A mutant background, it did not show an effect when knocked down (Ceol and Horvitz 2004). Another candidate RNAi screen, this time to identify factors involved in RNAi inheritance, revealed an effect for K03D10.3 (*mys-2*) in the inheritance of gene silencing induced by RNAi (Vastenhouw et al. 2006). A quite recent study dealt with the involvement of BET-1 in the establishment and maintenance of cell fates in *C. elegans*. BET-1 contains two bromodomains and was shown to bind acetylated histone H4 peptides. The authors reported that upon simultaneous downregulation by RNAi of *mys-1* and *mys-2,* subnuclear localization of BET-1 was disturbed, indicating that H4 acetylation provides a binding platform for BET-1. Furthermore, simultaneous knock-down of *mys-1* and *mys-2* caused a *bet-1*-like phenotype, resulting in abnormal cell-fate specification (Shibata et al. 2010).

An alignment of the MYS-2 protein sequence with dMOF, hMOF and Sas2 confirmed the homology that has been reported earlier (Sanjuan and Marin 2001). A further analysis of the sequence using interpro (Hunter et al. 2012) predicts the existence of the conserved MYST domain, as well as the chromo domain, which is also part of dMOF and hMOF (Figure 7). Chromo domains of different proteins were found responsible for the recruitment to specific states of chromatin, and there is evidence that methylated H3 tails on K9 can be the target for the chromo domain of *Drosophila* HP1 (Eissenberg 2012). Instead, the chromo domain of dMOF has been reported to be responsible for the *in vitro* binding of non-coding roX RNA that belongs to the MSL complex (Akhtar et al. 2000). This suggests a binding function to proteins and/or RNA that affects targeting to distinct chromatin domains (Eissenberg 2012).

Regarding the participation of the MYS-2 homologues from other organisms in multisubunit complexes, we queried the genome of the worm using BLASTn in order to find homologues of complex subunits of the MOF-containing complexes MSL and NSL. We did not find any homologs to MSL subunits, an observation that has been made previously and suggests that worms do not contain an MSL-like compensasome (Marin 2003). Although dosage compensation in worms also seems to be linked to H4K16Ac, the dosage compensation strategy here is distinct from the one in flies. Additionally, the worm dosage compensation complex is well investigated, making it unlikely that MYS-2 is directly involved in the downregulation of hermaphrodite X chromosomes. However, considering "Ohno's hypothesis", it is possible that MYS-2 has a function in upregulation of X chromosomes in both sexes, perhaps mediated by the acetylation of H4K16.

The *Drosophila* NSL complex consists of NSL1, NSL2, NSL3, MCRS2, MBD-R2, and WDS. Indeed, the search for NSL homologues revealed three possible candidates. WDR-5.1 (homologous to WDS) has been reported to be involved in H3K4 methylation in worms (Simonet et al. 2007). The two other candidates, namely H28O16.2 (homologous to MCRS1) and F54D11.2 (homologous to NSL3), have not been characterized so far and still have their generic names. There are no close homologues in the worm to other subunits of the NSL complex.

An interesting fact about *mys-2* is that it is part of the operon CEOP1731. Together with the two genes upstream, Y63D3A.7 and Y63D3A.8, it is likely to be transcribed as one large mRNA (Wormbase, WS234). Genes that reside in operon in worms have been reported to be functionally related in some cases, but that is not necessarily a general charcteristic of operons. Additionally, individual genes in an operon can be differently regulated on the mRNA level (Blumenthal and Gleason 2003). The gene Y63D3A.7 encodes a homologue of the NDUFA2/B8 subunit of the mitochondrial NADH dehydrogenase (ubiquinone) complex while Y63D3A.8 is predicted based on its domains to have a molecular function in sugar:hydrogen symporter activity (Tsang and Lemire 2003). This does not imply a functional relation between *mys-2* and those two genes.

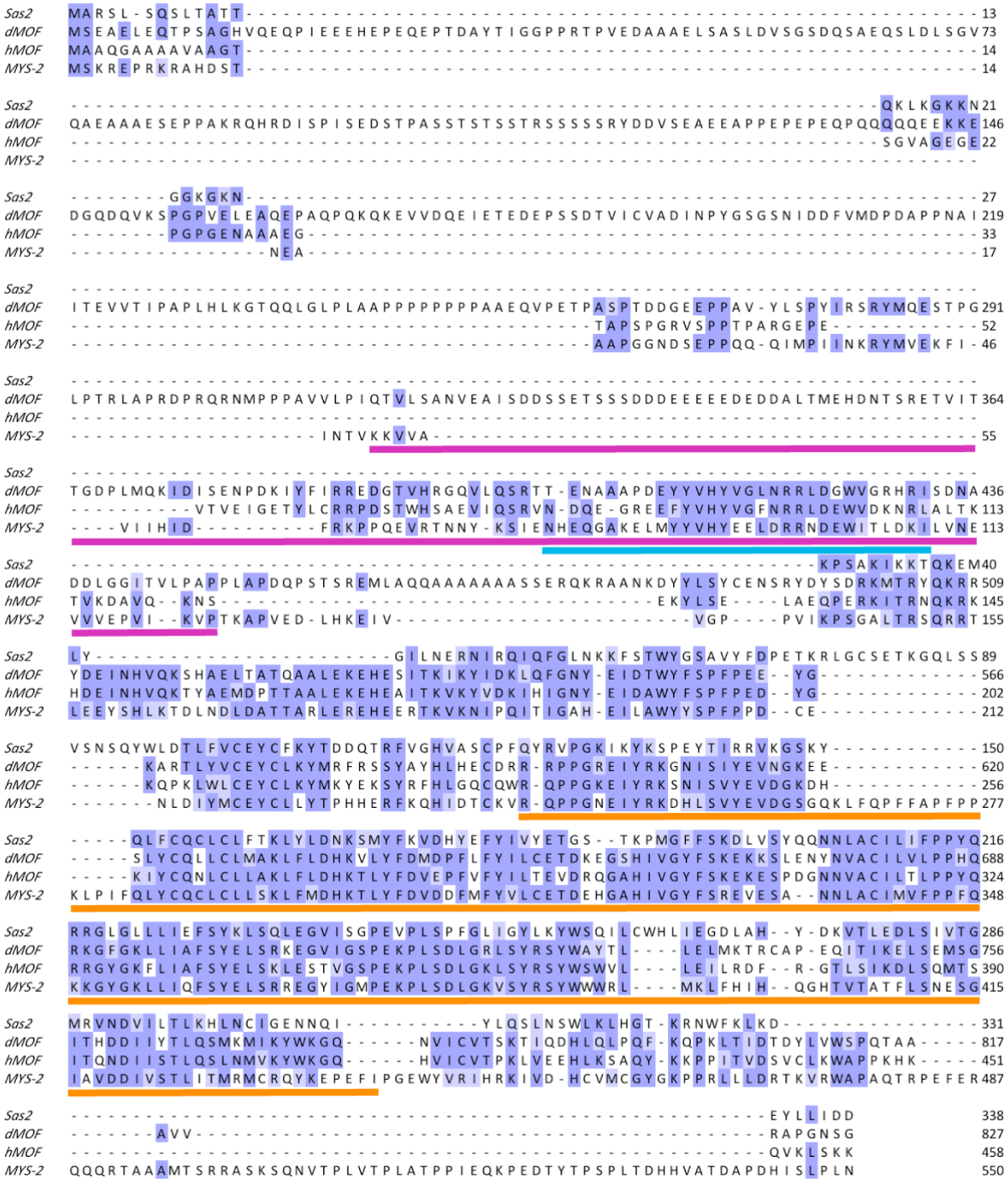


**Figure 7: Alignment of Sas2, dMOF, hMOF and MYS-2**; Alignment was performed using ProbCons (Do et al. 2005). Blue boxes indicate identities, colored bars indicate domains predicted by interpro (Hunter et al. 2012): magenta – chromo domain (INTERPRO:IPR000953), turquoise - RNA binding activity-knot of a chromodomain (INTERPRO:IPR025995), yellow – MYST domain (INTERPRO:IPR002717)

## 1.8. Aim of this thesis

Histone acetyltransferases of the conserved MYST family have been shown to influence elementary cellular processes like transcription, DNA replication and DNA repair. In particular, the homologous group of Sas2 (*yeast*), dMOF (*Drosophila*) and hMOF (humans) is

reported to be responsible for a major portion of H4K16Ac in their respective species (Sapountzi and Cote 2011). In flies, MOF is well characterized as the catalytical subunit of the MSL HAT complex that is responsible for dosage compensation via H4K16Ac (Akhtar and Becker 2000; Smith et al. 2000). MOF is furthermore part of a second HAT complex in flies, the NSL complex, which is found at promoters of housekeeping genes throughout the genome, where it is required to recruit RNA polymerase II (Lam et al. 2012). The MOF containing MSL complex is highly conserved in humans and, similar to the situation in flies, hMOF interacts with a second complex MOF-MSL1v1 that shares homology with the fly NSL complex (Dou et al. 2005; Smith et al. 2005; Taipale et al. 2005). Sas2 in yeast, as part of the SAS-I complex, was recently investigated by our group and shown to significantly contribute to genome-wide levels of the H4K16Ac mark in open reading frames (Heise et al. 2012).

This study was initiated with the motivation to expand the view on the impact of the Sas2/dMOF/hMOF group of enzymes on chromatin-mediated regulation. For this purpose, the well-established model organism *Caenorhabditis elegans* was used to characterize MYS-2, the closest homologue to the Sas2/dMOF/hMOF group. MYS-2 has been shown to mediate inheritance of RNAi and to play a role in the maintenance of cell fates, but beyond that, there have been no scientific reports on this MYST HAT (Vastenhouw et al. 2006; Shibata et al. 2010). We addressed questions that concerned elementary properties of MYS-2, by using approaches that made use of the worm as a model organism. Specific α-MYS-2 antibodies were generated in order to investigate the expression of *mys-2* by immunostaining embryos and dissected adult hermaphrodites. Analysis of the phenotypic consequences of the *mys-2*(ok2429) deletion addressed the general function of MYS-2. We were furthermore interested in the subunit composition of a putative MYS-2 containing HAT complex in worms. Therefore, MYS-2 was precipitated with α-MYS-2 antibodies, with the intention of co-purifying complex partners. Possible crosstalk or interaction of MYS-2 with components of the DCC in worms and a gene homologous to the fly NSL subunit NSL3 was addressed, by investigating genetic interactions using RNA interference in wild-type and mutant worms. A screen for interactors was initiated using the yeast two-hybrid system. The yeast properties in site-specific recombination were used in order to generate several *mys-2*::GFP reporter constructs that should be used to further investigate expression of *mys-2* in the worm.

Taken together, this study aimed at obtaining insight into elementary properties of MYS-2 and its possible function in the worm. It furthermore should provide a basis for further studies to expand our knowledge on this MYST HAT in *C. elegans*.

# 2. Materials and Methods

## 2.1. Strains

### 2.1.1. *Escherichia coli* strains

| | |
|---|---|
| TOP10 | F- mcrA Δ(mrr-hsdRMS-mcrBC) φ80lacZΔM15 ΔlacX74 nupG recA1 araD139 Δ(ara-leu)7697 galE15 galK16 rpsL($Str^R$) endA1 $\lambda^-$ |
| DH5α | $F^-$ endA1 glnV44 thi-1 recA1 relA1 gyrA96 deoR nupG Φ80d*lacZ*ΔM15 Δ(*lacZYA-argF*)U169, hsdR17($r_K^-$ $m_K^+$), λ– |
| BL21 (DE3) | $F^–$ ompT gal dcm lon $hsdS_B$($r_B^-$ $m_B^-$) λ(DE3 [lacI lacUV5-T7 gene 1 ind1 sam7 nin5]) |
| Rosetta(DE3)pLysS | $F^-$ ompT $hsdS_B$($R_B^-$ $m_B^-$) gal dcm λ(DE3 [lacI lacUV5-T7 gene 1 ind1 sam7 nin5]) pLysSRARE ($Cam^R$) |
| OP50 | nematode feeding strain, uracil auxotroph *E. coli* B. |
| HT115 (DE3) | F-, mcrA, mcrB, IN(rrnD-rrnE)1, lambda -, rnc14::Tn10(DE3 lysogen: lavUV5 promoter -T7 polymerase) (IPTG-inducible T7 polymerase) (RNAse III minus) |

### 2.1.2. *Saccharomyces cerevisiae* strains

**Table 1: *Saccharomyces cerevisiae* strains used in this study**

| Strain[a] | Genotype |
|---|---|
| AEY4217 | *MAT***a** *his3-Δ200 trp1-901 leu2-3,112 can1-100 ade2 lys2-801am LYS2*::(lexAop)4-*HIS3 URA3*::(lexAop)8-lacZ *GAL4* |
| AEY4218 | AEY4217 + pAE1336 |
| AEY4460 | AEY4217 + pAE1446 |
| AEY4929[b] | *MAT***a** *ade2-101 his3-11,15 trp1-1 leu2-3,112 lys2Δ ura3-1* (W303) + *CSE4*-GFP::*klTRP1* |
| AEY4980[c] | AB1380 (*MAT***a**, *ura-3, trp-1, ade2-1, can-1 100, lys 2-1, his-5*) + Y63D3 (in pYAC4) |
| AEY5027 | AEY4980 + Y63D3 *ura3Δ*::*KanMX* |
| AEY5079 | AEY5027 *mys-2*::GFP (between P20 and G21 of MYS-2) |
| AEY5080 | AEY5027 *mys-2*::GFP (between D210 and C211 of MYS-2) |
| AEY5081 | AEY5027 *mys-2*::GFP (between L549 and N550 of MYS-2) |

[a] Strains were constructed during this study or taken from the laboratory strain collection, unless indicated otherwise; [b] constructed by A. Samel; [c] Sanger Institute (Cambridge, UK)

### 2.1.3. *Caenorhabditis elegans* strains

**Table 2: *Caenorhabditis elegans* strains used in this study**

| Strain[a] | Genotype |
|---|---|
| N2 (Bristol)[b] | *wild type* |
| CB3249 | *unc-17*(*e245*)/*dpy-26*(*n199*)IV. |

| | |
|---|---|
| DR1410 | *dpy-27*(*y56*)/qC1 *dpy-19*(*e1259*) *glp-1*(*q339*) III. |
| TY824 | +/szT1[*lon-2*(*e678*)] I; *sdc-2*(*y74*)/szT1 X. |
| TY956 | *sdc-3*(*y132*)/*unc-76*(*e911*)V. |
| NL2099[b] | *rrf-3*(*pk1426*) II. |
| CA151 | *him-8*(*me4*) IV. |
| CB1489 | *him-8*(*e1489*)IV. |
| CB1561 | *her-1*(*e1561*)V. |
| VC1931 | K03D10.3(*ok2429*)/hIn1[*unc-101*(*sy241*)] I. |

[a] All strains provided by Caenorhabditis Genetics Center, unless stated otherwise; [b] Gift from A. Antebi

## 2.2.Media and growth conditions

### 2.2.1. *Escherichia coli* media and growth conditions

*E. coli* strains were grown using standard procedures (Sambrook et al. 1989) at 37°C in Luria-Bertani (LB) Medium. If selection for plasmids was required, one or two of the following antibiotics were added: 100 µg/ml ampicillin, 50 µg/ml kanamycin, 34 µg/ml chloramphenicol. To induce plasmid-driven gene expression, 1mM IPTG (Isopropyl β-D-1-thiogalactopyranoside) was supplemented.

### 2.2.2. *Saccharomyces cerevisiae* media and growth conditions

Yeast was grown as previously described (Sherman 1991) in either full medium (YPD) or yeast minimal medium (YM). YM was supplemented with 2% glucose and, upon requirement of marker selection, with one or more of the following supplements: adenine, uracil, tryptophan, methionine and histidine at 20 µg/ml, leucine and lysine at 30 µg/ml. To select against *URA3* containing plasmids, 1 mg/ml 5-FOA (5-Fluoroorotic Acid) was added in addition to the other supplements.

### 2.2.3. *Caenorhabditis elegans* media and growth conditions

Worms were maintained on Nematode Growth Media (NGM) agar plates seeded with a lawn of *E. coli* OP50 as a food source (Brenner 1974). Depending on the desired speed of growth, NGM agar plates were incubated at 15°C, 20°C or 25°C (from slowest to fastest). To obtain large quantities of nematodes, they were grown in liquid media (Lewis and Fleming 1995). For this purpose, the following S Medium components were prepared and autoclaved separately (except the cholesterol):

- 10x S Basal [58,5 g NaCl, 10 g $K_2HPO_4$, 60 g $KH_2PO_4$, $H_2O$ to 1 litre]
- Cholesterol [5 mg/ml in 95% ethanol]
- 1 M potassium citrate pH 6.0 [20 g citric acid monohydrate, 293.5 g tri-potassium citrate monohydrate, $H_2O$ to 1 litre]

- Trace metals solution [1.86 g disodium EDTA, 0.69 g $FeSO_4$ •7 $H_2O$, 0.2 g $MnCl_2$•4 $H_2O$, 0.29 g $ZnSO_4$ •7 $H_2O$, 0.025 g $CuSO_4$ •5 $H_2O$, $H_2O$ to 1 litre, stored in the dark.]
- 1 M $CaCl_2$
- 1 M $MgSO_4$

Furthermore, large quantities of OP50 overnight cultures were pelleted and stored at 4°C. In order to get synchronized cultures, six NGM agar plates (94 mm diameter), seeded with a lawn of OP50 were inoculated with agar chunks from starved NGM plates, containing only L1 larvae. Three days later, when the plates had just been cleared of bacteria by the worms, it was time to start the liquid culture. For this purpose, 400 ml of S Medium [40 ml 10x S Basal, 4 ml 1 M potassium citrate pH 6, 4 ml trace metals solution, 1,2 ml 1 M $CaCl_2$, 1,2 ml 1 M $MgSO_4$, 400 µl cholesterol, sterile $H_2O$ to 400 ml] were prepared using sterile techniques. 10 ml S Medium were removed to resuspend an OP50 pellet corresponding to 1 litre overnight culture and added thereafter. 20 ml S medium were removed and used to wash adult hermaphrodites off of six NGM agar plates. The worm suspension was then added to S medium, and the culture was incubated at 20°C with vigorous shaking. Cultures were monitored every day for the presence of food, and if needed, more OP50 was added. To avoid overcrowding, worms were usually grown for one generation in liquid media. After three to four days, when the majority of the next generation became adult, cultures were harvested.

### 2.2.4. Harvesting and bleaching of *C. elegans*

Liquid cultures were transferred into beakers and set on ice for at least 15 min. When worms were settled to the bottom, most of the liquid was aspirated. The remaining S medium was used to resuspend the worms and to transfer them to 50 ml falcon tubes. Worms were washed by adding cold M9 Buffer [3 g $KH_2PO_4$, 6 g $Na_2HPO_4$, 5 g NaCl, 1 ml 1 M $MgSO_4$, $H_2O$ to 1 litre, sterilized by autoclaving] to 50 ml, resuspending the pellet, and shortly centrifuging at 4000 rpm. The wash was repeated 3 or more times, until the supernatant was cleared of bacteria. After the last wash, the supernatant was removed and the wet weight of the pellet determined. Pellets were then either used for further application or frozen at -80°C until needed.

If embryos were required, worm pellets were bleached. For this purpose, 100 ml bleaching solution [70 ml $H_2O$, 20 ml sodium hypochlorite NaClO (12% Cl; Roth 9062.3), 10 ml 5 N NaOH] were prepared freshly. The worm pellet was resuspended in 45 ml bleaching solution, shaken extensively for four minutes and then shortly centrifuged at 4000 rpm. Supernatant was removed, the pellet washed once in M9 buffer and shortly centrifuged again at 4000 rpm.

After aspiration of supernatant, the pellet was resuspended in 45 ml bleaching solution a second time. The falcon tube was shaken extensively until worms were completely dissolved and only embryos remained, depending on the age of the sodium hypochlorite, this took 2 minutes or more. Instantly, embryos were shortly centrifuged at 4000 rpm, the bleaching solution was removed, and the embryos washed at least three times with M9 until the bleaching odour was gone. Bleached embryos were used to start synchronized liquid cultures or, after determination of the weight, for further applications. The same method in smaller scale was also used to decontaminate worm cultures.

## 2.3. Genetic methods

### 2.3.1. Molecular cloning

Unless stated otherwise, plasmids were generated using standard techniques (Sambrook et al. 1989). Kits for plasmid purification were purchased from Qiagen or Macherey-Nagel. Enzymes and respective buffers for DNA manipulation were obtained from New England Bioloabs, Roche, Invitrogen, Promega and Fermentas. Oligonucleotides used in this study were designed with "ApE – A plasmid Editor" and synthesised by "metabion International AG". They are listed in Table 4.

**Table 3: Plasmids used in this study**

| Plasmid[p] | Description | Purpose |
|---|---|---|
| pAE436 | pBTM117c-*SAS2* | Yeast two-hybrid (Y2H) control |
| pAE451 | pBTM117c-*SAS4* | Y2H control |
| pAE454 | pBTM117c-*CAC1* | Y2H control |
| pAE458 | pBTM117c-*CSE4* | Y2H control |
| pAE525 | pBTM117c | Y2H empty bait |
| pAE748 | L4440 | RNAi feeding vector |
| pAE1017 | L4440-*unc-22*[a] | RNAi positive control |
| pAE1019 | L4440-R07B5.9[e] | *mys-3* RNAi |
| pAE1020 | L4440-K03D10.3[e] | *mys-2* RNAi |
| pAE1021 | L4440-VC5.4[e] | *mys-1* RNAi |
| pAE1022 | L4440-C34B7.4[e] | *mys-4* RNAi |
| pAE1029 | pTG96 | Co-injection marker (*sur-5*::GFP) |
| pAE1030 | pRF4[a] | Co-injection marker (*rol-6*(su1006)) |
| pAE1031 | L3781[a] | GFP expression vector |
| pAE1212 | pK03D10.3::GFP | GFP driven by *mys-2* promoter |
| pAE1282 | K03D10 (Cosmid)[b] | *C. elegans* Cosmid carrying *mys-2* |
| pAE1299 | K03D10.3 (cDNA)[c] | *mys-2* ORF clone |
| pAE1333 | pET-15b-*mys-2*$^{1-795}$ | MYS-2 antigen expression vector |
| pAE1336 | pBTM117c-K03D10.3 | Y2H MYS-2 bait vector long |
| pAE1337 | pET-15b-*mys-2*$^{859-1650}$ | MYS-2 antigen expression vector |
| pAE1417 | pET-15b-*mys-2*$^{1-1650}$ | MYS-2 antigen expression vector |

| | | |
|---|---|---|
| pAE1446 | pBTM117c-K03D10.3$^{631-1653}$ | Y2H MYS-2 bait vector short |
| pAE1641 | L4440-*mys-2*$^{1-795}$ | *mys-2* RNAi A |
| pAE1642 | L4440-*mys-2*$^{859-1650}$ | *mys-2* RNAi B |
| pAE1689 | pCB-182[d] | contains GFP-*URA3*-GFP cassette |
| pAE1952 | L4440-F54D11.2 | F54D11.2 RNAi |
| pAE1954 | L4440-*dpy-27* | *dpy-27* RNAi |

[p] Plasmids were constructed during this study or taken from laboratory plasmid collection, unless stated otherwise; [a] Gift from A. Antebi; [b] Sanger Institute (Cambridge, UK);[c] Open Biosystems; [d] Gift from C.T. Beh (Hawkins et al. 2003); [e] constructed by S. Seitz

**Table 4: Oligonucleotides used in this study**

| **Oligonucleotide** | **DNA sequence 5'→3'** |
|---|---|
| Nco Promotor K03 | GCGCGCCCATGGGATCTCGTCGATCTT |
| reverse Promotor K03 | TTTGTCTGGAAATTTTTGCTGAAATCG |
| URAKO S1 | TCTTAACCCAACTGCACAGAACAAAAACCTGCAGGAAACG AAGATAAATCCGTACGCTGCAGGTCGAC |
| URAKO S2 | CTAATTTGTGAGTTTAGTATACATGCATTTACTTATAATAC AGTTTTTTAATCGATGAATTCGAGCTCG |
| URAKO A1 | GCGGAGAACTGTGAATGCGC |
| URAKO A4 | CGAAACACGGAAACCGAAGAC |
| MYSKO-1 | AACTGTTTGAACTCACCCCG |
| MYSKO-2 | AAATTTCCGGTTTTCTGGCT |
| MYSKO-6 | CGTGTGCTCGTTTCCTCGGCTCTC |
| F54-1 | GCCAACCACCTCGACAGAAG |
| F54-2 | ATGATCCGTCAGCATAGAGTCG |
| DPY27-1 | AGTTTGGAAATTGGTGCGAC |
| DPY27-2 | ATTGGAAGGGGTCGAAAGTT |
| GFP 1-1 | CTTTTCACTGGAGTTGTCCCAA |
| GFP 1-2 | CCATGCCATGTGTAATCCCAGC |
| K03D10.3 A-1 | GGCCATATGATGAGCAAACGAGAGCCG |
| K03D10.3 A-2 | GGCGGATCCCTGTCCACTTCCGTCCACTTCG |
| K03D10.3 B-1 | GGCCATATGCAGTGCTTATGCCTACTTTCC |
| K03D10.3 B-2 | GGCGGATCCGTTCAATGGCAATGAGATATGG |
| K03D10.3 Y2H-1 | GATTAGGCGTCGACGATGAGCAAACGAGAGCCG |
| K03D10.3 Y2H-2 | GATTAGGCGCGGCCGCTCAGTTCAATGGCAATGAG |
| K03D10.3 Y2H-3 | GATTAGGCGTCGACGTGTGAAAATTTGGACATTTATATGTG TG |
| pACT2 fwd | TACCACTACAATGGATG |
| pACT2 rev | CACAGTTGAAGTGAACTTGCC |
| T7 | CGTAATACGACTCACTATAG |
| K03D10.3 RNAi A-1 | GGCTCTAGAATGAGCAAACGAGAGCCG |
| K03D10.3 RNAi A-2 | GGCCTCGAGCTGTCCACTTCCGTCCACTTCG |
| K03D10.3 RNAi B-1 | GGCTCTAGACAGTGCTTATGCCTACTTTCC |
| K03D10.3 RNAi B-2 | GGCCTCGAGGTTCAATGGCAATGAGATATGG |
| MYS2-1 | CGAGAGCCGAGGAAACGAGCACACGACTCAACAAATGAG GCAGCTGCTCCCATGAGTAAAGGAGAAGAACTTTTCAC |
| MYS2-2 | GTTAATTATTGGCATTATTTGTTGTTGCGGGGGTTCACTGTC ATTTCCGCCGAATTCTTTGTATAGTTCATCCATGC |
| MYS2-3 | GGCGCTCACGAGATTCTCGCCTGGTACTATTCACCGTTTCC GCCTGACATGAGTAAAGGAGAAGAACTTTTCAC |

| | |
|---|---|
| MYS2-4 | GGTGTGTAGAGTAGGCAATATTCACACATATAAATGTCCA AATTTTCACAGAATTCTTTGTATAGTTCATCCATGC |
| MYS2-5 | CCACCATGTAGCTACGGATGCTCCCGACCATATCTCATTGC CATTGAACATGAGTAAAGGAGAAGAACTTTTCAC |
| MYS2-6 | CCATAAATTTCCATTTAAAAAAAACCGGCAAAATTTACAA ATTTTCAGAATTCTTTGTATAGTTCATCCATGC |
| MYS2-7 | GCAAACGAGAGCCGAGGAAAC |
| MYS2-8 | GTGTATAATTACGGCGACCACC |
| MYS2-9 | GCTCACGAGATTCTCGCCTGG |
| MYS2-10 | CACATCAATGTGCTGCTTGAATCG |
| MYS2-11 | CCACCATGTAGCTACGGATGC |
| MYS2-12 | CCCCGTTTCGTGGTAATCTCG |

All of the following bases and amino acids refer to the predicted gene- or protein models as proposed by Wormbase (www.wormbase.org), release WS234, 02.12.2012.

The transcriptional GFP-reporter pK03D10.3::GFP (pAE1031) was generated by amplifying a 2 kb region directly upstream of the *mys-2* ORF from the cosmid K03D10 using the oligonucleotides ncoPromotorK03 and reversePromotor. The resulting fragment was cloned into pGEM-T (Promega). The resulting vector and the plasmid L3781, which carries GFP, were digested with *Sph*I and *Pst*I and the isolated promoter insert was ligated with the digested L3781 to obtain the final vector pAE1212.

To express antigens for the generation of α-MYS-2 antibodies, two non-overlapping parts of *mys-2* were amplified from cDNA (pAE1299). For this purpose, two sets of primers were designed. A first fragment was amplified from *mys-2* cDNA using oligonucleotides K03D10.3A-1 and K03D10.3A-2. The fragment starts directly at the startcodon and has a length of 795 bp. A second fragment was amplified using oligonucleotides K03D10.3B-1 and K03D10.3B-2, starting at base 859 and ending at base 1650, immediately before the stopcodon of *mys-2*, resulting in a fragment of 792 bp length. Furthermore, the oligonucleotides contained restriction sites for *Nde*I (K03D10.3A-1 and K03D10.3B-1) and *Bam*HI (K03D10.3A-2 and K03D10.3B-2). Both fragments were adenylated prior to cloning into pGEM-Teasy (Promega). The resulting plasmids as well as the target vector pET-15b were digested with the restriction enzymes *Nde*I and *Bam*HI. The inserts were separated from pGEM-Teasy vector backbones by agarose gel electrophoresis, purified from isolated gel slices and ligated with pET-15b to give the final expression vectors. The identitiy of those final plasmids was confirmed by sequencing, and they were transformed into *E. coli* Rosetta(DE3)pLysS to allow for inducible expression of two 6xHis tagged antigens, MYS-$2^{1-265}$ (from pAE1333) and MYS-$2^{285-549}$ (from pAE1337). For control purposes, a nearly full-length fragment of *mys-2* cDNA was amplified from cDNA using oligonucleotides

K03D10.3A-1 and K03D10.3B-2. This fragment was cloned analogously to the two shorter fragments into the target vector pET-15b, allowing the expression of MYS-$2^{1-549}$ (from pAE1417), which only lacks the stop codon.

For the purpose of a yeast two-hybrid screen, two versions of a *mys-2* bait vector were constructed. The first version (pAE1336) was constructed by using oligonucleotides K03D10.3 Y2H-1 (includes a *Sal*I site) and K03D10.3 Y2H-2 (includes *Not*I site) to amplify the whole *mys-2* cDNA from start- to stop codon. After adenylation, the fragment was ligated into pGEM-Teasy. The *mys-2 Sal*I/*Not*I fragment was subsequently cloned into pBTM117c (*Sal*I/*Not*I). The second version of the bait vector (pAE1446) was constructed by using oligonucleotides K03D10.3 Y2H-3 (includes a *Sal*I site) and K03D10.3 Y2H-2 (includes *Not*I site) to amplify a fragment of the *mys-2* cDNA from base 631 to the stopcodon, a 1023 bp fragment that includes the predicted MYST domain. The following steps of cloning were performed analogously to the cloning of the full-length bait vector.

In order to downregulate *mys-2* by RNA interference, two vectors were constructed bearing either bases 1 to 795 or bases 859 to 1650 of the *mys-2* cDNA, analogous to the fragments used for antigen expression. The fragments were cloned into the vector L4440 (pAE748) that has two T7 promoter sites flanking the multiple cloning site (MCS). For this purpose, oligonucleotides K03D10.3 RNAi A-1 (includes *Xba*I site) and K03D10.3 RNAi A-2 (includes *Xho*I site) were used to amplify *mys-*$2^{1-795}$ from cDNA. After adenylation, the fragment was cloned into pGEM-Teasy. The *mys-*$2^{1-795}$ *Xba*I/*Xho*I fragment was subsequently cloned into L4440 (*Xba*I/*Xho*I). *Mys-*$2^{859-1650}$ was amplified from cDNA using oligonucleotides K03D10.3 RNAi B-1 (includes *Xba*I site) and K03D10.3 RNAi B-2 (includes *Xho*I site), cloning into the target vector L4440 was carried out analogous to cloning of *mys-*$2^{1-795}$.

To target *dpy-27* via RNA interference, oligonucleotides DPY27-1 and DPY27-2 were used to amplify a 1096 bp fragment from genomic DNA via single worm PCR (as described in 2.3.3). The fragment was adenylated and cloned into pGEM-Teasy. This vector was digested with *Not*I to cut out the insert. After separation from the backbone by agarose gel electrophoresis and purification from an isolated gel slice, the insert was cloned into L4440 (*Not*I).

To target the gene F54D11.2 via RNA interference, oligonucleotides F54-1 and F54-2 were used to amplify a 718 bp fragment from genomic DNA via single worm PCR. The fragment was adenylated and cloned into pGEM-Teasy. This vector was digested with *Not*I to cut out

the insert. After separation from the backbone by agarose gel electrophoresis and purification from an isolated gel slices, the insert was cloned into L4440 (*Not*I).

### 2.3.2. RNA Interference

RNA interference (RNAi, (Fire et al. 1998)) was performed to reduce transcript levels of the target gene by applying double-stranded RNA (dsRNA) with the sequence of the target gene to worms. This was done either by feeding worms with bacteria expressing the dsRNA, or by injection of dsRNA into worms (Fire et al. 1998; Timmons and Fire 1998).

RNAi by microinjection was carried out following a protocol previously described (Ahringer (ed.) ; Zipperlen et al. 2001). As described in 2.3.1, all DNA fragments for RNAi were cloned into L4440 that has two T7 sites flanking the insert. To obtain dsRNA, PCRs using oligonucleotide T7 were performed to amplify the desired insert from L4440. *In vitro* transcription was carried out with "TranscriptAid T7 High Yield Transcription Kit" (Fermentas) using 1 µl of unpurified PCR reaction as a template in a 20 µl transcription reaction. 1 µl of each transcription reaction was analyzed by agarose gel electrophoresis for correct size and adequate concentration of dsRNA. If necessary, dsRNA was diluted with DEPC water to adjust the concentration to 0.2-1.0 µg/µl. Without purification, dsRNA was injected to worms as described in 2.3.6. After recovery, injected worms were placed on NGM agar plates (60 mm) and incubated at either 15°C, 20°C or 25°C. Every 24 hours, injected worms were transferred to fresh plates to separate the progeny depending on their production subsequent to injection. The F1 generation was scored for phenotypes at every developmental stage.

RNAi by feeding was modified from a method previously described (Ahringer (ed.) ; Kamath et al. 2001). RNAi feeding plates (60 mm) were prepared at least 4 days before seeding with the bacterial feeding strain. For this purpose 50 µg/ml ampicillin and 1mM IPTG were added to NGM agar prior to pouring. The desired bacterial strains were grown in LB containing 50 µg/ml ampicillin and 10 µg/ml tetracycline overnight at 37°C. RNAi plates were seeded with 200 µl of the desired bacterial culture and, after drying, were incubated overnight at room temperature to induce expression of dsRNA. The next day, four L4 larvae of the desired worm strain were transferred to each plate, and the plates were then incubated at either 15°C, 20°C or 25°C. F1 progeny was scored for phenotypes. When most of the F1 progeny reached L4 stage, four L4 larvae were transferred to freshly prepared RNAi feeding plates seeded with the same bacterial strain. F2 progeny was also scored for phenotypes. RNAi feeding experiments were carried out in triplicates.

### 2.3.3. Single worm PCR

PCR on single worms (Barstead et al. 1991; Williams et al. 1992) was used to either genotype individuals of strain VC1931 at the *mys-2* locus or to test for the presence of transgenes bearing the GFP ORF. Individual worms were transferred into reaction tubes containing 2 µl single worm lysis buffer [fresh 100 µg/ml proteinase K in 10 mM Tris-HCl; 50 mM KCl; 2,5 mM $MgCl_2$; 0,45% Tween-20; 0,45% NP40; 0,01% gelatine], avoiding carryover of bacteria. Tubes were frozen for 30 min at -80°C followed by a 90 min incubation at 60°C. Proteinase K was inactivated for 15 min at 95°C. The whole lysate was used as template for a 25 µl PCR reaction of 35 cycles. The size of amplified fragments was analyzed by standard agarose gel electrophoresis.

Oligonucleotides GFP1-1 and GFP1-2 were used to amplify an 835 bp fragment of the GFP ORF. To genotype VC1931 worms at the *mys-2* locus, a duplex PCR was designed using oligonucleotides MYSKO-1, MYSKO-2 and MYSKO-6. MYSKO-1 and MYSKO-2 flank the 2168 bp deletion in *mys-2*, leading to a 1123 bp fragment on deletion alleles and a theoretical 3291 bp fragment on wild-type alleles, but the latter was not observed, most likely due to ineffectiveness of the amplification of long PCR-fragments in single worm PCR. MYSKO-6 anneals in the deleted region, giving, together with MYSKO-1, a 609 bp fragment on wild-type alleles and no fragment on deletion alleles. The combination of all three oligonucleotides in one PCR reaction allowed for a reliable test for the presence of alleles in one individual, giving only the short 609 bp fragment in wild-type worms, only the long 1123 bp fragment in worms homozygous for the deletion and both fragments in heterozygotes.

### 2.3.4. Generation and purification of *mys-2*::GFP fusions

Yeast artificial chromosomes (YACs) and cosmid clones played an essential role during the genome sequencing of *C. elegans*. Those YACs contain a large genomic region of the worm's genome (up to several hundred kilobases) and can be propagated in *S. cerevisiae*. They were initially used to generate the physical map of the genome, by closing gaps between smaller, sequenced clones for example cosmids. Furthermore, some parts of the *C. elegans* genome were sequenced from YACs directly (1998). In order to construct a precise GFP reporter, we wanted to integrate GFP into the open reading frame of *mys-2* in its genomic environment. The cosmid K03D10 contains the genomic locus of *mys-2*, therefore the gene initially obtained the generic name K03D10.3. However, the cosmid does not contain the complete operon CEOP1731 which *mys-2* is a part of. The yeast artificial chromosome Y63D3 offered the possibility of tagging *mys-2* with GFP in its genomic environment on the YAC. Most of

the YACs have never been sequenced completely but partially. The sequenced region of Y63D3 is called Y63D3A. While we know that the sequenced part is about 50 kilobases in size, we do not know the size of the complete YAC.

#### 2.3.4.1. Homologous recombination in yeast

Utilizing the site-specific recombination properties of *S. cerevisiae*, integration was carried out using yeast homologous recombination adapted from a method previously reported (Hawkins et al. 2003). The ends of the YAC Y63D3 are marked with the *S. cerevisiae* selection markers *TRP1* and *URA3*. Since subsequent selection steps required *ura3Δ* cells, *URA3* on the YAC was deleted using *kanMX* (Wach et al. 1994). Oligonucleotides URAKO S1 and URAKO S2 were used to amplify the *kanMX* cassette and to target it to *URA3*. Oligonucleotides URAKO A1 and URAKO A4 were designed to perform test PCR reactions to verify the *URA3* deletion on the YAC. Using this procedure, the strain AEY5027 was generated and used for the subsequent integration of GFP.

In a next step, the GFP-*URA3*-GFP cassette was amplified from pCB182 (pAE1689) using three different sets of oligonucleotides, depending on the desired site of GFP insertion in *mys-2*. Sets were designed to target the cassette to three different positions throughout the *mys-2* ORF, leading to in-frame-fusion of GFP between the following amino acids of the predicted MYS-2 protein: P20 and G21 via MYS2-1 and MYS2-2 (in yeast strain AEY5079); D210 and C211 via MYS2-3 and MYS2-4 (in yeast strain AEY5080); L549 and N550 via MYS2-5 and MYS2-6 (in yeast strain AEY 5081). Sites of integration were chosen under the premise to not disturb the predicted chromo and MYST domain of MYS-2. Amplified cassettes were transformed into the yeast strain carrying the YAC (AEY5027). Transformants were selected on solid medium lacking uracil, and integration of the cassette at *mys-2* on the YAC was confirmed by PCR (Table 5) with oligonucleotides flanking the respective sites.

In a second recombination event, *URA3* was looped out of the integrated cassette. For this purpose, candidates were initially streaked on complete medium to avoid selection for *URA3*, and afterwards transferred to YM containing 5-FOA to select against the presence of *URA3*. Loss of *URA3* can occur from rare recombination events between the two GFP copies flanking *URA3* (Hawkins et al. 2003). The final integrations were confirmed by PCR on genomic DNA preparations from candidate strains. A first PCR using the oligonucleotides GFP 1-1 and GFP1-2 showed the presence of the GFP sequence and confirmed the loss of *URA3*. Three further PCR reactions were performed to confirm the integration of GFP at each of the three positions. The primer pairs that were already used to test for the first recombination event, MYS2-7/MYS2-8, MYS2-9/MYS2-10 and MYS2-11/MYS2-12

encompass the integration sites. The amplicon size confirmed the loss of *URA3* by recombination at the respective sites (Table 5). In order to ensure a correct in-frame-integration of GFP, amplicons derived from the control PCR reactions were analyzed by single read sequencing (GATC Biotech AG) from both directions using the primers given in Table 5. GFP-integrations were confirmed to be in frame in the YACs from AEY5079 and AEY 5080. The amplicon from the PCR on the YAC from AEY5081 turned out to be too large, the borders between GFP and the *mys-2* ORF were not properly sequenced. Since all integrations were carried out analogous, we assumed the integration in AEY5081 to be correct.

**Table 5: Overview of amplicon sizes of control PCR reactions at the sites of GFP integration in the *mys-2* ORF.**

| Primer pair | Size of amplicon at respective integration site | | |
|---|---|---|---|
| | unmodified | integrated GFP-*URA3*-GFP cassette | integrated GFP |
| MYS2-7/MYS2-8 | 295 bp | 2.7 kb | 1015 bp |
| MYS2-9/MYS2-10 | 128 bp | 2.5 kb | 848 bp |
| MYS2-11/MYS2-12 | 1284 bp | 3.7 kb | 2004 bp |

### 2.3.4.2. Preparation of yeast artificial chromosome DNA

Prior to microinjection of the three different GFP-tagged YACs, they had to be separated from the endogenous yeast chromosomes. Following a method previously described (Peterson 2007), high-mass DNA plugs were prepared from the respective yeast strains. Pellets of overnight cultures in YPD were resuspended in solution 1 [1 M sorbitol; 20 mM EDTA, pH 8.0; 14 mM ß-mercaptoethanol; 2 mg/ml zymolyase-20T] at 8 x $10^9$ cells/ml and afterwards mixed with an equal volume of solution 2 [like solution 1 with additional 2% Sea Plaque GTG low melting point agarose] at 50°C. The mixture was poured into ice-chilled plug molds. Solid plugs were treated with 8 ml solution 3 [like solution 1 with additional 10 mM Tris] per ml of plugs for 2 h at 37°C with gentle rocking to digest yeast cell walls. To solubilise cell membranes and to denature proteins, plugs were incubated at 37°C for 1 h with LDS [1% lithium dodecyl sulphate; 100 mM EDTA, pH 8.0; 10 mM Tris, pH 8.0], and 2 times for 2 h at room temperature with 0.2x NDS [1x NDS: 0.5 M EDTA; 10 mM Tris, pH 7.5; 1% *N*-laurylsarcosine, pH 9.0]. Plugs were washed twice with TE (pH 8.0) and finally stored in fresh TE (pH 8.0) until needed.

Since large DNA fragments cannot be separated by conventional agarose gel electrophoresis, pulsed field gel electrophoresis (PFGE) using a contour-clamped homogeneous electric field (CHEF) was performed to separate the yeast chromosomes. A CHEF Mapper XA System (Bio-Rad), located at the Institute of Medical Radiation Biology at the Universitätsklinikum in Essen was used with the kind permission of Prof. Dr. George Iliakis. With the assistance of Dr. Mario Moscariello, the system was set up following the manufacturers instructions. 1 % agarose MP (multipurpose agarose; Roche) gels in 0.5x TBE were loaded with the desired plugs and wells were sealed with 1% agarose MP in 0.5x TBE. Gel runs were performed using the systems "auto algorithm" mode, which determines optimal conditions for the given range of molecular weight. Using the values 120 kb for "molecular weight: low" and 300 kb for "molecular weight: high" led to the following parameters defined automatically by the system: Int. Sw. Tm. = 14.84 s; Fin. Sw. Tm. = 26.29 s; included angle = 120°; Run Time = 31.5 h.

YACs were identified by southern blotting using standard methods (Sambrook et al. 1989). A GFP fragment was amplified from L3781 (pAE1031) using oligonucleotides GFP-1 and GFP-2. The probe was labelled with [α-$^{32}$P]dCTP by Dr. Mario Moscariello, using the "rediprimeII DNA labelling system" (Amersham).

For preparative PFGE gels, the comb was taped to give a single, large well for yeast plugs and two single wells at the edges for the yeast chromosome marker (NEB). After the gel run, the outer lanes containing the marker were cut off and stained with ethidiumbromide. Bands were visualized on an UV-table and the desired position marked with a scalpel. The whole gel was reassembled and the YAC containing region of the unstained part was cut out following the marked positions of the outer lanes. For concentration purposes, the gel slice was integrated at a 90° angle into a standard mini-gel of 4% Nusieve GTG agarose in 0.5x TBE. The gel was run at 40 V for 144 h. A gel slice of approximately 0.5 cm x 0.5 cm immediately below the integrated large gel slice was excised. Agarose was melted at 68°C for 10 min and the equilibrated for 5 min at 42.5°C. 2 U of ß-agarase I were added and incubated overnight. The solution was refrigerated, and complete digestion was confirmed when no clumps of agarose were present. The solution was stored at 4°C until needed. Identity of each of the YACs was confirmed with PCR analysis as described in 2.3.4.

### 2.3.5. Yeast Two-Hybrid Screen

In order to find possible interaction partners of MYS-2 *in vivo*, a yeast two-hybrid screen was performed (Gyuris et al. 1993). The method was carried out following the manual of Hybrid Hunter (Invitrogen). The yeast two-hybrid system is based on the activation of reporter genes

upon recruitment of the Gal4 activation domain to the respective operator sequence. The bait vector (pAE1336/pAE1446, construction described in 2.3.1) expressed a fusion of MYS-2 to the LexA binding domain. As prey, the pACT2.2 C. elegans yeast 2-hybrid library (Addgene) was used. Each preyvector expressed a fusion of the Gal4 activation domain to a *C. elegans* protein. Through interaction of the MYS-2 bait with one of the prey fusions, the Gal4 activation domain was recruited to the LexA operator in AEY4217, leading to expression of the reporter genes.

To amplify the cDNA library, three portions of *E. coli* DH5α were transformed with 1 µg cDNA library each. Each transformation was streaked on ten LB agar plates containing ampicillin. Transformants were washed off the plates, pooled and stored in aliquots at -80°C. Those aliquots were used to start cultures, from which the cDNA library was purified using the Qiagen Plasmid Maxi Kit.

The yeast strain AEY4217 was transformed with the *mys-2* containing bait plasmids pAE1336 or pAE1446, in order to create the bait strains AEY4218 and AEY4460, respectively. Proper expression of the LexA-MYS-2 fusion in AEY4460 was verified by immunoblots probed with an α-LexA antibody (Millipore), as positive controls for this blot pAE436, pAE451, pAE454 and pAE458 were transformed into AEY4217, while the untransformed strain served as a negative control. Autoactivation of the *HIS3* reporter gene by the bait plasmids was tested on medium lacking histidine.

2 ml of competent yeast cell suspension (80 OD) were transformed with 100 µg of the cDNA library, 100 µl each were then streaked on 20 agar plates with media lacking leucine and histidine to select for the presence of a pACT2.2 prey plasmid and for reporter gene activation. Another 100 µl was streaked on medium lacking only leucine but containing histidine, in order to determine transformation efficiency and estimate the number of screened transformants. Transformations were repeated until the desired number of transformants had been screened. $His^+$ colonies were saved and tested for LacZ activation, the second reporter gene, by performing a ß-galactosidase filter assay (Breeden and Nasmyth 1985). Colonies passing this test were considered primary candidates for further testing.

Primary candidates were streaked on full media and then transferred to media containing 60 µg/ml canavanine. Canavanine is a toxic arginine analogue. The *CAN1* gene encodes the yeast arginine permease. While the endogenous gene was mutated in AEY4217, a *CAN1* copy was on the backbone of the mys-2 containing bait vector pBTM117c. Therefore, only cells that had lost the bait vector were able to grow on canavanine. Plasmid loss was verified on media lacking tryptophan, where cells should not be able to grow without *TRP1*, which is also

present on pBTM117c. On media lacking histidine, candidates were tested for whether they are able to activate the *HIS3* reporter from the prey plasmid alone. Primary candidates that failed to grow in both tests were then considered secondary candidates.

In order to amplify the cDNA from the respective prey plasmids, colony PCR reactions were performed using the oligonucleotides pACT2 fwd and pACT2 rev. PCR reactions were analyzed by standard agarose gel electrophoresis for the presence of an amplified fragment, fragments were isolated from excised gel slices, subsequently ligated to pGEM-Teasy and transformed into *E. coli* DH5α. The plasmids from positive clones were isolated with Qiagen Plasmid Mini Kit. In order to identify each cDNA, the clones were sequenced using the T7 primer (GATC Biotech AG). The *C. elegans* genome was queried with the obtained sequences using BLASTn at NCBI (via a tool of ApE – A plasmid Editor).

### 2.3.6. Microinjection

Microinjection (Evans (ed.) ; Mello et al. 1991; Mello and Fire 1995) was used to either transform adult hermaphrodites with transgenes or to induce RNA interference by injecting dsRNA. Prior to injection, agarose pads and injection needles were prepared. 2% agarose in water was boiled and a drop of 100 µl was placed on a 22x50 mm glass coverslip (Menzel-Gläser), a second coverslip was put on top and slightly tapped to give a flat pad. After agarose solidification, the coverslips were separated and baked at 170°C for 3 h. Pads were stored until needed. Injection needles were pulled using borosilicate glass capillaries (1.0 mm O.D. x 0.78 mm I.D. (Harvard Apparatus)) in a P-97 needle puller (Sutter Instruments). The pulling program was adjusted frequently according to changing characteristics of the heating filament, an example is given below:

| | |
|---|---|
| Heat | 310 |
| Pull | 90 |
| Velocity | 90 |
| Time | 120 |

This program was used with a "Ramp test value" of 277 and gave needles of the desired properties with a closed tip. Microinjection needles were stored until needed. For injection, an inverted microscope IX51 (Olympus) was equipped with a gliding stage (IX2-GS), a standard 4x Objective (Plan C N, 4x/0.10), a 40x Nomarski oil-immersion objective (UPlanApo, 40x/1.00 Oil Iris, BFP1 C2) and a MN-151 micromanipulator (Narishige). Injection mixes were prepared prior to injection. The vector pRF4 was used as a co-injection marker in DNA injection mixes, since it carries the dominant *rol-6(su1006)* allele, inducing the easily detectable Roller phenotype. The transcriptional GFP-reporter pAE1212 and pRF4 were

injected at 100 ng/µl, the YACs were injected at concentrations from 8 to 20 ng/µl. RNA was injected at concentrations between 0.2 and 1.0 µg/µl. If necessary, injection mixes were diluted with water. Injection needles were loaded from the back with 2 µl of either DNA injection mix or dsRNA and fastened in the needle holder attached to the micromanipulator. Up to ten well-fed adult hermaphrodites were transferred into a 5 µl drop of halocarbon oil 700 (Sigma) on an agarose pad. Using an eyebrow, worms were positioned and gently pressed onto the pad until fixed properly. Slides were taped onto the middle of the gliding stage. Using the 4x objective, worms were brought into the centre of the visual field and the tip of the needle was positioned in close proximity to the worms. Using the 40x objective, the agarose surface was brought into focus, and the needle tip was positioned next to a piece of debris or similar. By moving this object against the tip, it was broken, and proper flow of solution was confirmed by applying air-pressure with a 60 ml syringe attached to the end of the needle holder. Afterwards, gonads of worms were brought into focus, and the tip of the needle was positioned at an angle of approximately 30°C relative to the worm's dorsal side. By sliding the table, needles were inserted into the gonad and the solution injected. If possible, both arms of the gonad were injected. Instantly after injecting a group of worms, 5 µl M9 buffer were applied to relieve and rehydrate the animals. When worms started swimming, after about 10 min, they were transferred to fresh agar plates seeded with the OP50 feeder strain.

Groups of three injected worms were transferred to 94 mm agar plates, when DNA was injected. Animals of the F1 generation, which showed the Roller phenotype, were transferred to individual plates and allowed to lay eggs. The F2 generation was analyzed for the expression of GFP using a fluorescence microscope. Furthermore, F1 mothers were analyzed with single worm PCR for the presence of GFP sequence (described in 2.3.3) after they laid down eggs.

If dsRNA was injected in order to induce RNA interference, animals were treated as described in 2.3.2 after injection.

## 2.4. Biochemical methods

### 2.4.1. SDS-PAGE and Immunoblotting

Protein samples were separated on 8, 10 or 12 % SDS gels according to standard techniques (Laemmli 1970). Proteins were transferred to nitrocellulose membranes (Amersham Hybond ECL, GE Healthcare) in transfer buffer [39 mM glycine, 48 mM Tris base, 0.037 % SDS, 20 % methanol (Sambrook et al. 1989)] using a BIO-RAD Tank Transfer System with either

constant voltage at 95V for 90 min or constant current at 30 mA overnight. Membranes were then blocked for one hour at room temperature with 3 % non-fat dry milk in TBST (NFDM). Incubation with primary antibody was carried out overnight at 4°C with gentle agitation. After three 5 min washes with TBST, membranes were incubated with secondary antibody in NFDM for two to four hours at room temperature with gentle agitation. After five 5 min washes with TBST, signals were detected using Amersham ECL Western Blotting Analysis System (GE Healthcare) and Amersham Hyperfilm ECL chemiluminiscence films (GE Healthcare)

### 2.4.2. Generation of α-MYS-2 antibodies

In order to generate antigens for the subsequent immunization, MYS-$2^{1-265}$ (from pAE1333) and MYS-$2^{285-549}$ (from pAE1337) were expressed in *E. coli* Rosetta(DE3)pLysS.

In a first step, the expression and the solubility of both MYS-2 fragments was determined, the empty pET-15b vector served as a negative control. 20 ml of LB media were inoculated with 1 ml of the respective overnight culture and shaken at 37°C. As soon as the $OD_{600}$ was between 0.5 and 0.7 (after approximately 2 h), the expression was induced by adding 1 mM IPTG. 1 ml aliquots of the cultures were removed immediately before induction and one, three and five hours after induction. The cells of the obtained aliquots were pelleted and resuspended in lysis buffer [50 mM $NaH_2PO_4$; 300 mM NaCl; 10 mM imidazol; pH 6.3] at 0.01 OD per µl. 1 mg/ml lysozyme was added and the solution incubated on ice for 30 min. The solutions were sonicated in a Bioruptor (Diagenode) set to "high" for 6 cycles of 10 s with 10 s pauses in between. The lysates were centrifuged at 10000 x g at 4°C for 20 min. The supernatants, representing the soluble fraction, were saved for later analysis. The pellets were resuspended in a volume of 1 x Laemmli corresponding to the volume of lysis buffer. The pellets represent the insoluble fraction. All fractions were analyzed by SDS-PAGE and in western blots using an α-6xHis antibody.

Both of the expressed 6xHis-tagged MYS-2 fragments were found to be insoluble. The amount of expressed protein peaked after 5 h of induction, and the expression of MYS-$2^{1-265}$ (from pAE1333) was stronger than the expression of MYS-$2^{285-549}$ (from pAE1337). The purification was therefore carried out following "Protocol 10. Preparation of cleared *E. coli* lysates under denaturing conditions" followed by "Protocol 17. Batch purification of 6xHis-tagged proteins from *E. coli* under denaturing conditions" of the fifth edition of "The Qia*expressionist*" (Qiagen, June 2003) with modifications. The cells of 1 litre culture were pelleted after 5 h of IPTG induction and resuspended in 30 ml lysis buffer [500 mM NaCl; 20 mM imidazol]. After addition of 1 mg/ml lysozym the solution was frozen overnight at -20°C.

The lysate was subsequently thawed and centrifuged at 10000 x g at 4°C for 30 min. The supernatant (soluble proteins) was removed and the pellet resuspended in 30 ml of buffer B [100 mM $NaH_2PO_4$; 10 mM Tris-HCl; 8 M urea; pH 8.0]. After overnight stirring at 4°C, cellular debris was removed by centrifugation for 30 min at 10000 x g. 1 ml of the 50 % Ni-NTA slurry (Qiagen; previously equilibrated with buffer B) was added to 4 ml of the lysate and gently shaken at room temperature for 60 min. The lysate-resin mixture was loaded into an empty column (10 ml PolyPrep; Bio-Rad), and after flow-through was complete, the resin was washed twice with 4 ml buffer C [100 mM $NaH_2PO_4$; 10 mM Tris-HCl; 8 M urea; pH 6.3]. Elution was carried out by adding 0.5 ml of buffer E [100 mM $NaH_2PO_4$; 10 mM Tris-HCl; 8 M urea; pH 4.5] four times, producing fractions E1 to E4. All fractions were saved for later analysis by SDS-PAGE and immunoblotting. Fractions E2, E3 and E4 of the MYS-$2^{1-265}$ purification showed the highest yield of the antigen, they were pooled and used to immunize animals. Purification of MYS-$2^{285-549}$ was not successful, the obtained amount was insufficient for immunization.

Immunization was carried out by Pineda Antibody Services (Berlin), animals for immunization were chosen by testing their pre-immunesera in immunoblots of worm protein lysates. Two rabbits and two guinea pigs were chosen that gave the lowest signals in pre-immuneserum especially of proteins around 64 kDa, the calculated size of MYS-2. After 120 days of immunization, the four sera were obtained, from now on called K1 (rabbit 1), K2 (rabbit 2), M1 (guinea pig 1) and M2 (guinea pig 2).

### 2.4.3. Affinity purification of α-MYS-2 antibodies

In order to improve specificity of the antibodies, they were affinity purified using nitrocellulose membranes (Duerr ; Smith and Fisher 1984; Duerr et al. 1999). 400 µl proteinlysates, correlating to 4 OD, of *E. coli* expressing the MYS-$2^{1-265}$ antigen were separated by SDS-PAGE using one large well and then blotted onto a nitrocellulose membrane. The prominent MYS-$2^{1-265}$ antigen band was visualized by staining the membrane with Ponceau S (Sigma). The MYS-$2^{1-265}$ containing membrane was cut out with a scalpel on a clean glass plate and placed in a 94 mm petri dish (Greiner). Membrane and petri dish were blocked by adding 10 ml NFDM [TBST with 3% non-fat dry milk] and shaking at room temperature for 1 h. After rinsing three times with TBST [50 mM Tris; 150 mM NaCl; 0.05% Tween-20; pH 8.0] and once with water, 10 ml glycine buffer [5 mM glycine; 0.01% BSA; 0.05% Tween-20; 500 mM NaCl; pH 2.3] was added and the dish swirled for exactly 60 s. After rinsing again three times with TBST and once with water, 10 ml NFDM was added and the dish shaken for 30 min at room temperature. After dish and membrane were rinsed twice

with TBST, 10 ml TBST and 0.5 ml of the respective serum were added and the dish shaken for 60 min at room temperature. Dish and membrane were then rinsed six times for 5 min each with TBST. In the meantime, a 15 ml Falcon tube was prepared with 150 µl 1 M Tris pH 8.2. After the sixth TBST rinse followed by a brief rinse with water, 5 ml glycine buffer were added to the dish and swirled for exactly 20 s, in order to release the antibody from the MYS-2 antigen on the membrane. The glycine buffer was removed and added to the 150 µl 1 M Tris pH 8.2 in the prepared 15 ml Falcon tube. Immediately, another 5 ml glycine buffer were added to the dish and swirled for exactly 20 s. Glycine buffer was removed and pooled with the first 5 ml. The membrane was quickly rinsed three times with TBST and then covered with NFDM. The covered membrane was stored in the dish at -20°C for later reuse. The pH of the eluate was checked with pH strips and adjusted to 7.5 if necessary by adding 1 M Tris pH 8.2. Eluates were then stored at 4°C until further use.

### 2.4.4. Immunoprecipitation of MYS-2

In order to identify proteins that interact with MYS-2, a strategy was applied that has successfully been used in *C. elegans* before (Moresco et al. 2010). We sought to immunoprecipitate MYS-2 with the α-MYS-2 antibodies K1 and K2. The antibodies were crosslinked to protein A-Sepharose beads, in order to to minimize their signals in western blots and coomassie stained SDS gels. Bands in the coomassie stained gels of the immunoprecipitation were excised and analysed by mass spectrometry.

#### 2.4.4.1. Crosslinking of antibodies to Protein A-Sepharose beads

The rabbit α-MYS-2 antibodies K1 and K2 and their corresponding preimmunesera K1p and K2p were crosslinked to protein A-Sepharose beads prior to immunoprecipitation following a protocol from www.abcam.com, “Procedure for crosslinking the antibody to the beads”. Without that step, the antibodies were eluted from the beads together with precipitated protein in the final step of immunoprecipitation. This masked the signals in western blot analysis of the IP. If not stated otherwise, all of the following centrifugation steps were peformed in a microcentrifuge for 2 min at 510 x g, and all washing steps include rotation at the given temperature and end with a centrifugation to separate beads and supernatant. Protein A-Sepharose beads (Sigma, P9424) were shortly washed twice with PBS to give a 50% slurry, and the slurry was rotated overnight at 4°C. The next day, beads were centrifuged, and the supernatant was removed. One volume of dilution buffer [1 mg/ml BSA in PBS] was added to the beads, and they were rotated for ten minutes at 4°C and subsequently centrifuged. To ensure saturation with antibodies, antibody sera and preimmune sera were added to the beads

in excess. For qualitative purposes, 100 µl serum of K1 or K2 were added to 100 µl of beads. For quantitative purposes, 500 µl of each serum was added to 500 µl of beads. For control purposes the same amounts of preimmunesera K1p and K2p were used. Beads and sera were rotated at 4°C for 2 hours and then centrifuged. After centrifugation, the supernatant was removed, and the beads were washed with one volume of dilution buffer for 5 min, followed by a short wash with PBS. Dimethyl pimelimidate (DMP, Sigma) solution was prepared freshly by dissolving 13 mg/ml in water and mixing it with wash buffer [0.2 triethanolamine in PBS] in a 1:1 ratio. The pH of the solution was verified to be between 8 and 9. One volume of DMP solution was added to the beads, and the beads were rotated for 30 min at room temperature. After centrifugation and removal of the supernatant, the beads were washed with wash buffer for 5 min at room temperature. The 30 min incubation with fresh DMP solution was repeated twice, for a total of three incubations, followed by washing each time. In order to quench residual DMP, one volume of quenching buffer [50 mM ethanolamine in PBS] was added to the beads, and they were rotated for 5 min at room temperature. After centrifugation and removal of the supernatant, the procedure was repeated once, followed by a short wash with PBS. To remove unlinked antibody, 1 M glycine at pH 3 was added and rotated for 10 min at room temperature. After centrifugation and removal of the supernatant, the procedure was repeated once. Thereafter, the beads were washed three times for 5 min at room temperature with homogenization buffer [50 mM HEPES-KOH pH 7.6; 1 mM EDTA; 140 mM KCl; 0.5 % NP-40; 10 % glycerol; one tablet protease inhibitor cocktail (Roche complete) was added to every 25 ml of buffer directly before use, as well as 1 mM DTT]. Beads could be stored in the final wash for a few days, but were usually used immediately for immunoprecipitation.

#### 2.4.4.2. Immunoprecipitation

Immunoprecipitation (IP) was performed as previously described (Shaham (ed.)). Frozen worm pellets, harvested from liquid cultures of mostly adult hermaphrodites, were thawed on ice and resuspended in homogenization buffer at 1 ml per gram worms. 10 ml of resuspended worms were homogenized in 50 ml tubes on ice in a Bioruptor (Diagenode) set to “high” for 20 cycles of 30 s with pauses of 1 min in between for cooling. Cellular debris was removed by centrifugation in a SS-34 rotor for 20 min at 5000 x g and 4°C, and the supernatant was transferred to a clean 50 ml tube. Sonication was repeated, followed by a centrifugation in a SS-34 rotor for 20 min at 25000 x g and 4°C. Protein concentration of the supernatant was determined with a Bradford assay, and aliquots of 1 ml were quick-frozen in liquid nitrogen and stored at -80°C.

For immunoprecipitation, protein lysates were thawed on ice, and 100 µl of protein A-Sepharose beads were added per ml lysate. After rotation for two hours at 4°C, the beads were spun down for 2 min at 510 x g, and the supernatant was used for immunoprecipitation. 1 ml of precleared lysate (18 mg total protein) was added to 100 µl (qualitative IP) or 500 µl (quantitative IP) of beads crosslinked with antibodies, and rotated overnight at 4°C. The antibody-antigen complexes captured on protein A-Sepharose beads were spun down for 2 min at 500 x g. The supernatant was removed and saved for later analysis, the beads were washed four times with ChIP buffer [50 mM HEPES-KOH pH 7.6; 1 mM EDTA; 140 mM KCl; 0.05 % NP-40; one tablet protease inhibitor cocktail (Roche complete) was added to every 25 ml of buffer directly before use, as well as 1 mM DTT] for 5 min at 4°C. Supernatants from washing steps were saved for later analysis. To elute the captured proteins, 2 volumes of 0.5 M glycine at pH 2 were added to the beads, and the solution was rotated for 10 min at 4°C. After centrifugation for 2 min at 500 x g, the supernatant was removed and saved for later analysis. A second round of elution was done by adding 2 volumes of 1 M glycine pH 2 to the beads. After rotation for 10 min at 4°C and a centrifugation at 500 x g for 2 min, the supernatant was saved for later analysis.

#### 2.4.4.3. Analysis of immunoprecipitation

To control the precipitation of MYS-2, wash fractions and eluates were analyzed by immunoblots that were probed the guinea pig α-MYS-2 serum M1. In order to identify interaction partners that possibly co-immunoprecipitate with MYS-2, both eluates of each IP were pooled, concentrated by precipitation with trichloroacetic acid (TCA) and analyzed by SDS-PAGE. For this purpose, one volume of TCA was added to 4 volumes of the samples, and the solutions were incubated on ice for 30 min. After centrifugation for 5 min at 14000 rpm at 4°C in a microcentrifuge, the supernatant was removed. Pellets were washed two times by adding 200 µl of cold acetone and centrifuged again. Residual acetone was removed by placing the tubes in a 95°C heat block for 5-10 min. Dried pellets were resuspended in 2x Laemmli which turned yellow, due to the low pH. 1 M Tris pH 9.5 was titrated to the solution until it turned blue.

Signals unique to eluates from IPs with K1 and K2 were cut out from the SDS gel for subsequent protein identification by mass spectrometry (MS/MS). Mass spectrometry was carried out by ChromaTec GmbH (Greifswald).

## 2.5. Cytological methods

### 2.5.1. Immunostaining of embryos

The method described here was learned under the kind supervision of Prof. Ralf Schnabel (TU Braunschweig) and is modified from his lab protocol. Ten 94 mm NGM plates with well-fed adult hermaphrodites were washed off with M9 buffer. Worms were bleached as previously described to obtain embryos. Worms and embryos were cooled on ice during the procedure to arrest development. A small drop containing several hundred embryos was transferred to a commercial polylysine-coated slide (Menzel-Gläser) and covered with a 50x22 mm coverslip overlapping on one edge. The slide was placed on a metal plate cooled by a block of dry ice and incubated there for at least 10 min. The coverslip was removed by swiftly hitting it with a finger on the overlapping edge. Slides were then incubated in methanol at -20°C for at least 5 min, followed by an incubation in acetone at -20°C for at least 5 min. Slides were transferred to TBST and incubated for 10 min at room temperature. Slides were removed from TBST, and excessive liquid was removed using a water-jet vacuum pump. The spot containing the embryos was covered with 20 µl suspension of the primary antibody. Affinity purified antibodies were used without dilution, non-purified sera as well as preimmunesera were diluted 1:200 in TBST. Slides were incubated in a humid chamber overnight at 4°C. Slides were subsequently rinsed once with TBST and then incubated in fresh TBST for 10 min at room temperature. Slides were removed from TBST, and excessive liquid was removed. The spot containing the embryos was covered with 20 µl suspension of the secondary antibody. Secondary antibodies were diluted 1:250 with TBST. Slides were incubated for 2-4 h at room temperature, followed by a rinse with TBST and a 10 min incubation with fresh TBST. Slides were now ready for mounting. Excessive liquid was removed, and 20 µl mounting medium [for 10 ml: 200 mg n-Propyl gallate; 0.3 ml 1 M Tris. pH 9.0; 2.7 ml dd$H_2O$; 7 ml glycerol; 8 µl DAPI (2.5 mg/ml in dd$H_2O$)] were spread in several drops around the area containing the embryos. A 50x22 mm coverslip was gently lowered on the slide starting at the frosted edge of the slide and avoiding air bubbles. Excessive liquid was removed from the edges with the water-jet vacuum pump without moving the coverslip. Slide and coverslip were sealed using commercial, transparent nail polish. Slides were now ready to be observed under a fluorescence microscope.

### 2.5.2. Immunostaining of dissected hermaphrodite gonads

Dissecting gonads of adult hermaphrodites prior to immunostaining allows for a better staining of the germline and early embryos. The method described here was modified from

several previously described methods (Duerr ; Shaham (ed.) ; Crittenden et al. 1994; Wu et al. 2012b). 4% paraformaldehyde solution was prepared as follows. 2.0 g reagent grade paraformaldehyde (Fluka) was added to 25 ml dd$H_2O$ and 50 µl of 1 M NaOH. The solution was heated to 60°C, and when it became clear after approximately 15 min, it was cooled on ice. 25 ml of buffer containing 0.2 g $KH_2PO_4$ and 0.94 g $Na_2HPO_4$ was adjusted to pH 7.2 and mixed with 25 ml of the paraformaldehyde solution. It was aliquoted immediately and stored at -20°C until needed.

Ten adult hermaphrodites were transferred into a 5 µl drop of 0.2 mM levamisole (anthelminthic) in dd$H_2O$ on a polylysine-coated slide (Menzel-Gläser). Using two 27 gauge needles like a scissor, the worms were cut either between the pharynx and the gonad, between the tail and the gonad or at the vulva to release the gonad. A second drop of 5 µl freshly thawed 4% paraformaldehyde solution was carefully mixed with the first drop. A 50x22 mm coverslip was applied, overlapping on one edge. Slides were incubated in a humid chamber at room temperature for 30 min. The slide was put on a metal plate cooled by a block of dry ice or liquid nitrogen and incubated there for at least 10 min. The coverslip was removed by swiftly hitting it with a finger on the overlapping edge. After freeze-crack, the slides were incubated in methanol at -20°C for 120 min followed by a 15 min incubation in acetone at -20°C. From this point on, immunostaining was carried out as described in 2.5.1.

# 3. Results

## 3.1. Analysis of *mys-2* cDNA

In the course of this study, we obtained a cDNA clone containing *mys-2* from the *C. elegans* ORF collection (Open Biosystems), which was subjected to sequence analysis in order to confirm its identity and to compare it to the predicted *mys-2* gene model (Wormbase, WS234). An alignment of the sequencing result with the *mys-2* coding sequence revealed that our clone lacked 51 bases (Figure 8). Specifically, bases 801 to 851 (counting from the ATG) are absent in the cDNA, which results in the absence of a predicted *Hind*III restriction site (bases 796 to 801).

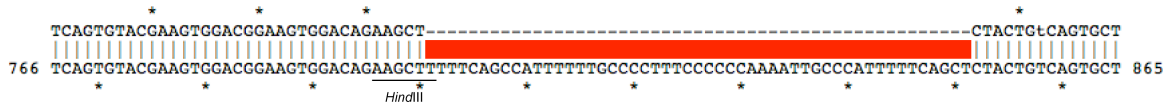


**Figure 8: Sequence analysis of cDNA clone revealed 51 base deletion;** Alignment of the sequencing result (top) with the predicted *mys-2* coding sequence (bottom) from base 766 to 865 (counting from ATG); Asterisks indicate decades; *Hind*III restriction site as indicated

This deletion results in a change in the predicted protein model. In particular, the residues F268 to L284 are removed and the codon for L267 changes from CTC to CTT.

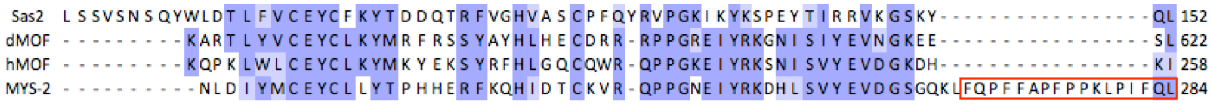


**Figure 9: Alternative MYS-2 amino acid sequence aligned better within the MYST domain to homologue MYST HATs Sas2, dMOF and hMOF;** the alternative MYS-2 sequence (bottom) lacks a stretch of 17 amino acids (red square) that was unique to MYS-2, resulting in higher identity within the MYST domain; Blue boxes indicate identities; Numbers on the right indicate the last shown amino acid residue; Alignment was performed using ProbCons (Do et al. 2005)

This deletion in the amino acid sequence affects the predicted MYST domain of MYS-2 and removes a stretch of 17 amino acids, resulting in a higher identity with the MYS-2 homologs Sas2, dMOF and hMOF (Figure 9). In order to prevent confusion, bases and amino acid numbering according to Wormbase (WS234) were retained in this study.

## 3.2. Generation of α-MYS-2 antibodies

In order to be able to determine the localization of MYS-2 as well as for further biochemical studies, antibodies were raised against MYS-2. For this purpose, recombinant 6xHis-tagged MYS-2(1-265) was purified from *E. coli* and used to immunize two rabbits and two guinea

pigs. The immunesera were subsequently assessed for their ability to detect recombinant MYS-2.

In a first test, protein lysates from *E. coli* expressing MYS-2(1-265), a second, non-overlapping MYS-2(285-549) fragment or full length MYS-2(1-549) were immunoblotted and probed with the four α-MYS-2 antisera.

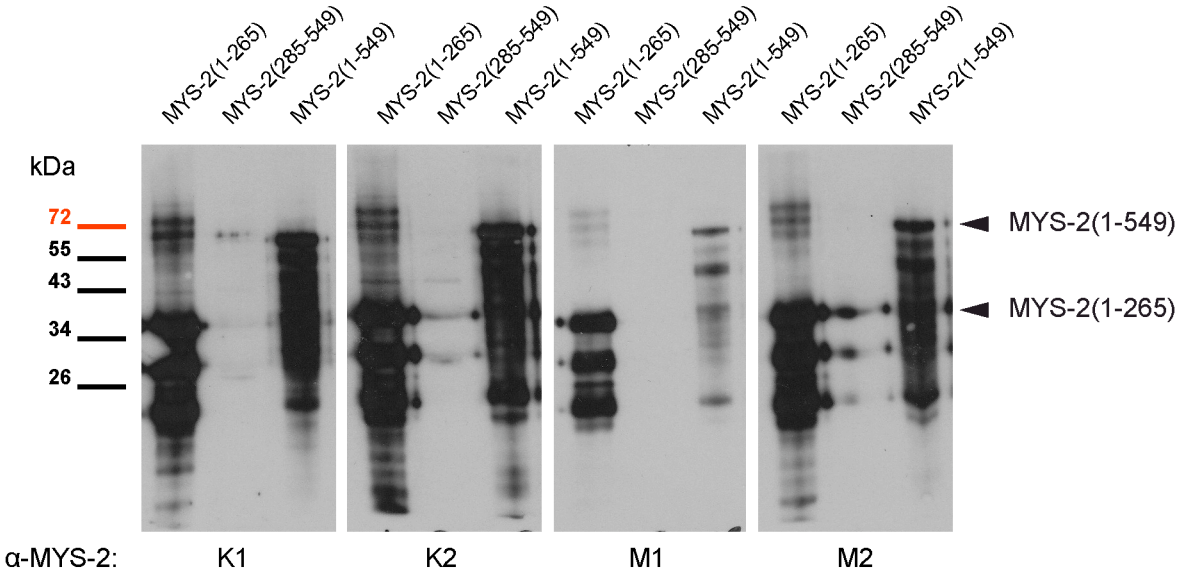


**Figure 10: Generated antibodies detected recombinant MYS-2;** Western blots of protein lysates from *E. coli* expressing the indicated MYS-2 fragment (top) probed with α-MYS-2 antisera (1:2000) from two rabbits (K1, K2) and two guinea pigs (M1, M2) as indicated (bottom); Signals of MYS-2 fragments are indicated on the right

The calculated molecular weight of MYS-2(1-265) and MYS-2(285-549) is 31.7 kDa and 31.4 kDa, respectively. The calculated molecular weight of MYS-2(1-549) is 62.6 kDa, this reflects the possible change in MYS-2 sequence (section 3.1). For an antibody specific for MYS-2(1-265), a signal in immunoblots from *E. coli* expressing MYS-2(1-265) and MYS-2(1-549) was expected, whereas no signal should be present with MYS-2(285-549). As shown in Figure 10, all four antisera detected both MYS-2(1-265) and MYS-2(1-549), but not MYS-2(285-549). There was substantial protein degradation in the *E. coli* extracts as illustrated by the detection of multiple bands of lower molecular weight by all four α-MYS-2 antisera. Altogether this showed that the four antisera were able to detect recombinant MYS-2.

We next assessed the ability of the α-MYS-2 antisera to detect MYS-2 in worm extracts. For this purpose, protein lysates from mixed culture wild-type worms were probed with the antisera using western blotting. The expected molecular weight of MYS-2 is 62 kDa.

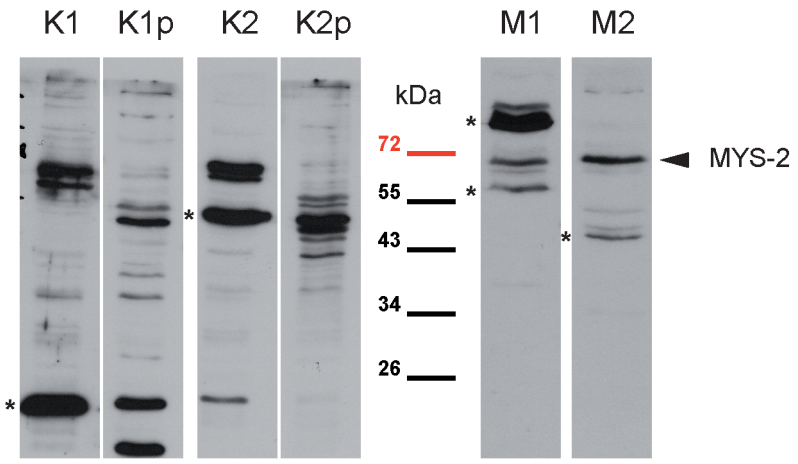


**Figure 11: α-MYS-2 antisera detected MYS-2 in wild-type worms extracts;** Western blots of wild-type worm extracts probed with α-MYS-2 antisera (K1, K2, M1, M2; 1:2000) and respective preimmune sera from the two rabbits (K1p, K2p; 1:500) as indicated on top; specific MYS-2 signal (arrowhead) and unspecific signals (*) are indicated

All four antisera showed a prominent signal at the expected size that was not present in immunoblots with the respective preimmune sera, as shown for the two rabbit preimmune sera (Figure 11). The signals from rabbit immune sera were stronger than those of the guinea pig antisera. However, with each of the antibodies, several additional signals were detected in the worm lysates, indicating that each of them detected some other protein(s).

### 3.2.1. Affinity purification of α-MYS-2 antibodies

In order to minimize unspecific signals, we subjected the antibodies to affinity purification, and they subsequently were tested in immunoblots on wild-type protein lysates. Figure 12 shows a comparison of the antibodies before and after affinity purification, which showed that each of the antibodies gave rise to a single band or two bands of similar molecular weight after affinity purification. As before, the signals of the rabbit antibodies (K1, K2) were stronger than those of the guinea pig antibodies (M1, M2), even though the identical antibody dilutions were used. The rabbit antibodies also showed a band of slightly higher mobility that may constitute a degradation product or an alternative form of MYS-2. Further testing of antibody specificity was carried out in immunostainings of worms deleted for *mys-2* (section 3.6.3).

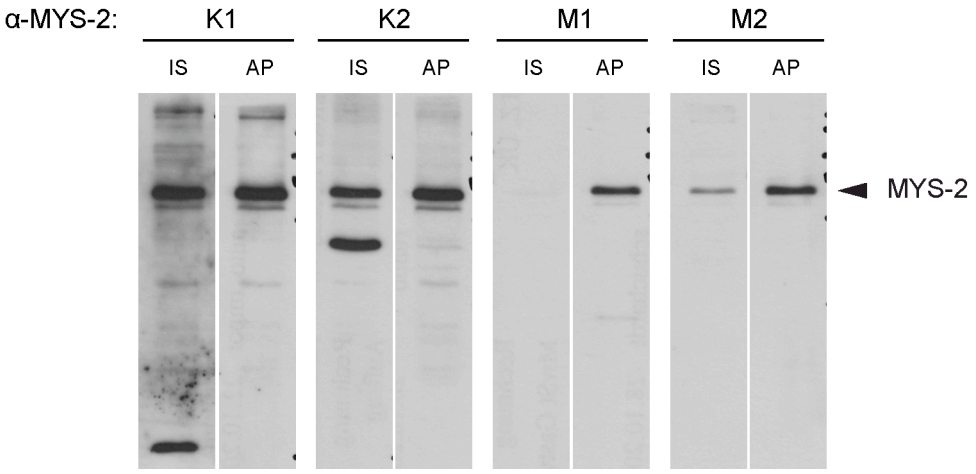


**Figure 12: Affinity purification improved specificity of α-MYS-2 antibodies;** immunoblots on wild-type protein lysates probed with immune sera (IS) or affinity purified antibody (AP) of the two rabbits (K1, K2) and guinea pigs (M1, M2); immunesera used at dilution 1:5000, affinity-purified antibodies used at dilution 1:5

The immunoblots on N2 wild type protein lysates furthermore indicated that MYS-2 is expressed in wild-type worms under standard laboratory conditions.

## 3.3. MYS-2 is ubiquitously expressed and localizes to chromatin

In order to gain insight into the function of MYS-2, we asked where and when it is expressed in the worm. While immunoblots showed that it was expressed in mixed wild-type cultures, we were interested in the details of the temporal and spatial expression pattern. In addition, we were interested in the subcellular localization of MYS-2. These questions were addressed by immunostainings, using the specific α-MYS-2 antibody. In the following experiments the affinity purified antibodies from rabbits (K1, K2) were used, since they gave stronger signals than the guinea pig antibodies. K1 and K2 were usually used in parallel, and we did not see differences in their staining pattern.

The MYS-2 homologues in yeast, flies and humans are chromatin modifiers, so we hypothesized that MYS-2 would be enriched in the nucleus associated to chromatin. Furthermore, its homologues are the prime histone acetyltransferases for the abundant H4K16Ac mark, raising the expectation that MYS-2 is expressed in many, if not all of the tissues in the worm.

In a first experiment whole animals from all developmental stages were stained, but the antibody in most cases did not permeate the cuticle sufficiently, resulting in partially stained animals. Therefore we subsequently stained dissected hermaphrodites. This makes tissues like the gonad or the intestine more accessible to the antibody and allows for a better view of single cells. We also specifically stained embryos, which were easily accessible to antibodies due to their small size.

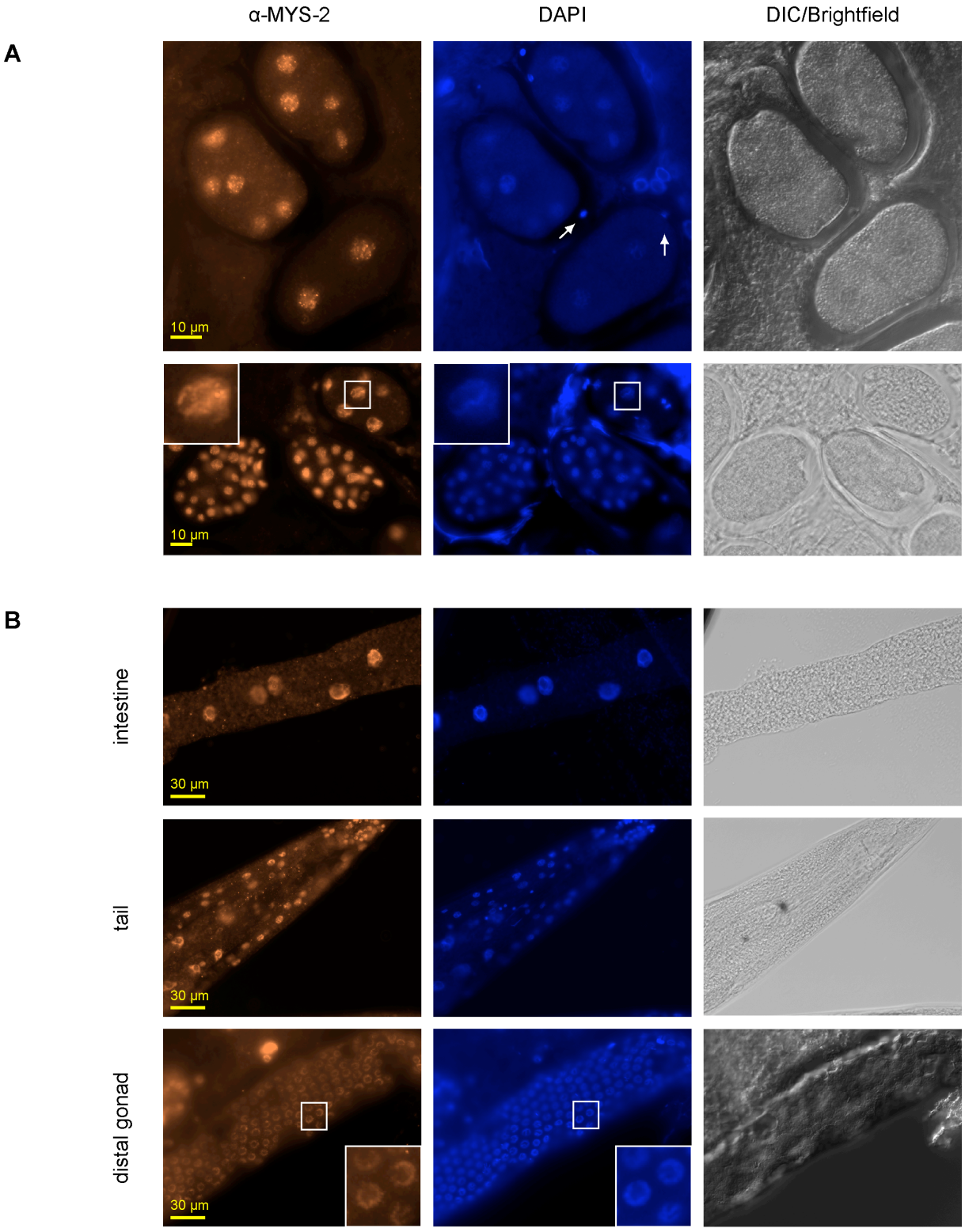


**Figure 13: MYS-2 was ubiquitously expressed and localized to chromatin;** Immunostaining of dissected wild-type adult hermaphrodites with α-MYS-2 antibody (K1), DNA stained with DAPI; (**A**) Early embryos show robust MYS-2 signals in each nucleus, the MYS-2 signal is absent from pole bodies (arrows); (**B**) Nuclei of somatic cells (intestine and tail) and germ nuclei (distal gonad) show robust MYS-2 expression; (**A**, **B**) MYS-2 precisely colocalized with DNA, as shown in magnified sections of individual nuclei in bottom panels

In stained animals, MYS-2 was specifically enriched in nuclei of all cells, and no nucleus seemed to lack a MYS-2 signal. From early embryo on, throughout all of the four larvae stages up to adult hermaphrodites, each nucleus in each tissue showed prominent MYS-2 signals (Figure 13).

Moreover, germline nuclei showed the same robust MYS-2 signals as somatic nuclei (Figure 13B). Starting with mitotic germ cells in the distal gonad throughout meiosis and fertilization to the onset of embryonic development, all nuclei contained MYS-2.

The main MYS-2 signal was consistently found in the nucleus. In particular, MYS-2 signals precisely colocalized with the DAPI signals (magnified sections Figure 13). However, in polar bodies on early embryos, which contain DNA, we did not observe any signal (Figure 13 A). Low levels of MYS-2 signal were also visible in the cytoplasm. This might be background staining, though we cannot exclude a cytoplasmatic portion of MYS-2.

Taken together, these findings showed that MYS-2 is ubiquitously expressed in wild-type worms under standard laboratory conditions. We observed that MYS-2 colocalized with chromatin in the nucleus.

Global transcription is repressed in early *C. elegans* embryos until the 4-cell stage at least (Seydoux and Dunn 1997). The embryo is dependent on maternally provided gene products during that time. MYS-2 was found in very early embryos, indicating that it is provided by the mother either as mRNA or as protein, suggesting an important function early in development, perhaps in the fundamental regulation of chromatin in early embryogenesis.

We also stained non-dissected *him-8*(me4) males, which showed the same abundant nuclear MYS-2 signal (data not shown). The respective strain CA151 produces males at a high frequency due to chromosome non-disjunction during meiosis. Thus, there was no sex-specific difference in MYS-2 expression, unlike for the fly homologue dMOF.

## 3.4. MYS-2 was precipitated with α-MYS-2 antibodies

The closest MYS-2 homologues, Sas2, dMOF and hMOF, have been found to be part of at least one multisubunit HAT complex (Scott et al. 2000; Meijsing and Ehrenhofer-Murray 2001; Dou et al. 2005; Smith et al. 2005; Raja et al. 2010). The strategy to immunoprecipitate (IP) a protein of interest with the aim of co-immunopurifying complex partners has been successfully applied before in *C. elegans*. For instance, the kinetochore component KNL-1 has been shown by co-IP to interact with HIM-10 and NDC-80, conserved *C. elegans* homologues of the kinetochore components Nuf2p and Ndc80p (Desai et al. 2003).

We were most interested in the interaction partners of MYS-2. Using the rabbit α-MYS-2 antibodies K1 and K2, MYS-2 was precipitated from protein lysates of mixed stage wild-type worms. In order to minimize signals from the antibodies in both coomassie-stained gels and western blots from the IPs, the antibodies were crosslinked to the Protein A-Sepharose beads prior to the IP. IPs were carried out with both rabbit α-MYS-2 antibodies and compared to control IPs with the corresponding preimmune sera. MYS-2 was expected to be precipitated by K1 and K2, while being absent from the control IPs. The success of IP was confirmed by western blotting the glycine eluates of precipitated proteins and probing them with the guinea pig α-MYS-2 antibody M1 (Figure 14). Two signals were detected in each immunoprecipitation that were absent in the control IP. The two signals might reflect two isoforms of MYS-2 or a degradation product. The fact that the guinea pig antibody detected the protein precipitated by both rabbit antibodies and that the same pattern of signals is found with both K1 and K2 IP indicates that this band constitutes immunoprecipitated MYS-2.

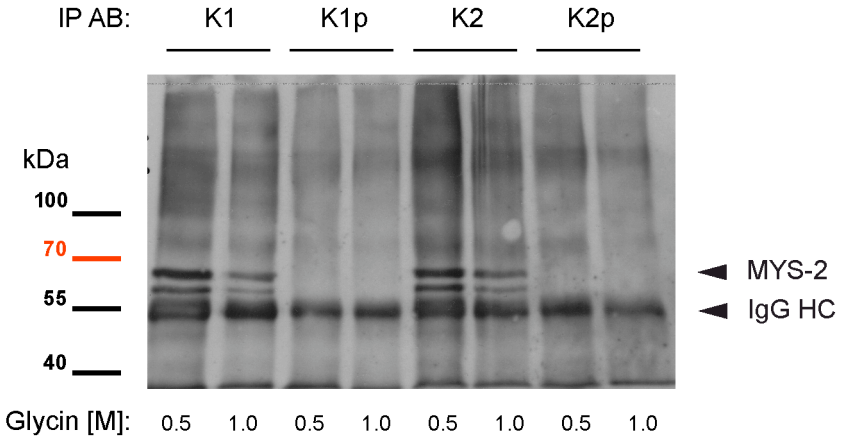


**Figure 14: MYS-2 was precipitated with rabbit α-MYS-2 antibody.** Western blot of 15 µl of elutions from immunoprecipitations with rabbit α-MYS-2 antibodies K1 and K2 and corresponding preimmunesera K1p and K2p as indicated; Elutions were carried out with 0.5 M Glycin followed by 1.0 M Glycin as indicated. Western blot probed with guinea pig α-MYS-2 antibody M1. Signals of MYS-2 and rabbit IgG heavy chains (IgG HC) are indicated.

We further sought to identify additional co-immunoprecipitated proteins in coomassie-stained gels from the IPs. We expected to detect signals corresponding to the signals from western blots that represent MYS-2. Additional signals present in IPs with K1 and K2, but absent from the control IPs, might represent proteins interacting with MYS-2. Faint signals (data not shown) were detected, and the gel bands isolated. The bands were sent to Chromatech AG (Greifswald) for identification by mass spectrometry (MS/MS). However, the analysis by mass spectrometry was not successful due to insufficient amounts of protein.

## 3.5. Trials for *mys-2*::GFP expression

*C. elegans* is one of the best models to use GFP protein fusion for expression and localization analysis of proteins of interest. Due to its transparency, the expression of a GFP reporter construct can be observed in the living animal at each stage of development. The genome of *C. elegans* is comparatively compact, and a common approach therefore is to clone the region upstream of the gene of interest into a GFP expression vector and introduce it into the worm, in order to quickly assess temporal and spatial expression patterns. We sought to follow this technique and created a transcriptional GFP reporter that is expressed under the control of the 2 kb genomic region upstream of *mys-2* (pAE1212). The reporter construct was injected into gonads of wild-type adult hermaphrodites together with the co-injection plasmid pRF4 (pAE1030) that expressed the dominant allele *rol-6*(su1006) as a marker. Both were injected together at 100 ng/µl in water. Animals displaying the Roller phenotype indicate the presence of the co-injection marker, which allows the identification of transformed worms. Although 18 transgenic lines were established here that inherited the Roller phenotype at least up to the F3 generation, expression of GFP was never observed. We sought to control the method by transforming the *rol-6*(su1006) co-injection marker (pAE1030) in combination with another common co-injection marker expressing the *sur-5*::GFP fusion (pAE1029), both at 100 ng/µl. In seven out of ten transgenic lines, both markers co-segregated, two displayed GFP expression but were not Roller and one line was Roller without GFP expression. We concluded that the co-injection in principal was succesful, but that the reporter construct (pAE1212) expressed no GFP. The reasons are discussed in section 4.5.

Since *mys-2* is annotated to be part of an operon that is likely to be regulated as one transcriptional unit, a yeast artificial chromosome (YAC) that contained *C. elegans* genomic sequence was manipulated to construct in-frame-fusions of *mys-2* and GFP. Three versions of a translational *mys-2*::GFP reporter (AEY5079, AEY5080, AEY5081) were generated using the YAC Y63D3 (AEY4980). Since the YAC contained *mys-2* in its genomic environment, all regulatory elements should be present. Thus, the three versions of the GFP reporter were expected to accurately reflect endogenous *mys-2* expression. Genomic DNA preparations from the respective yeast strains containing a version of the *mys-2*::GFP reporter were injected into wild-type hermaphrodite gonads. Concentrations of 100 ng/µl or 1.7 µg/µl were injected together with the Roller co-injection marker at 100 ng/µl. Transgenic lines could not be established from those transformations. For unknown reasons, no animals were detected that showed the Roller phenotype indicative positive transformants.

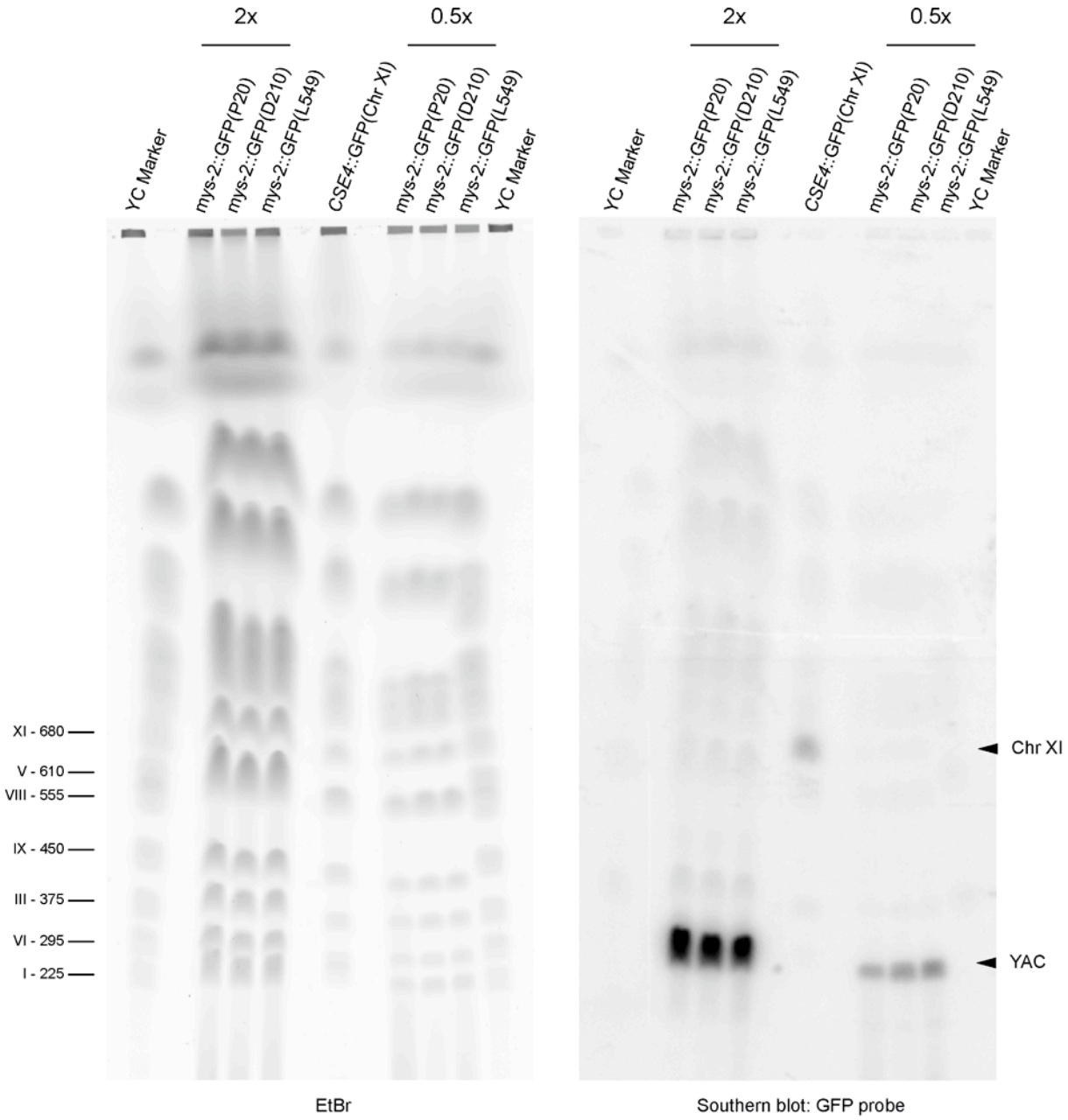


**Figure 15: YACs containing the *mys-2*::GFP fusions were identified by southern blotting;** left panel shows the CHEF gel separating the yeast chromosomes stained with ethidium bromide (EtBr), YC Marker: Yeast Chromosome PFG Marker (NEB) loaded on outer lanes, relevant chromosomes and their sizes in kilobases are indicated on the left; gel loaded with DNA plugs (2x or 0.5x) from yeast strains containing YAC-based *mys-2*::GFP fusions (the residue of GFP fusion is given in brackets), DNA plug from endogenous *CSE4*-GFP::*klTRP1* (on Chr. XI)) as positive control for southern blotting; right panel shows the southern blot of the CHEF gel from left panel hybridized with [α-$^{32}$P]dCTP-labelled GFP probe (by Dr. Mario Moscariello); the signal of *CSE4*::GFP (Chr XI) was at the expected 680 kb, confirming specificity of the GFP probe, the equally sized YACs were found to migrate at the same size as Chr. I at 225 kb

We therefore isolated each YAC from the endogenous yeast chromosomes by clamped homogeneous electrical field (CHEF) pulsed field gel electrophoresis (PFGE). Dr. Mario Moscariello identified the YACs by southern blotting of a CHEF gel, and they were

determined to co-migrate with the yeast chromosome I at 225 kb (Figure 15). Respective bands were then excised from preparative CHEF gels and, after a 2D gel run for concentration purposes, agarose was digested to generate the YAC solutions. The identities of the YACs were confirmed by control PCR reactions, and integrity of each of the YACs was confirmed on standard agarose gels. The YACs were then injected into wild-type hermaphrodite gonads together with the *rol-6*(su1006) co-injection marker. Each of the three YACs containing a version of the *mys-2*::GFP fusion was injected into 45 (P) adult hermaphrodites. The F1 generations were scored for the Roller phenotypes, and positive animals were transferred to individual agar plates. They were allowed to produce progeny for three days. The F2 progeny was scored for Roller phenotypes and if found positive, their mothers were analyzed by single worm PCR for the presence of GFP (Figure 16). Altogether, 440 F1 Roller individuals were found, and 98 of them produced Roller in the F2 generation. 32 of the respective F1 mothers were determined positive for the presence of GFP sequence, reflecting 32 transgenic lines that carry at least a fragment of the YAC.

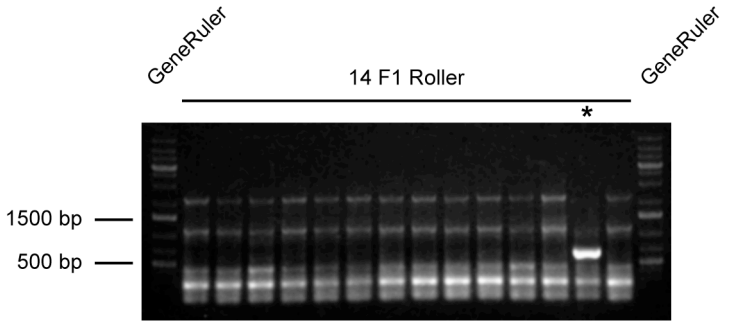


**Figure 16: single worm PCR confirmed the presence of the YAC in transgenic worms;** 14 F1 Roller that produced F2 Roller assayed in swPCR using primers GFP 1-1 and GFP 1-2, one individual was found positive by presence of the 600 bp GFP amplicon (*) indicative of the presence of *mys-2*::GFP

All lines were extensively analyzed for the expression of *mys-2*::GFP at all developmental stages, but expression was not observed. Since MYS-2 was found to be expressed ubiquitously in immunostainings, each YAC was also injected into 20 wild-type hermaphrodites without the co-injection marker. F1 progeny was then directly scored for GFP signals under a fluorescent dissecting microscope, but no *mys-2*::GFP was observed.

Taken together, although a number of transgenic lines were produced that stably inherited the co-injection marker together with the *mys-2*::GFP sequence, none of those was found to express *mys-2*::GFP. Injections of the *mys-2*::GFP reporter constructs without the *rol-6*(su1006) marker, also did not lead to animals expressing *mys-2*::GFP. We suspected the expression of the GFP reporter constructs to be lethal due to overexpression of *mys-2*, as will be discussed in section 4.5, and tried another approach. To circumvent this potential problem,

the YACs were injected into phenotypically wild-type worms of the *mys-2*(ok2429) deletion strain without the co-injection marker (see chapter 3.6.1 for a detailed description of this strain. We thus hoped to complement the potential lethality of the overexpression with the endogenous deletion, thereby allowing expression of the *mys-2*::GFP fusion and rescuing the deletion phenotype at the same time. The F1 progeny of injected mothers was scored for GFP expression. Furthermore, F1 progeny was scored for the Mys phenotype, indicating whether the injected mother was homozygous for the allele *mys-2*(ok2429). This progeny was examined for the occurrence of rescued animals. However, neither GFP expression, nor rescue of progeny from homozygous mothers was observed. For an interpretation of these results see the Discussion.

## 3.6. *mys-2* was maternal-effect lethal

The phenotype caused by mutation or the deletion of a gene can provide information about its function. Hence we sought to determine the effect of deleting *mys-2*. Since no simple gene knock-out procedure in worms was at our disposal, we addressed this issue by targeting *mys-2* via RNA interference, and we obtained a deletion *mys-2* allele (*mys-2*(ok2429)) that was generated by the *C. elegans* Gene Knockout Consortium.

### 3.6.1. Maternal contribution rescued the *mys-2*(ok2429) deletion phenotype

We obtained a strain bearing the *mys-2*(ok2429) allele balanced by an inversion on chromosome I (strain VC1931). The strain comprises phenotypically wild-type hermaphrodites that are trans-heterozygous. These individuals carry the *mys-2*(ok2429) allele on one homologue of chromosome I, while the other homolog of chromosome I carries the *unc-101*-marked inversion, which prevents undesired recombinantion events on that chromosome. If not crossed to males, the trans-heterozygous hermaphrodite (P) reproduce by selfing and segregate *mys-2* and *unc-101* according to the laws of Mendelian inheritance. The progeny (F1) is statistically composed of 50 % trans-heterozygotes with genotype identical to the mother, 25 % are homozygous for the *unc-101*-marked inversion and another 25 % are homozygous for the *mys-2*(ok2429) allele. The Consortium reported the trans-heterozygotes to be phenotypically wild-type (WT), the *unc-101* homozygotes to be Uncoordinated (hereafter referred to as Unc/Dpy) and the *mys-2*(ok2429) homozygotes to be lethal at an unknown stage.

The strain report implies the phenotypically occurrence of wild-type and Unc/Dpy at a ratio of 2:1 (50 % : 25 %). However, phenotypically analysis revealed that phenotypically wild-types and Unc/Dpy animals occurred at a ratio of roughly 3:1 in the F1 generation. A further

analysis of the F2 selfing progeny of phenotypically F1 wild-types displayed a difference among the F1 mothers. While two-thirds produced the expected F2 progeny identical to the F1 progeny, one-third produced progeny with a completely penetrant phenotype of small and slow growing worms (Figure 17).

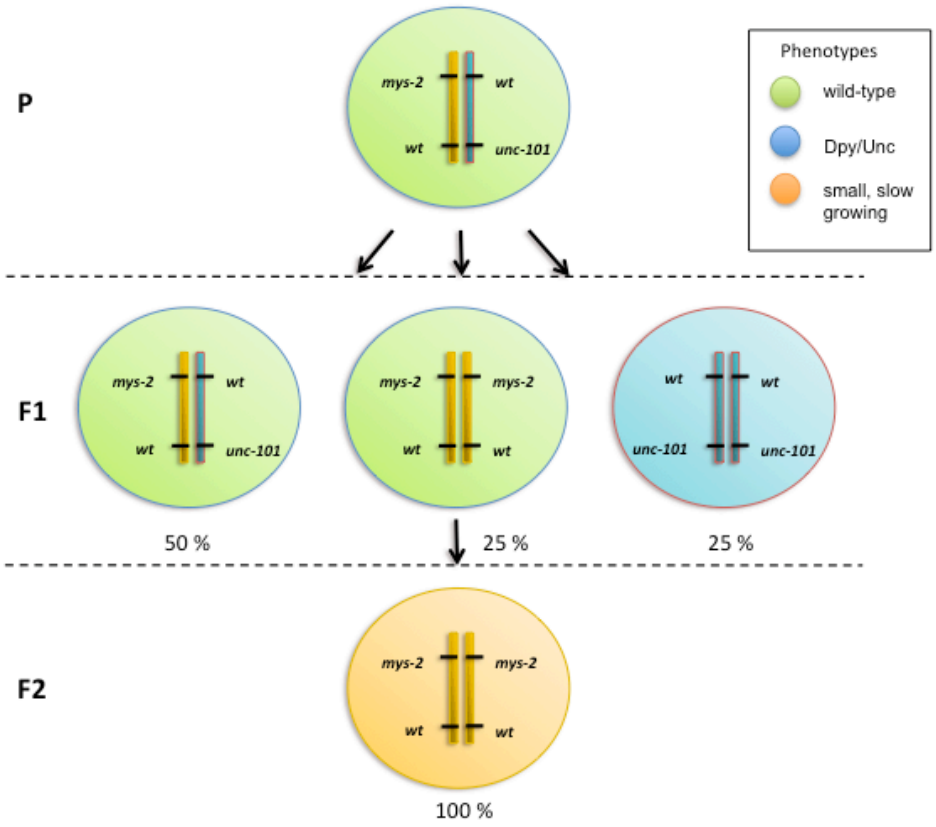


**Figure 17: Scheme of genotypes and phenotypes in the *mys-2*(ok2429) strain (VC1931).** The heterozygous mother (P) carries one chromosome I homologue with *mys-2(ok2429)*(yellow) and another chromosome I homologue with hIn1[*unc-101*(sy241)] (blue). Chromosomes get distributed in the F1 with regards to the laws of Mendelian inheritance. Homozygous *mys-2(ok2429)* individuals look wild-type (green background), indistinguishable from heterozygotes. Homozygous F2 individuals from homozygous F1 mothers are small and slow growing (yellow background)

We sought to determine the genotype of phenotypically wild-type worms at the *mys-2* locus. This was addressed by performing single worm PCR reactions on mothers, after they had laid enough eggs to additionally analyze their progeny. In addition to the primers given by the *C. elegans* Gene Knockout Consortium that encompass the deletion (MYSKO-1/MYSKO-2), a third primer that anneals in the deletion sequence was designed (MYSKO-6). The corresponding duplex single worm PCR confirmed with a perfect correlation that phenotypically wild-type worms were either heterozygous or homozygous for the *mys-2*(ok2429) deletion allele. We tested 149 phenotypically wild-type mothers and analyzed their

progeny. While 94 were determined to be heterozygotes and gave progeny with the expected segregation of phenotypically wild-types and Dpy/Unc animals, 55 were homozygous for *mys-2*(ok2429) and gave rise to progeny that displayed the severe phenotype. Not only was the correlation between the PCR result and the progeny perfect, the ratio of nearly 2:1 also reflects the laws of Mendelian inheritance.

Taken together, these findings showed that severe phenotypically consequences arose upon deletion of *mys-2*, but only if both mother and zygote were depleted for *mys-2* gene products (m-z-). As long as the mother was at least heterozygous for *mys-2*, the mutant phenotype was rescued in homozygous *mys-2*(ok2429) zygotes (m+z-). This was in agreement with the immunostainings of MYS-2 that indicated a maternal contribution of *mys-2* gene products. It is therefore most likely that the mother provides the egg with *mys-2* gene products that compensate for the loss of MYS-2 in the F1 generation. However, it is also possible that MYS-2 has a function in the germ cells of the mother, which provides epigenetic information for the next generation.

### 3.6.2. The homozygous *mys-2*(ok2429) deletion is lethal

The phenotype observed in worms homozygous for *mys-2*(ok2429) from homozygous mothers affected all animals with complete penetrance. However, expressivity differed among the affected animals. The brood size of *mys-2*(ok2429)m-z- progeny was reduced in comparison to *mys-2*(ok2429)m+z- progeny. This reduction was not quantified, since it ranged from less than ten animals to more than 100 animals. Viable *mys-2*(ok2429)m-z- animals developed significantly slower than wild-type worms. Wild-type worms develop from egg to the adult hermaphrodite in roughly 3 days at 20°C. The first adult *mys-2*(ok2429)m-z- animals were detected after five days, at the earliest, and were often sterile when they reached adulthood. The rare fertile *mys-2*(ok2429)m-z- worms gave rise to a next generation that suffered identical phenotypes. It was in rare cases possible to maintain a homozygous line for up to four weeks. While most lines died with the second *mys-2*(ok2429)m-z- generation, some lines did not show any fertile adults and died within the first *mys-2*(ok2429)m-z- generation. Viable *mys-2*(ok2429)m-z- animals that did not reach adulthood either died at differing stages of development or arrested at one of the four larvae stages.

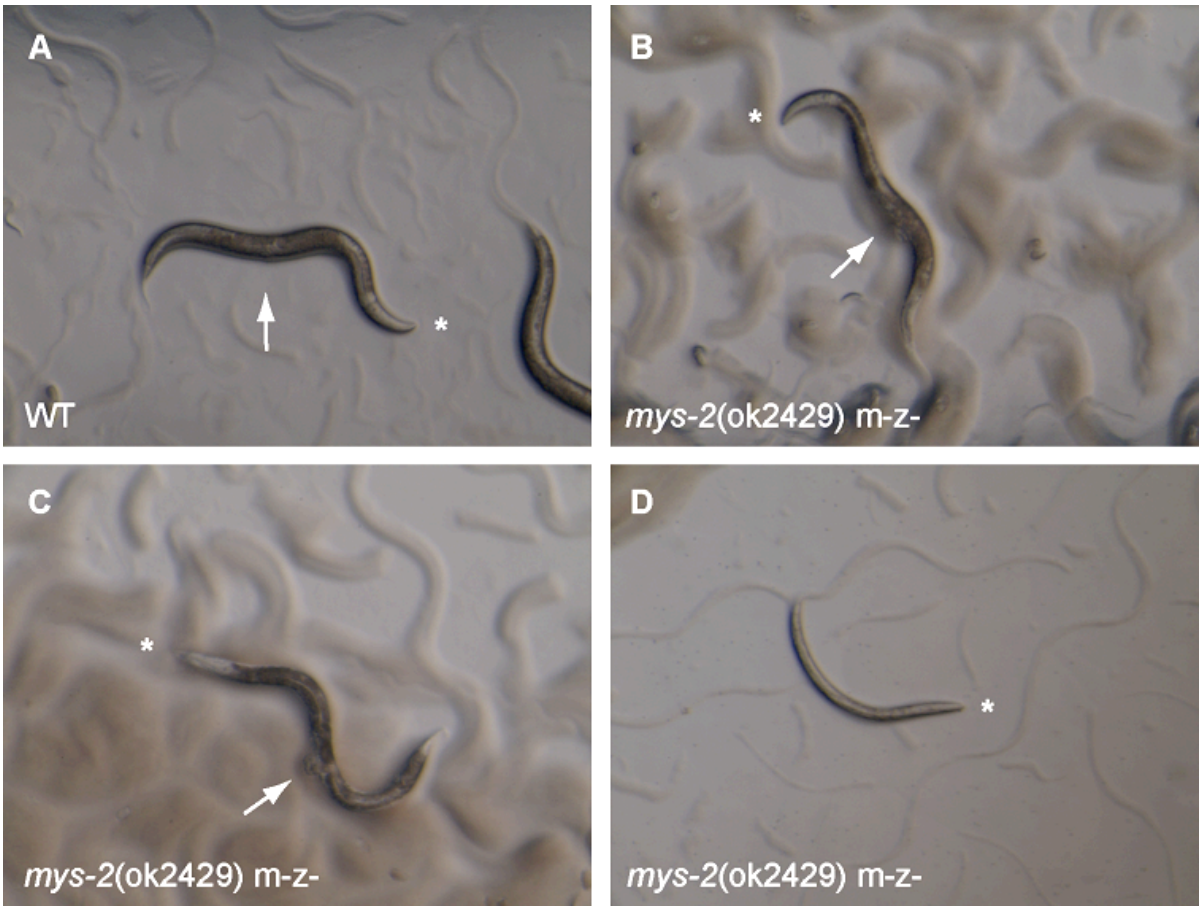


**Figure 18:** ***mys-2*****(ok2429)m-z- worms were small and showed vulval defects;** Dissecting microscopical photographs of four worms of the VC1931 strain are shown, their heads (*****) and vulvae (arrows) are indicated. (**A**) shows a phenotypically wild-type worm (WT) which was either heterozygous or homozygous for *mys-2*(ok2429). (**B-D**) show *mys-2*(ok2429) m-z- worms with ascending severeness of the mutant phenotype, (**B**) was a fertile adult hermaphrodite which was equally long compared to WT but thinner in the anterior part of its body. (**C**) was smaller and thinner as WT and infertile. (**D**) was very small and thin and about to die. Mutant worms often showed vulval defects like protruding vulva (Pvl) (**B, C**).

The observed mutant phenotypes were of variable severeness. Animals that escaped embryonic or larval lethality were smaller and thinner compared to wild-type (Figure 18). In addition, worms often suffered from vulval defects. Vulval integrity was impaired, leading to the protruding vulva phenotype (Pvl) or the more severe ruptured or "exploded through vulva" phenotype (Rup) where the gonad and the intestine excavate through the vulva (Figure 18 and Figure 19). Furthermore, vulvaless (Vul) animals and "bags of worms" were observed, where the progeny hatches in the body of the mother.

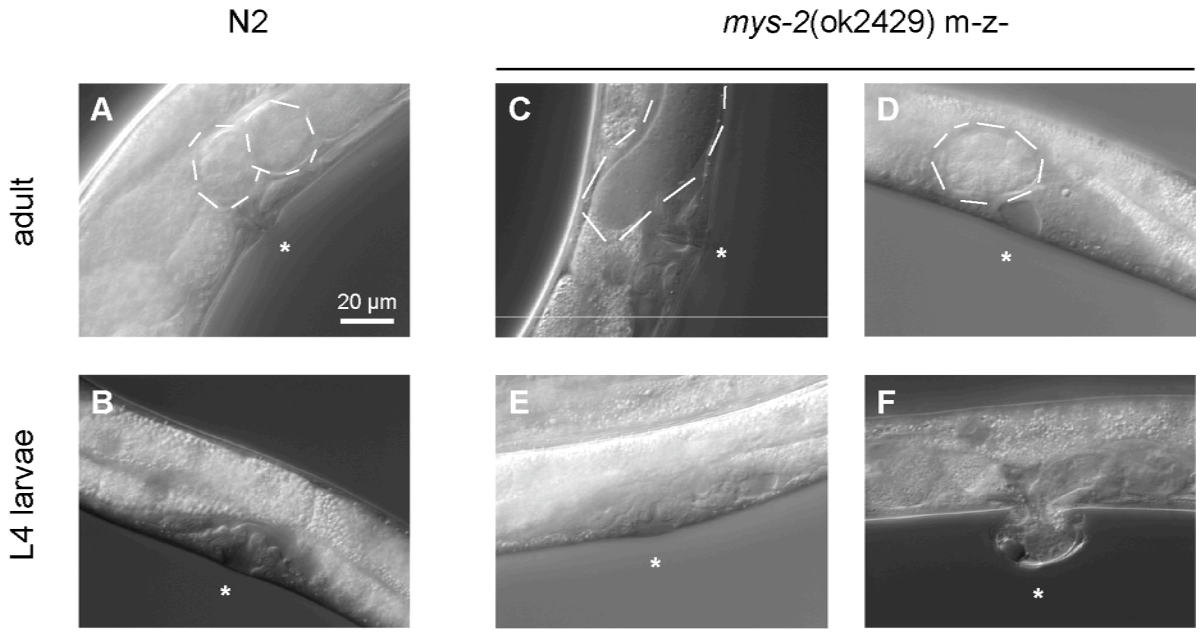


**Figure 19: *mys-2*(ok2429) m-z- worms suffered from vulval defects;** Nomarski images of the middle body part of adult or L4 larvae hermaphrodites from strain wild-type (N2) and *mys-2*(ok2429)m-z- worms. The vulva (*), situated at the ventral body side, is shown in detail. (**A**) Wild-type situation, two embryos are highlighted, the vulva was fully developed. (**B**) Developing vulva in a wild-type L4 larvae. (**C**) while the vulva looked wild-type, this worm was sterile (no embryos) and the distal gonad (highlighted) was mislocated to the ventral half of the body. (**D**) Vulvaless worm, no vulval cells observable. This worm developed a single embryo (highlighted). (**E**) The morphology of vulval cells is different from wild type. (**F**) Initial stage of "exploded through vulva" phenotype.

Taken together, the homozygous deletion of *mys-2* caused severe developmental defects that were rescued by maternal contribution. This indicated that *mys-2* is an essential gene, since the majority of affected animals died at different stages of development. Furthermore, the observed phenotypes in animals that escaped lethality suggested that there exists a low degree of rescue that can act over several generations. While it was possible to propagate homozygous lines over approximately three generations, all lines died eventually. The observed phenotypes were variable, and it is likely that more misdevelopment takes place besides the described vulval defects.

### 3.6.3. MYS-2 was depleted in *mys-2*(ok2429)m-z- worms

Our analysis above showed that worms with the mutant phenotype were homozygous for the deletion of *mys-2* as determined by genotyping the animals using single worm PCR. We next tested whether they also showed reduced immunostaining with the α-MYS-2 antibodies. For this purpose, dissected gonads derived from a *mys-2*(ok2429)m-z- adult hermaphrodite were stained. In addition, phenotypically wild-type adult hermaphrodites that derived from a heterozygous mother were stained in the same manner. The genotype of each mother was

determined by single worm PCR. While this ensures that mutant worms were homozygous for the deletion, the genotype of phenotypically wild-type worms can be either heterozygous or homozygous for the deletion.

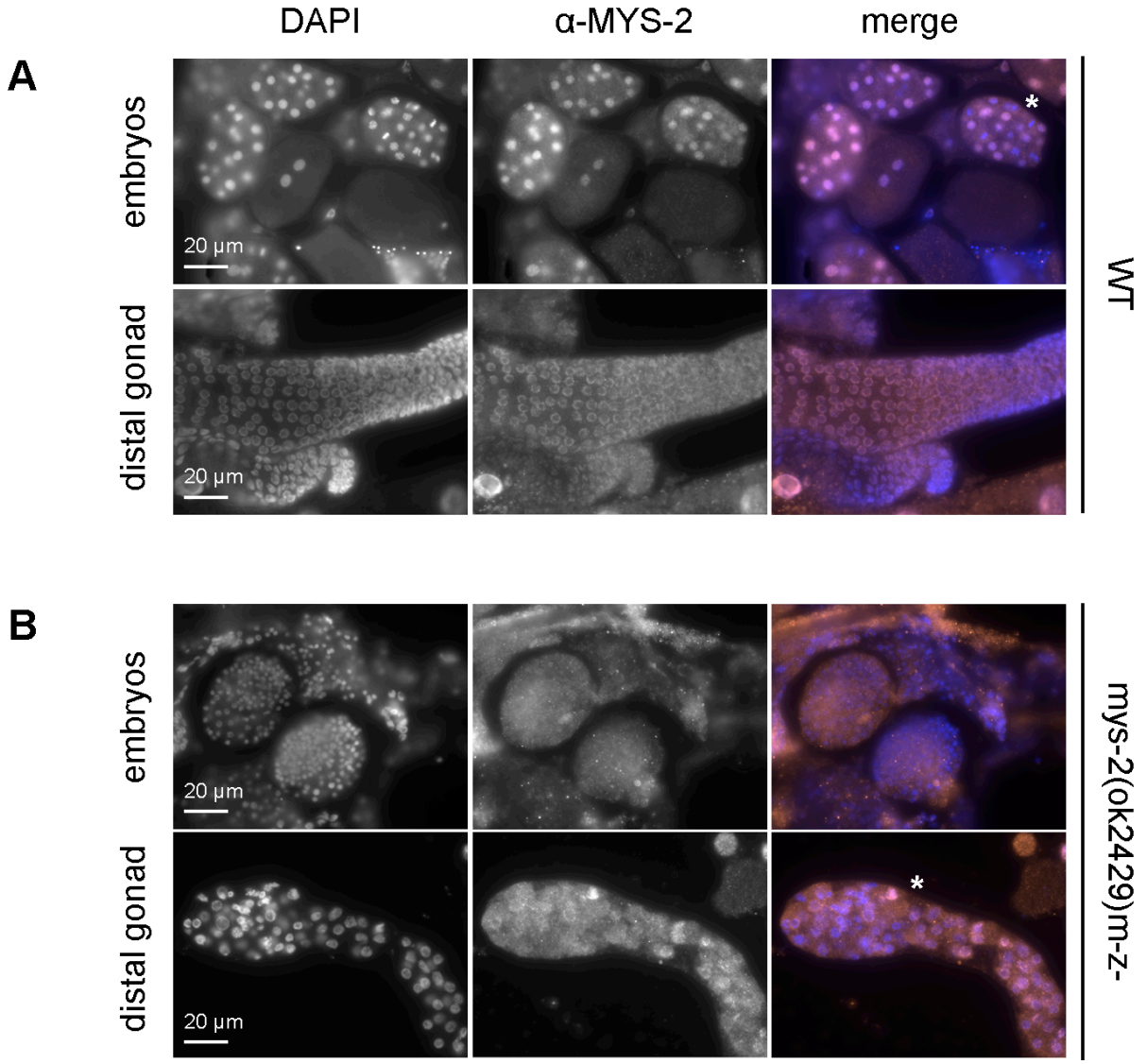


**Figure 20: MYS-2 was depleted from *mys-2*(ok2429) m-z- worms;** MYS-2 immunostainings (orange), counterstained with DAPI (blue); (**A**) dissected, phenotypically wild-type (**WT**), adult hermaphrodites of the *mys-2*(ok2429) strain (VC1931); (**B**) dissected, homozygous *mys-2*(ok2429)m-z- worms Embryos of phenotypically wild-types (**A** - upper panels) showed robust MYS-2 signals, individual cells of an embryo (*) might have been depleted of MYS-2, all nuclei in the distal gonad of a phenotypically wild-type hermaphrodite (**A** – lower panel) showed robust MYS-2 signals, notice the well-ordered alignment of nuclei; embryos of *mys-2*(ok2429)m-z- worms (B – upper panel) were completely depleted of MYS-2, most nuclei in the distal gonad (**B** – lower panel) were depleted of MYS-2, individual nuclei (*) showed weak signals. Nuclei in the distal gonad differed in size (refer to the DAPI panel) and are not as well ordered as in phenotypically wild-type worms, morphology of the distal gonad was altered.

The stained phenotypically wild-type hermaphrodites showed robust MYS-2 signals. A significant, abundant depletion of MYS-2, indicating a homozygous *mys-2*(ok2429) genotype,

was not observed among the stained phenotypically wild-type worms. However, individual embryos were found that displayed depletion of MYS-2 in individual cells, suggesting a homozygous *mys-2*(ok2429) genotype for the embryo (Figure 20A).

In contrast, the stained *mys-2*(ok2429) m-z- worms were depleted of MYS-2. Only in rare cases, a low level staining was observed in nuclei, which might reflect residual MYS-2 levels that are responsible for the rescue from lethality. Moreover, the immunostainings revealed that the morphology of organs, particularly the gonad, was altered in these mutants. Mitotic germ nuclei that are located in the distal gonad showed abnormal sizes and heterogeneous DNA staining, suggesting that fundamental processes in the nucleus are disturbed (Figure 20B). Since the size of nuclei is dependent on the content of DNA, one could speculate about impaired DNA replication or defects in mitosis. These findings link the mutant phenotypes to the deletion of *mys-2*. The entirety of the described phenotypes will be referred to as the Mys phenotype in the following sections.

## 3.7. H4K16Ac is not depleted upon loss of MYS-2

The homologues of MYS-2 in yeast, flies and humans are all reported to acetylate H4K16, and deletions of the MYS-2 counterparts result in a significant decrease in global H4K16Ac levels (Akhtar and Becker 2000; Kimura et al. 2002; Dou et al. 2005). Accordingly we asked whether the loss of MYS-2 affected the abundance of H4K16Ac in worms. For this purpose, immunostainings with an α-H4K16Ac antibody in *mys-2*(ok2429) m-z- worms were performed and compared to stainings in wild type N2 worms. Mutant adult hermaphrodites that contained embryos were subjected to dissection and staining, thus including embryos in the staining.

The H4K16Ac staining in wild-type worms showed prominent signals in each nucleus of every tissue. It has been reported that X chromosomes are silent in the germline and are depleted for H4K16Ac in a SIR-2.1 dependent manner (Wells et al. 2012). In our H4K16Ac stainings, germ nuclei in the distal gonad exclusively showed a “u”-like shaped staining, which was in contrast to the “o”-like shape of the corresponding DNA signal (Figure 21). This reflected the reported depletion of X in the germline for H4K16Ac and was consistent with the earlier study (Wells et al. 2012).

Stainings of *mys-2*(ok2429) m-z- worms did not reveal a substantial reduction in the signal of the α-H4K16Ac antibody. We also did not detect any changes in the staining pattern of the antibody, suggesting that MYS-2 either has a substrate specificity that does not include H4K16Ac, or this residue is redundantly acetylated by additional HATs in *C. elegans*.

However, our approach only addressed global levels of H4K16Ac and does not exclude local changes in the pattern of H4K16Ac enrichment on the genomic level.

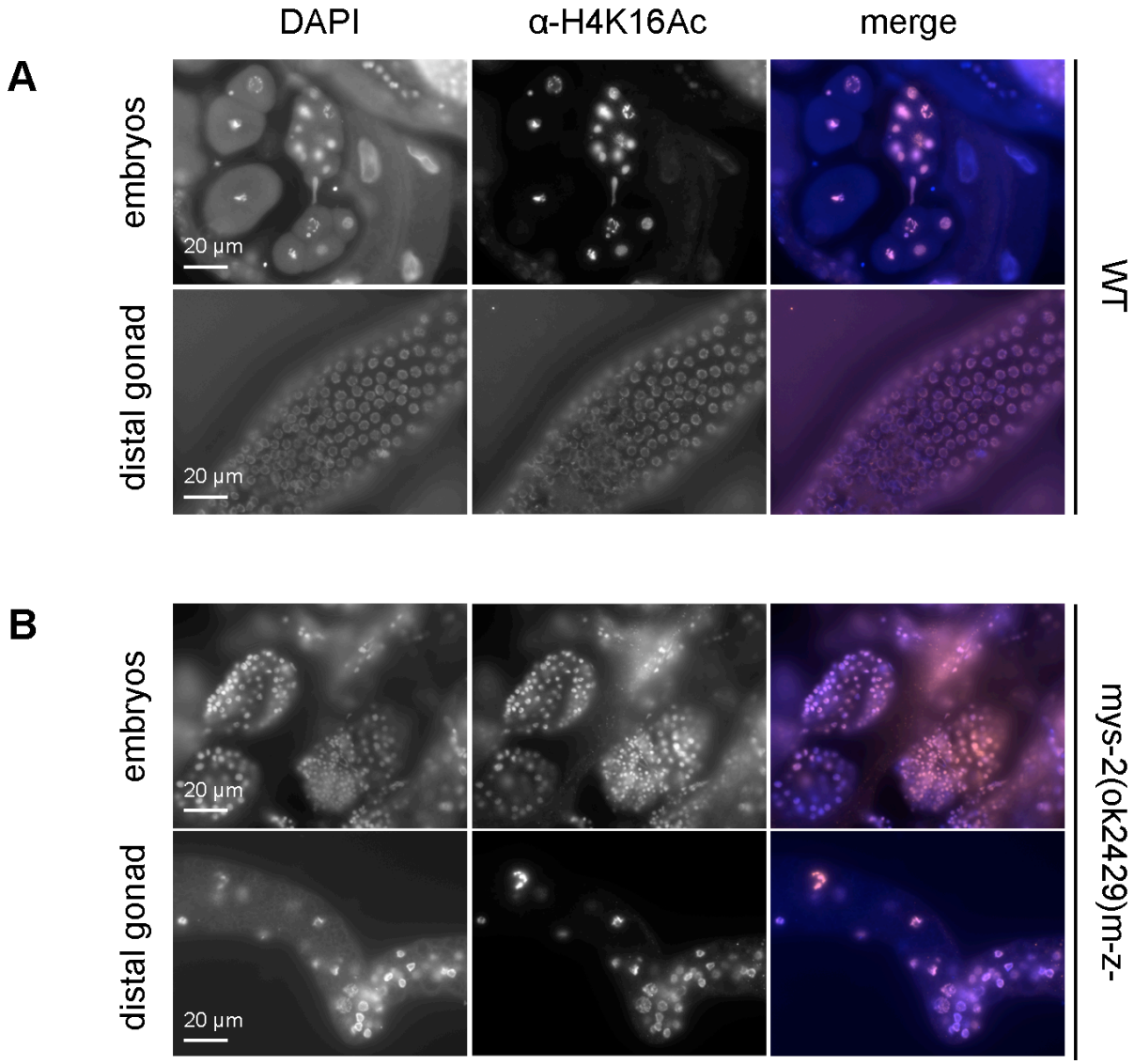


**Figure 21: Global levels of H4K16Ac were not affected upon loss of MYS-2;** H4K16Ac immunostainings (orange), counterstained with DAPI (blue); (**A**) dissected wild-type adult hermaphrodites (**WT**); (**B**) dissected, *mys-2*(ok2429) m-z- worms; wild-type embryos (**A** - upper panels) showed robust H4K16Ac signals in each nucleus; all nuclei in the distal gonad of a wild-type hermaphrodite (**A** – lower panel) showed robust H4K16Ac signals, notice the "u"-shaped H4K16Ac signals in contrast to the "o"-shaped DAPI signals; embryos of *mys-2*(ok2429) m-z- worms (**B** – upper panel) showed robust H4K16Ac signals in each nucleus, comparable to wild-type; nuclei in the distal gonad (**B** – lower panel) showed robust H4K16Ac signals

## 3.8. RNAi disrupted the maternal rescue of *mys-2*(ok2429)

In order to further explore the function of *mys-2*, the gene was targeted by RNA interference. An existing construct expressing dsRNA with *mys-2* sequence (pAE1020) was used in RNAi feeding experiments. The empty RNAi vector L4440 served as negative control, and an RNAi construct targeting *unc-22* (pAE1017) served as positive control. Bacteria expressing dsRNA

corresponding to the respective genes were fed to wild-types and worms carrying the deletion *rrf-3*(pk1426), which renders them more sensitive to gene knock-down by RNAi (Simmer et al. 2002). No phenotypes were observed when targeting *mys-2* in both strains, while the *unc-22* control caused the expected Uncoordinated (Unc) phenotype (data not shown).

In a second approach, RNAi was performed by injecting dsRNA into adult hermaphrodites. For this purpose, two additional constructs were generated that either targeted roughly the first or the second half of the *mys-2* open reading frame. They will be referred to as *mys-2* A or *mys-2* B, respectively. As negative control, dsRNA with the sequence of GFP was used. Injected animals were transferred to new plates every 24 hours. This served two purposes. First, the progeny is separated in 3 chunks that are of equal age, facilitating the detection of worms that develop slower. Second, eggs produced before the RNAi mediated gene knock-down is established cannot show a corresponding effect. The required time for the knock-down to be established differs, depending on the targeted gene. Thus, the progeny of the first 24 h post injection an incalculable number of worms that are not yet affected by the knock-down. Additionally, the worms were incubated at 15°C, which reduces the amount of progeny per chunk and facilitates the scoring of phenotypes.

Injections of *mys-2* A *and mys-2* B resulted in the rare occurrence of mutant phenotypes, at a frequency of less than 5 % (data not shown), suggesting that *mys-2* knock-down was inefficient in wild-type or *rrf-3*(pk1426) worms. The *mys-2* deletion strain offered the possibility to test this hypothesis, since the *mys-2* expression levels are expected to be reduced in *mys-2*(ok2429) heterozygous animals. In *mys-2*(ok2429)m+z- animals rescued by the maternal contribution, a knock-down of *mys-2* in the heterozygous mother might impair the maternal rescue, resulting in phenotypes resembling the Mys phenotype.

We then injected phenotypically wild-type adult hermaphrodites of the *mys-2*(ok2429) strain with dsRNA of either *mys-2* A, *mys-2* B or GFP as negative control. Since phenotypically wild-type worms can be either heterozygous or homozygous for the *mys-2* deletion, the occurrence of the *unc-101* related Unc/Dpy phenotype in the progeny was a reliable indicator for the genotype of the injected animal, because only heterozygous worms carry the *unc-101* allele and give rise to *unc-101* homozygotes. The phenotypes were scored as soon as the progeny was adult, which was 4 days after the mother was removed from the plate. Progeny of homozygous *mys-2*(ok2429) mothers had not reached adulthood at that time, due to their developmental defect, nor was there any progeny with a Unc/Dpy phenotype. They were not included in the analysis (Table 6).

**Table 6: Overview of phenotypes caused by RNAi against *mys-2* in strain VC1931;** Occurrence of wild type (WT), the *unc-101* related uncoordinated/dumpy (Unc/Dpy) and additional mutant (Mut) phenotypes is given as number and as percentage of the total number of animals (in brackets); "Worms per plate" gives the mean value of worms per plate and the standard deviation

| Time after injection | RNAi target | WT | Unc/Dpy | Mut | Total | Worms per plate |
|---|---|---|---|---|---|---|
| 0 – 24 h | GFP | 326 (74%) | 99 (23%) | 15 (3%) | 440 | 55 ± 28,2 |
| | *mys-2* A | 464 (55%) | 130 (15%) | 251 (30%) | 845 | 85 ± 29 |
| | *mys-2* B | 550 (65%) | 145 (17%) | 151 (18%) | 846 | 58 ± 22 |
| 24 – 48 h | GFP | 403 (75%) | 93 (17%) | 43 (8%) | 539 | 68 ± 25 |
| | *mys-2* A | 236 (38%) | 89 (14%) | 298 (48%) | 623 | 63 ± 26 |
| | *mys-2* B | 383 (42%) | 155 (17%) | 380 (41%) | 918 | 63 ± 27 |
| 48 – 72 h | GFP | 223 (75%) | 48 (16%) | 25 (8%) | 296 | 37 ± 25 |
| | *mys-2* A | 110 (41%) | 57 (21%) | 104 (38%) | 271 | 33 ± 32 |
| | *mys-2* B | 349 (49%) | 118 (16%) | 250 (35%) | 717 | 46 ± 28 |

Altogether, 18 phenotypically wild-type worms were injected with the *mys-2* A dsRNA, eight of them were later determined to be *mys-2*(ok2429) homozygous. 19 phenotypically wild-type worms were injected with the *mys-2* B dsRNA, three of them were later determined to be *mys-2*(ok2429) homozygous, and ten phenotypically wild-type worms were injected with the GFP dsRNA, two of them were *mys-2*(ok2429) homozygous. We scored for phenotypically wild-type worms and the Unc/Dpy phenotype of *unc-101* homozygous, all other phenotypes were categorized as Mutant (Mut) in Table 6 and will be further described later in this section. The RNAi targeting GFP showed roughly the expected ratio of three phenotypically wild-type to one Unc/Dpy. About 75 % of the animals are phenotypically wild-type, regardless of the time after injection. Some mutant animals were observed in the control, which most likely reflects a variance in the *unc-101* related phenotype. In contrast to that, RNAi targeting *mys-2* showed a decreased percentage of phenotypically wild-type animals. Progeny of the first 24 hours after injection was reduced to of 55 % or 65 % phenotypically wild-type animals upon knock-down of *mys-2*. These values were further decreased in progeny from the second 24 hours, to 38 % and 42 %, respectively. In the third 24 hours, those values increased slightly to 41 % and 49 % respectively, for the two *mys-2* RNAi constructs. We conclude that the RNAi effect is established during the first 24 hours, and the effect is the strongest between 24 and 48 hours after injection. While the number of phenotypically wild-type worms decreased, the

amount of Unc/Dpy animals is comparable to the negative control. The percentage of mutant animals increases, peaking in the second 24 hours at 48 % or 41 %, respectively.

In order to account for the possibility of missing individuals that die early in development, the mean number of worms per plate was scored. No significant difference between the *mys-2* RNAi and the GFP control was observed, indicating that embryonic or larval lethality did not occur frequently.

The most abundant of the observed mutant phenotypes was small (Sma) and/or slow growing worms. They accounted for roughly 80 % of the animals categorized as mutant (Mut). This phenotype ranged from very small worms that were severely misdeveloped to worms that looked wild-type but lagged behind in development. Similarly abundant (80%) was the protruding vulva phenotype (Pvl), ranging from slightly visible to worms that were about to become ruptured (Rup). The Sma and the Pvl phenotype frequently occurred in combination. About 20 % of the mutant (Mut) worms had exclusively the Pvl phenotype. Furthermore, the mutant worms were unusually transparent in comparison to WT worms (clear – Clr), and some serious misdevelopments were observed in rare cases (Figure 22). About 10 % of the mutant animals were dumpy (Dpy) in combination with Pvl. These worms were phenotypically similar to the *unc-101* related Unc/Dpy worms. This similarity most likely accounts for the miscategorization of some Unc/Dpy animals as Mut in the GFP control. A precise quantification of each phenotype was not possible, since they frequently occurred in differing combinations. A recurring pattern concerning the combinations was not recognized.

Taken together, the results of the RNAi against *mys-2* showed a significant effect of both constructs. The observed phenotypes were the same, and they occured with similar frequency. Additionally, no phenotypes were observed upon the same RNAi in wild-type worms. Hence, we conclude that the observed effects are likely caused by the knock-down of *mys-2* and are not off-target effects, although we cannot completely exclude effects related to a knock-down of the genes that reside in the same operon, as discussed in section 4.5.

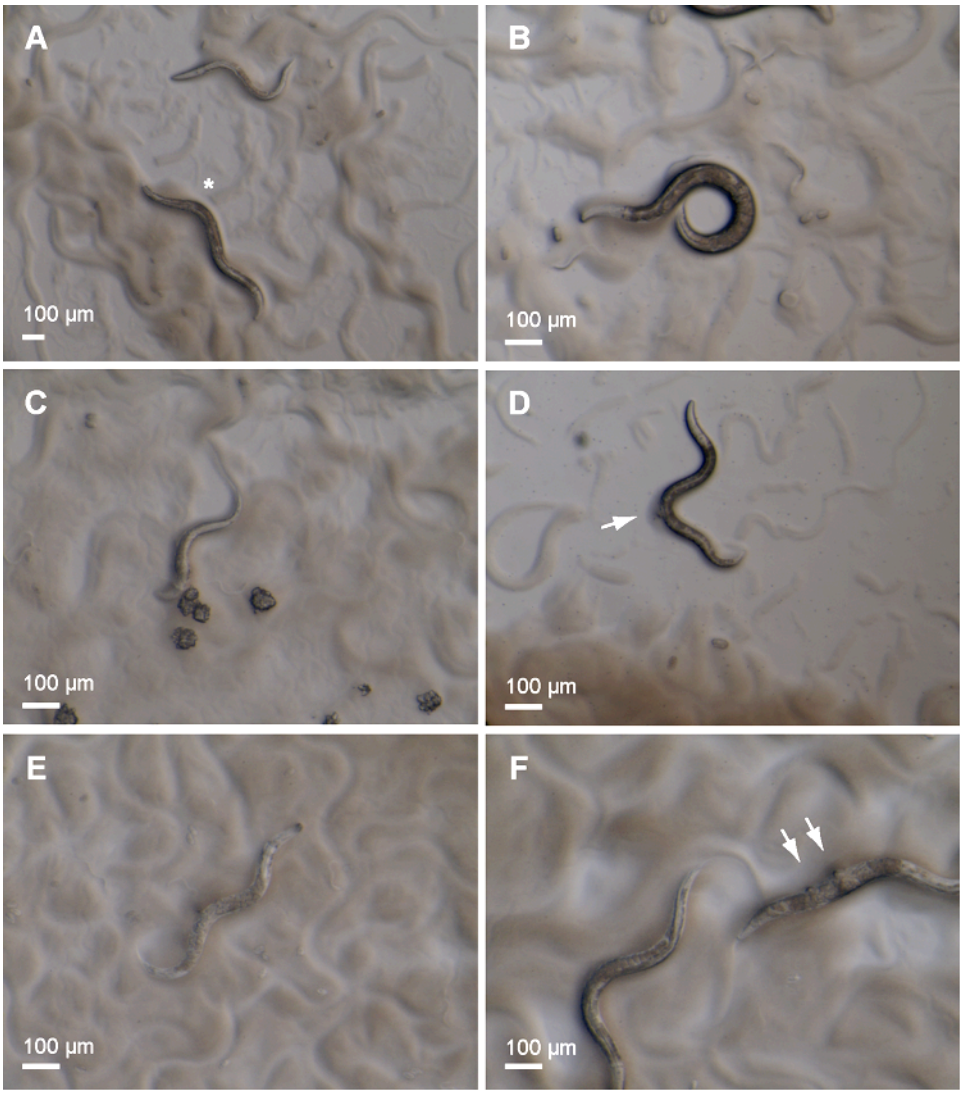


**Figure 22: RNAi against *mys-2* in *mys-2*(ok2429) heterozygotes caused diverse phenotypes;** Dissecting microscopical photographs of**:** (**A**) a phenotypically wild-type (*) compared to Sma; (**B**) typical Unc/Dpy (*unc-101* related); (**C**) severe Sma phenotype; (**D**) strong Pvl (arrow) on slow growing worm (still at L4 larvae stage); (**E**) severe transparent or clear phenotype (Clr); (**F**) severe misdevelopment, possibly multivulvae (Muv, arrows)

The RNAi phenotypes were partially overlapping with the phenotypes observed in *mys-2*(ok2429)m-z- worms. A substantial number of embryonic or larval lethality was observed in the *mys-2*(ok2429)m-z- animals that was not phenocopied in the RNAi, suggesting that the RNAi phenotypes were weaker than the phenotypes of the genetic deletion. The morphology of the small worms in the RNAi was not the same as in *mys-2*(ok2429)m-z- worms. The genetic deleted worms were thinner and sick, while animals depleted for *mys-2* by RNAi, apart from the very severe cases, were usually fertile and tended to be fitter. In general, morphology was more variable among the animals in the RNAi experiments. However, the types of mutant phenotypes were similar.

The characterization of the Mys phenotype and the immunostainings suggested that the maternal contribution with *mys-2* gene products is important in the very early, transcriptionally silent embryo. The higher variety of the RNAi related phenotypes might therefore reflect worms that are heterozygous for the deletion but lack the maternal *mys-2* gene products, causing defects in early gene regulation. With the onset of embryonic transcription, the embryo might express basal levels of *mys-2* that withstand the knock-down by RNAi and are sufficient to regulate later stages of development, resulting in milder phenotypes.

The RNAi results further show that the knock-down of *mys-2* was not strong enough to result in abundant phenotypically consequences in wild-type worms, whereas in animals with only one wild-type *mys-2* allele, reflecting a weaker genomic background, the knock-down was sufficient to cause abundant phenotypes. This opens up the possibility to make use of RNAi in uncovering genetic interactions. It seems possible that the knock-down of *mys-2* can cause effects if other factors that are involved in the same mechanisms or pathways, are weakened by mutations or deletions. Analogous to that approach, the knock-down of such unknown factors in the *mys-2* strain might also reveal genetic interactions.

## 3.9. The knock-down of *mys-2* in dosage compensation deficient mutants

The MYS-2 homologue in flies, dMOF, plays an essential role in the dosage compensation of the male X chromosome, which is transcriptionally upregulated due to hyperacetylation of H4K16 (Hilfiker et al. 1997). In order to determine whether MYS-2 has a role in *C. elegans* dosage compensation, we sought to knock it down in combination with mutations in subunits of the Dosage Compensation Complex (DCC). Since the dosage compensation in worms is achieved through downregulation of both X chromosomes in hermaphrodites (Meyer 2010), we hypothesized a MYS-2 function antagonistic to the DCC that would result in weaker phenotypes.

In order to test this hypothesis, strains with mutations in genes encoding subunits of the DCC, namely *sdc-2*, *sdc-3*, *dpy-26* or *dpy-27*, were fed with bacteria expressing *mys-2* dsRNA (pAE1020). Neither a weakening, nor a strengthening of the DCC-related Dumpy phenotype was observed (data not shown). To test this further, the *dpy-27* and *sdc-2* strains were injected with *mys-2* A dsRNA, since it had a slightly stronger effect in the *mys-2* deletion strain than *mys-2* B. GFP dsRNA served as the negative control again. However, no effects related to the injection of *mys-2* A dsRNA were detected (data not shown).

The false-negative rate of RNAi in *C. elegans* is about 30% (Kamath et al. 2003). Therefore, *dpy-27* was targeted by RNAi in the *mys-2*(ok2429) deletion strain, analogous to the approach above. We recapitulated a published RNAi experiment targeting *dyp-27* in wild-type (Piano et al. 2002). The *dpy-27* RNAi in wild-type led to the expected phenotypes of 11 % dumpy (Dpy) worms, 7 % larval arrest (Lva) and 3 % of other phenotypes, like for instance locomotion variant (Table 7). We then targeted *dpy-27* for knock-down in animals heterozygous for *mys-2*(ok2429) and compared the scored phenotypes to the RNAi in wild-type (Table 7).

The progeny of a *mys-2*(ok2429) heterozygote is composed of phenotypically wild-type and *unc-101* related Unc/Dpy animals at a ratio of 3:1 (Figure 17). To indicate a genetic interaction of *dpy-27* and *mys-2*, a significant change in this 3:1 ratio was expected. Following the hypothesis above of a MYS-2 function antagonistic to the DPY-27 containing DCC, weaker phenotypes were expected in animals that were hetero- or homozygous for the *mys-2*(ok2429) deletion allele. The homozygous *unc-101* animals are homozygous for the *mys-2* wild-type allele and should therefore be affected more strongly by the knock-down of *dpy-27*, thus perhaps increasing lethality or developing phenotypes distinct from the *unc-101*-related Unc/Dpy phenotype. This would result in less animals displaying the *unc-101* related Unc/Dpy phenotype, shifting the ratio towards phenotypically wild-types, for instance 4:1 or higher.

The RNAi of *dpy-27* in the *mys-2*(ok2429) deletion strain was complicated to interpret, since the *dpy-27* related phenotype (Dpy) overlapped with the *unc-101* related phenotype (Unc/Dpy). Progeny of homozygous mothers showed no additional effect and are not included in the results given in Table 7. The percentage of phenotypically wild-type animals is reduced, and 22 % of mutant animals with phenotypes other than Dpy or Unc/Dpy were observed. This might suggest an effect, but most important is the ratio of phenotypically wild-types to Unc/Dpy, which is still roughly 3:1 (46% : 16% equals 2.9:1). This indicates that *unc-101* animals, which are homozygous for the *mys-2* wild-type allele, are equally strongly affected by the dpy-27 knock-down as animals that are hetero- or homozygous for the *mys-2* deletion. Taken together, this indicates that there is no genetic interaction between *mys-2* and *dpy-27*.

**Table 7: Overview of phenotypes upon RNAi of *dpy-27* in wild-type and in the *mys-2* (ok2429) deletion background;** Occurrence of phenotypically wild-types (WT), dpy-27 related dumpy (Dpy), dpy-27 related larval arrest (Lva), *unc-101* related Unc/Dpy and other (including Sma, Pvl) are given as number and as percentage of the total number of animals (in brackets);

| strain | RNAi target | WT | Dpy | Lva | other | total |
|---|---|---|---|---|---|---|
| wild-type | *dpy-27* | 934 (78%) | 124 (11%) | 78 (7%) | 30 (3%) | 1166 |
| **strain** | **RNAi target** | **WT** | **Dpy** | **Unc/Dpy** | **other** | **total** |
| *mys-2* (ok2429) | *dpy-27* | 613 (46%) | 213 (16%) | 212 (16%) | 288 (22%) | 1326 |

We then tested the hypothesis that MYS-2 might have a function in dosage compensation, possibly in the upregulation of X in both sexes, with regards to "Ohno's hypothesis" (Deng et al. 2011). The strain CB1489 carries the *him-8*(e1489) allele. This leads to increased levels of chromosome non-disjunction, causing the occurrence of 37 % XO males and 6 % XXX hermaphrodites, which are dumpy. This strain offered the possibility of testing two issues. Firstly, the high occurrence of males might reveal whether MYS-2 has a sex-specific effect. Secondly, males only have one X chromosome. If MYS-2 is involved in general X upregulation, then the knock-down of *mys-2* might have more severe effects in males than in hermaphrodites, where the two X chromosomes are additionally regulated by the DCC.

**Table 8: Overview of phenotypes caused by RNAi against *mys-2* in a *him-8* mutant background;** Occurrence of wild type males (WT XO), wild type hermaphrodites (WT XX), dumpy hermaphrodites (Dpy XXX) and additional mutant (Mut) phenotypes is given as number and as percentage of the total number of animals (in brackets);

| Time after injection | RNAi target | WT (XO) | WT (XX) | Dpy (XXX) | Mut | total |
|---|---|---|---|---|---|---|
| 0 – 24 h | GFP | 79 (43%) | 95 (52%) | 8 (4%) | 0 | 182 |
| | *mys-2* A | 160 (40%) | 225 (56%) | 6 (1%) | 8 (2%) | 402 |
| | *mys-2* B | 225 (46%) | 232 (48%) | 16 (3%) | 13 (3%) | 486 |
| 24 – 48 h | GFP | 93 (47%) | 99 (50%) | 7 (4%) | 1 (1%) | 200 |
| | *mys-2* A | 136 (32%) | 252 (60%) | 11 (3%) | 24 (6%) | 423 |
| | *mys-2* B | 211 (41%) | 271 (52%) | 11 (2%) | 24 (5%) | 517 |
| 48 – 72 h | GFP | 43 (44%) | 48 (49%) | 6 (6%) | 1 (1%) | 98 |
| | *mys-2* A | 63 (37%) | 87 (51%) | 5 (3%) | 14 (8%) | 169 |
| | *mys-2* B | 112 (41%) | 146 (53%) | 2 (1%) | 16 (6%) | 276 |

As shown in Table 8, the occurrence of males in the *him-8*(e1489) strain was not strongly affected upon knock-down of *mys-2*. Some mutant phenotypes were observed that are likely caused by *mys-2* RNAi, but both males and hermaphrodites were equally affected. A sex-specific effect of the *mys-2* knock down was not detected.

The gene *her-1* is repressed in hermaphrodites and initiates male sex determination in males (Hodgkin 1980). The strain CB1561 comprises animals with only one X chromosome (XO) and a mutation in *her-1*, which represses male sex determination. Although having a male genotype, all animals develop into phenotypically wild-type hermaphrodites due to the *her-1* (hermaphrodization) mutation. Since dosage compensation is dependent on the ratio of autosomes to X chromosomes, no dosage compensation is established in these animals. Similar to the *him-8* strain, we had the possibility of testing whether MYS-2 has effects on a single X chromosome that is not additionally regulated by the DCC, though this time in hermaphrodites. Upon knock-down of *mys-2*, only rare mutant individuals were scored that reflect the RNAi effect in wild-type worms (data not shown). This did not indicate a function of MYS-2 in general X upregulation.

In order to test the hypothesis of a MYS-2 containing HAT complex that shares homology with the MOF containing NSL complex in flies, the gene F54D11.2 was targeted by RNAi. This gene is the worms closest homologue to NSL3 in flies, encoding a subunit of the NSL complex (Raja et al. 2010). The corresponding dsRNA was injected in wild-type worms and in the *mys-2* deletion strain. No phenotypes were observed in wild-type, and no additional phenotypes were observed in the deletion strain (data not shown).

## 3.10. A yeast two-hybrid screen revealed possible interactions of MYS-2

The homologues of MYS-2 in yeast, flies and humans are reported to be part of multisubunit HAT complexes. Sas2 is the catalytical subunit of the SAS-I complex , MOF in *Drosophila* is part of the MSL and the NSL complex and MOF in humans is reported to be part of two distinct complexes, homologous to the fly complexes (Smith et al. 2000; Meijsing and Ehrenhofer-Murray 2001; Dou et al. 2005; Smith et al. 2005; Raja et al. 2010). It is therefore possible that MYS-2 also is part of a complex in *C. elegans*. With the RNAi experiments described above, we tested candidates for an interaction with MYS-2 that were chosen based on their homology to NSL components or their involvement in dosage compensation.

In order to take an unbiased approach to identify possible interaction partners of MYS-2, we screened *C. elegans* proteins for interaction with MYS-2 in a yeast two-hybrid screening system. We sought to identify subunits of a possible MYS-2 containing complex that bind

directly to MYS-2. Furthermore, this approach might also reveal acetylation substrates that can be bound by MYS-2. Due to the identity of MYS-2 as a possible HAT, we primarily expected to find factors involved in chromatin modification, chromatin remodelling or chromatin subunits, or perhaps histones as a potential substrate.

A construct was generated to express a fusion of the LexA DNA-binding domain and full-length MYS-2 (pAE1336). Additionally, a construct that lacks 210 amino acids of the MYS-2 N-terminus was generated (pAE1446). The expression of both constructs in yeast was confirmed by western blots probed with an α-LexA antibody (data not shown).

In total, approximately 1.5 million transformants were screened, which equals a 75 x coverage of the predicted 20000 proteins in *C. elegans*, assuming 100% coverage by the cDNA library. The screen yielded 356 primary candidates, of which 35 passed the final tests and were identified by sequencing analysis (see Materials and Methods section 2.3.5). They are presented in Table 9.

**Table 9: Candidates identified in a yeast two-hybrid screen against MYS-2;** n - times found independently, if higher than 1; GO Term – Gene Ontology term Molecular function; Homology – closest homologue in yeast or humans; Description – as given by Wormbase (WS234)

| | n | Gene | GO Term (Molecular function) | Homology | Description |
|---|---|---|---|---|---|
| LexA-MYS-2(211-550) | 3 | C39E9.12 | Nucleic acid binding | Nematode-specific | - |
| | 2 | *csn-2* | Protein binding | RPN6 (yeast) | Signalosome complex subunit 2 |
| | | *hcp-3* | DNA binding | CENP-A | Centromeric histone H3 variant |
| | | *his-72* | DNA binding | Histone H3 | Canonical histone H3 |
| | | *iff-1* | Translation elongation factor activity; RNA binding | HYP2 (yeast) | Translation elongation factor eIF-5A |
| | | *ubq-2* | Protein binding, structural component of ribosome | RPL40A (yeast) | Fusion protein, cleaved into ubiquitin and ribosomal protein of 60S large subunit |
| | | *rla-1* | Ribosome | RPP1A (yeast) | Encodes an acidic ribosomal subunit protein P1 |
| | | *rpl-18* | Structural constituent of ribosome | RPL18A (yeast) | Large ribosomal subunit L18 |
| | | *rpl-19* | Structural constituent of ribosome | RPL19A (yeast) | Large ribosomal subunit L19 |
| | | *rps-15* | Structural constituent of ribosome; RNA binding | RPS15 (yeast) | Encodes a small ribosomal subunit S15 protein |
| | | *pbs-5* | Proteasome core complex | PRE2 (yeast) | Proteasome beta subunit |

| | | | | | |
|---|---|---|---|---|---|
| | | *act-3* | ATP-binding | ACT1 (yeast) | Actin |
| | | *act-4* | ATP-binding | ACT1 (yeast) | Actin |
| | | *nmy-1* | ATP binding | MYO1 (yeast) | Encodes a class II non-muscle myosin |
| | | *clec-265* | Carbohydrate binding | REG1A (human) | C-type lectin |
| | | *mai-2* | Enzyme inhibitor activity | ATPIF1 (human) | Mitochondrial ATPase inhibitor |
| | | *far-1* | Lipid binding | Nematode-specific | Nematode fatty acid retinoid binding |
| | | *spk-1* | Protein SR kinase activity | SKY1 (yeast) | Encodes a serine/threonine kinase |
| | | *idh-1* | Isocitrate dehydrogenase (NADP+) activity | IDP1 (yeast) | Encodes a predicted cytosolic isocitrate dehydrogenase |
| | | *pas-5* | Endopeptidase activity | PSMA5 (human) | Encodes a proteasome alpha-type five subunit of the core 20S proteasome subcomplex |
| | | Y62E10A.2 | Ribonuclease P activity; nucleic acid binding | POP7 (human) | Ribonuclease P protein subunit p20 |
| | | *glt-1* | Sodium:dicarboxylate symporter activity | SLC1A2 (human) | Encodes a predicted plasma membrane glutamate transporter |
| | | Y82E9BR.3 | Hydrogen ion transmembrane transporter activity | OLI1 (yeast) | - |
| LexA-MYS-2 | 3 | *his-45* | DNA binding | Histone H3 | Canonical histone H3 |
| | | *his-74* | DNA binding | Histone H3.3 | Histone variant H3.3 |
| | | *his-72* | DNA binding | Histone H3 | Canonical histone H3 |
| | | *act-1* or *act-3* | ATP-binding | Actin | Actin |
| | | *col-139* | structural constituent of cuticle | Collagen | Collagen |
| | | F45H11.5 | n.d. | COX19 yeast | required for cytochrome c oxidase assembly |
| | | Y34B4A.9 | n.d. | Nematode-specific | - |

Interestingly, histone H3 was identified several times independently as a MYS-2 interactor. Like most other organisms, worms contain multiple genes encoding H3. *his-45* was found three times independently, and *his-72* was found two times independently (once in each screen). Both encode the highly conserved histone H3. Furthermore, two candidates encoding variants of H3, *his-74* (H3.3) and *hcp-3* (CENP-A), were found, suggesting that MYS-2 is able to interact specifically with H3, at least under non-physiological conditions in the yeast two-hybrid screen, and thus, that H3 or H3 variants may be MYS-2 substrates.

Notably, the unknown gene C39E9.12 was found three independent times as a MYS-2 interator and is predicted by Gene Ontology to have a molecular function in nucleic acid binding due to its SAP DNA-binding domain. It only has homologues in other nematodes, and has not been investigated in detail yet, so its function is unknown.

Moreover, we found multiple interactor clones for ribosomal proteins, several cytoskeleton related factors (actin, myosin and collagen), a translation elongation factor and others. Interactors identified in the Yeast two-hybrid system, have to be reviewed carefully. Although conditions in the yeast nucleus are technically *in vivo*, they do not exactly simulate conditions in a *C. elegans* nucleus. The occurrence of false positives is likely, common false-positive interactors include ribosomal proteins, mitochondrial proteins, cytochrome oxidases, proteasome subunits and collagen-related proteins (Hengen 1997). Eleven of the identified interactors belong to one of those groups. Whether the remaining 13 candidates are also false-positives or reflect real interactors can only be addresses in directed approaches. In summary, the screen identified on epotential MYS-2 complex component (C39E9.12), a possible DNA binding protein, as well as three histine H3 variants as potential substrates of a hypothesized MYS-2 HAT complex.

# 4. Discussion

Members of the MYST family of histone acetyltransferases have so far been shown to be involved in gene regulation by their catalytical function, the acetylation of specific histone residues (Sapountzi and Cote 2011). One of the *C. elegans* members of this protein family, MYS-2, was the subject of this study. It has so far been linked to the inheritance of RNAi and to the maintenance of cell identity, but has not been characterized in detail. Using a combination of RNAi, microscopy, a yeast two-hybrid screen, immunostainings and immunopurification, we have addressed elemental questions concerning the expression, localization and interactions of MYS-2 in order to characterize it in more detail.

In immunostainings, we found MYS-2 to be expressed ubiquitously throughout development and to be enriched in the nucleus, where it localized to chromatin. Furthermore, we found MYS-2 to be essential, since a deletion was lethal. Interestingly, the phenotype was fully rescued by maternal contribution for one generation, and partially rescued in subsequent generations. Partially rescued animals grew more slowly than wild-type and showed severe developmental defects, including vulval defects and abnormal gonad and germ nuclei morphology, indicating a fundamental function in global gene regulation. A knock-down of *mys-2* by RNAi disrupted the maternal rescue and increased the number of mutant phenotypes, thus further supporting an important function in early embryonic development. Furthermore, several potential interaction partners of MYS-2 have been identified, which provide interesting leads for future analysis of MYS-2 interactors.

## 4.1. *mys-2* was expressed ubiquitously

We found *mys-2* to be expressed ubiquitously, with MYS-2 localized in each nucleus from the egg to the adult hermaphrodite, and the signal colocalized with DNA. While the results do not exclude an additional cytosolic localization, the majority was located inside the nucleus. A significant increase or decrease of the MYS-2 signal was neither detected in specific tissues nor at specific developmental stages. Instead, uniform levels of MYS-2 were observed, which is consistent with the data from a recent study that determined mRNA levels of the whole transcriptome throughout embryonic development in a high-throughput assay. The data for *mys-2* display an even expression level up to the first larvae stage L1, with a temporary reduction in the early embryo (Levin et al. 2012).

The ubiquitous expression of MYS-2 suggests that it has a very elementary function, perhaps as a house-keeping factor working on chromatin. Indeed, known histone modifiers in *C. elegans* show very similar expression profiles during embryogenesis, as for instance the

HDAC *sir-2.1*, the histone methyltransferases *set-2* and *mes-4*, or two further MYST HATs, *mys-1* and *mys-4* (Levin et al. 2012).

## 4.2. *mys-2* was essential for normal development

In *C. elegans*, three types of mutations identify essential functions: zygotic lethal mutations, maternal-effect sterile mutations and sterile mutations. All of these prevent the development from an egg to a fertile adult. Zygotic lethal mutations cause the animal to die at a certain stage of development, and sterile mutations prevent the reproduction of an animal. Maternal-effect sterile mutations are a special class of sterilizing mutations, in that they prevent the development of the progeny of a mother homozygous for the mutation. The *mes* (maternal-effect sterile) genes are the most prominent example, where homozygous hermaphrodites are themselves fertile when born by a heterozygous mother, but their progeny fails to develop a functional germline (Strome 2005).

We found worms to be viable when born by a mother heterozygous for the allele *mys-2*(ok2429). They were phenotypically indistinguishable from their mother and from wild-type worms. However, the progeny produced by homozygous individuals was found to suffer severe developmental defects. They were lethal at differing stages of development, grew more slowly and showed abnormal morphology in a variety of tissues. In particular, morphology of the vulva, the gonad and the mitotic germ nuclei was affected. A small portion of these animals developed into fertile adult hermaphrodites, which produced progeny suffering from similar phenotypes. We observed this rescue for up to three generations, but all lines died eventually. These findings indicate lethality upon the loss of MYS-2, which is well rescued in the first homozygous generation, most likely by maternal contribution, and viability can be rescued in subsequent generations, though with severe defects. We confirmed the maternal contribution of *mys-2* gene products, since robust MYS-2 signals were observed in immunostainings of 2-cell and 4-cell embryos. mRNA transcription is repressed in the embryo up to the 4-cell stage, and even up to the 100-cell stage in the germ cell lineage (Seydoux and Dunn 1997). Therefore, the embryo is completely dependent on maternally provided gene products. Thus, the observed signals reflect maternally provided MYS-2. Together with the strong phenotype, this strengthens the hypothesis of MYS-2 having an essential function in early development.

With respect to the maternal rescue of the *mys-2* mutant phenotype, it is interesting to speculate whether this is only dependant on the maternal contribution, or whether there is a function of MYS-2 in the maternal germ cells that provides epigenetic information for the

next generation. Such a mechanism has been reported for the H3K36 methyltransferase MES-4, which transmits a memory of germline expression to the progeny via histone modification (Rechtsteiner et al. 2010). A temperature-sensitive *mys-2* allele would provide a powerful tool to further study the most important time of the MYS-2 function.

The histone variant HTZ-1 (H2A.Z) has been linked to the maintenance of specific chromatin states at promoters that are dynamically regulated during development. It is ubiquitously expressed and embryonic lethal when depleted by RNAi. However, embryos carrying a homozygous deletion can be rescued by maternal contribution and develop into adult hermaphrodites with grossly normal morphology, although 80 % are sterile (Whittle et al. 2008). CBP-1 is a HAT in worms, belonging to the p300/CBP family. Upon depletion by RNAi, embryos die early due to defects in cell differentiation. Interestingly, these defects can be partially suppressed by an additional depletion of the HDAC *hda-1* (Shi and Mello 1998). In another study, a protein recombinantly expressed from the gain of function allele *cbp-1*(ku258) displayed a sevenfold increased HAT activity *in vitro*. It was shown to suppress the Muv phenotype caused by overinduction of Ras signalling. Animals carrying the *cbp-1*(ku258) allele were generally sick and displayed pleiotropic defects, including sterility, embryonic and larval lethality, a protruding vulva and slow growth. The authors proposed a function for CBP-1 in transcriptional activation and furthermore suggested that alterations in the equilibrium of acetylation levels result in disturbance of global transcription (Eastburn and Han 2005). The *hda-1* gene is homologous to HDAC1 (human) and Rpd3 (yeast), which are class (I) HDACs. Interestingly, maternal and zygotic knock-down of the ubiquitously expressed *hda-1* results in embryonic lethality. Disruption of zygotic expression alone by a point mutation in the gene resulted in defective vulval development and gonadogenesis (Dufourcq et al. 2002).

These examples demonstrate that chromatin states, including acetylation levels, play a key role in transcriptional regulation in the worm. Mutations affecting such factors like *cbp-1* and *hda-1* display pleiotropic phenotypes that are similar to our observations in *mys-2*-depleted worms.

## 4.3. A role for MYS-2 in dosage compensation?

Dosage compensation in *C. elegans* is achieved by a twofold downregulation of both X chromosomes in the hermaphrodite, such that expression levels then are equal to the expression from the single male X chromosome. The downregulation is mediated by the dosage compensation complex (DCC), which specifically localizes to the hermaphrodite X

chromosomes. Chromatin modifications are likely to be involved in this mechanism, since hermaphrodite X chromosomes differ in the pattern of chromatin marks from the autosomes. For instance, the X chromosome is depleted of H4K16Ac in the maternal germline (Meyer 2010). The X chromosomal depletion of H4K16Ac is dependent on the HDAC SIR-2.1 (Wells et al. 2012). *Drosophila* evolved the opposite strategy to achieve dosage compensation, namely that the MOF-containing MSL complex targets the single male X chromosome and hyperacetylates H4K16, resulting in a twofold upregulation to match the average expression levels of the two female X chromosomes (Smith et al. 2000).

Another aspect of dosage compensation is the equalization of expression levels between the autosomes and the X chromosomes, since a twofold downregulation of X chromosomes in hermaphrodites and a single X in males in *C. elegans* imply halved expression levels of X-linked genes in comparison to autosomal genes. RNA-Seq analysis has shown that this is not the case in worms, flies and mammals. Instead, the average expression levels are equal between X-linked and autosomal genes. It therefore has been hypothesized that the X chromosomes are upregulated, regardless of the sex, by an unknown mechanism, also referred to as "Ohno's hypothesis" (Deng et al. 2011).

Based on the homology of MYS-2 with Sas2, hMOF and dMOF in particular, we hypothesized a function for MYS-2 in dosage compensation mediated by the acetylation of H4K16. It may be involved in the sex-specific downregulation, possibly by fine-tuning H4K16 acetylation levels that are reduced by SIR-2.1. The sex-independent upregulation of X is another possible option, where MYS-2 might regulate expression levels by its catalytical function. Both options would imply antagonistic functions to the DCC.

We tested this hypothesis by RNAi-mediated depletion of *mys-2* in several genetic backgrounds mutated in DCC subunits, and by the knock-down of *dpy-27* in a *mys-2*(ok2429) mutant background. The results did not support a genetic interaction between MYS-2 and the DCC. The RNAi-mediated depletion of *mys-2* in *him-8* males and XO *her-1* hermaphrodites also showed no effect. Additionally, in immunostainings, no specific localization of MYS-2 to a certain chromosome was detected. The X chromosome in the maternal germline, which is depleted for H4K16Ac, showed MYS-2 signals that were indistinguishable from autosomes at the cytological level. Thus, our findings do not support the hypothesis of an involvement of MYS-2 in dosage compensation, though the possibility cannot be completely excluded. Taking into account that *mys-2* RNAi in wild-type was very inefficient, and that depletion of *mys-2* was reported to disrupt inheritance of RNAi mediated silencing (Vastenhouw et al.

2006), it is possible that the RNAi mechanism itself is affected upon depletion of *mys-2*, thereby masking effects that *mys-2* may have in this experimental setup.

## 4.4. Is MYS-2 a chromatin modifier?

The close relationships between MYS-2 and Sas2, dMOF and hMOF, particularly in the catalytical MYST domain (Figure 7), strongly suggested a histone acetyltransferase activity for MYS-2. We hypothesized specificity towards H4K16, since all three homologues were shown to acetylate H4K16 and are responsible for a major portion of that histone mark (Akhtar and Becker 2000; Meijsing and Ehrenhofer-Murray 2001; Taipale et al. 2005). One approach to address this issue were immunostainings with an α-H4K16Ac antibody. We observed the reported abundant signal, as well as the depletion from germline X chromosomes in wild-type (Wells et al. 2012). However, in worms depleted for MYS-2, a significant decrease in the signal was not observed. It is therefore rather unlikely that MYS-2 is the prime H4K16 acetyltransferase in *C. elegans,* but these findings do not exclude the possibility of a MYS-2 contribution to H4K16Ac. In this study, only global levels of H4K16Ac were examined, and a more extensive analysis of the genome-wide H4K16Ac distribution in a *mys-2* mutant is necessary in order to further investigate this question.

The identification of potential interactors or substrates of MYS-2 can potentially provide information on the molecular environment of MYS-2. An immunopurification with rabbit α-MYS-2 antibodies precipitated MYS-2, but did not yield high-enough amount of co-purifying protein to identify possible interactors. NSL3 is a subunit of the NSL complex, a second MOF-containing HAT complex in *Drosophila* that is distinct from MSL (Lam et al. 2012). There is evidence, that both complexes are conserved in humans (Dou et al. 2005; Smith et al. 2005). We hypothesized that a MYS-2 containing HAT complex in the worm might contain homologues to NSL subunits in flies. The *C. elegans* genome contains no homologues to subunits of the MSL complex, apart from *mys-2*, but three genes are homologous to members of the NSL complex, namely H28O16.2 (MCRS1), F54D11.2 (NSL3) and *wdr-5.1* (WDS). The depletion of the NSL3 homologue, F54D11.2, in *mys-2*(ok2429) worms, served to investigate a genetic interaction with *mys-2* that would suggest an NSL-like complex in *C. elegans*. Our findings did not support this hypothesis. Taking the above-mentioned possible problems with RNAi into account, this however does not rule out the possibility of a conserved, NSL-like complex in *C. elegans*.

A screen for MYS-2 interactors using the yeast two-hybrid system was an unbiased approach to identify interaction partners or substrates of MYS-2. Identified candidates from such a

screen must be reviewed carefully, because false-positive interactions can arise, for instance through folding and post-translational modifications of expressed proteins that do not reflect *in vivo* folding in worm nuclei. Additionally, proteins are brought together in the two-hybrid assay that might never get in contact with each other under physiological conditions due to different spatial or temporal regulation. We anticipated to identify homologues of known factors involved in chromatin modification or remodelling, which could subsequently be confirmed by independent approaches. Among the candidates found, the gene C39E9.12, which was identified in the yeast two-hybrid screen three independant times, might be a candidate in that context. It is predicted to have a nucleic acid binding function, and an expression analysis shows an even profile throughout embryonic development, similar to *mys-2* (Levin et al. 2012). Having only homologues within the nematode phylum, it could be a possible nematode-specific factor involved in chromatin regulation that targets a MYS-2 containing complex to the promoters of a number of house-keeping or developmental genes in the worm genome.

Furthermore, seven independent clones encoding histone H3 or an H3 variant, like H3.3 and CENP-A, were identified. Additionally, both versions of the *mys-2* bait interacted with them. This suggests H3 as a starting point for a closer analysis of MYS-2 substrate specificity. Results confirming this substrate specificity would be somewhat surprising, since H4K16 is the major target of the closest MYS-2 homologues. However, it should be noted that the SAS-I complex in *S. cerevisiae* shows activity towards H3K14 (Sutton et al. 2003). Also, Sas2 interacts by yeast two-hybrid with the yeast homologue of CENP-A (Cse4), though the relevance of this interaction remains to be determined (Seitz 2004). Further binding partners or non-histone substrates could be among the other identified clones, though only further studies can separate them from false-positives.

## 4.5.The *mys-2* sequence and its genomic environment

Our analysis of the *mys-2* cDNA clone displayed a difference to the annotated coding sequence. We did not further analyze the issue, whether this reflects the actual coding sequence or not. In order to circumvent potential problems, RNAi constructs and the antigen for antibody production were designed to not contain the part deleted in the cDNA clone. Nevertheless, the resulting altered amino acid sequence a more significant alinement to the closest MYS-2 homologues Sas2, dMOF and hMOF, as it removes a stretch of 17 amino acids inside of the MYST domain that was unique to the MYS-2 sequence (Figure 9). Furthermore, the composition of the 51 basepair sequence appears to be rather intronic, with

long stretches of the same nucleotide (Figure 8), making it seem unlikely that this would be exonic sequence.

Operons are a common form of gene organization in bacteria, where two or more genes are under the control of a single promoter that regulates transcription of a polycistronic RNA. Nematodes have re-evolved this feature. Clusters of up to eight genes are transcribed to one polycistronic pre-mRNA, which is co-transcriptionally spliced (Blumenthal 2012). Those operons can have internal promoters, allowing operon-independent regulation of single genes (Huang et al. 2007).

The *mys-2* gene is located downstream of the two genes Y63D3A.7 and Y63D3A.8, and all three together are annotated as the operon CEOP1731 (Wormbase, WS234). This brings up the problem that we cannot exclude the possibility that the observed effects of the knock-down of *mys-2* are due to a disruption of the whole operon, as it has been reported that RNAi can also target pre-mRNA (Bosher et al. 1999). However, the *mys-2*(ok2429) deletion allele lacks approximately two kilobases that contain the first three exons of *mys-2*, but do not affect the coding sequence of the gene upstream. We therefore consider the deletion-related effects to be exclusively due to the absence of *mys-2* function.

Being the last gene of the operon makes it rather unlikely that *mys-2* expression is regulated from a region immediately upstream. A promoter upstream of Y63D3A.7 is more likely to regulate expression of the whole operon. This is presumably the explanation why no expression of GFP was observed, when under the control of a region two kilobases upstream of *mys-2*. This furthermore indicates that *mys-2* does not possess an internal, *mys-2* specific promoter, at least not in the upstream region tested here. Thus, we reasoned that only a construct containing the complete operon is suitable to construct a *mys-2*::GFP-reporter. The cosmid K03D10 contains the *mys-2* open reading frame, but not the complete operon. Therefore, the YAC Y63D3 represented a possibility to integrate GFP into the *mys-2* coding sequence. Additionally, the YAC is expected to contain all regulatory elements needed to express a *mys-2*::GFP fusion like the endogenous *mys-2*. However, expression of *mys-2*::GFP was never observed, although the presence of the GFP DNA sequence was confirmed by single worm PCR in individual animals. DNA injected into *C. elegans* gonads forms extrachromosomal arrays with repeats of the transformed DNA molecules (Stinchcomb et al. 1985). Repetitive elements are silenced in the *C. elegans* germline, but since immunostainings displayed ubiquitous expression of MYS-2, this is unlikely to be the explanation for why MYS-2::GFP expression from the YACs was not observed. The finding that a gain of function allele of the HAT *cbp-1* with increased catalytical activity resulted in severe mutant

phenotypes demonstrates that accurate expression levels can be highly important for genes to maintain wild-type function (Eastburn and Han 2005). Other essential genes can also be lethal when overexpressed (Prof. Ralf Schnabel, personal communication). This might be a possible explanation for the lack of GFP expression from the *mys-2*::GFP in-frame-integrations on the YAC. One can expect that the YAC breaks when passing the narrow injection needle. The worms found positive for GFP in the single worm PCR might therefore reflect transgenes that only contain a portion of the *mys-2* containing operon including GFP, which fails to express the operon. However, intact operons would be selected against, due to lethality in this scenario, which would further explain why transformations of the YAC failed to rescue the *mys-2*(ok2429)deletion.

## 4.6. Summary and outlook

This study was initiated in order to characterize the function of MYS-2, a member of the MYST family of histone acetyltransferases in *C. elegans*. The closely related Sas2 in yeast has been studied extensively in our group and was shown to maintain euchromatic identity in subtelomeric regions and has been linked to genome-wide transcription elongation by acetylating H4K16 (Kimura et al. 2002; Suka et al. 2002; Heise et al. 2012). The *Drosophila* homologue MOF is well-known for its essential function in male dosage compensation and the hyperacetylation of the X chromosome to enhance transcriptional activation (Akhtar and Becker 2000). MOF in humans is also associated to transcriptional activation and has been shown to acetylate H4K16 (Li et al. 2009). A loss of H4K16Ac is furthermore a characteristic of many human cancer forms (Fraga et al. 2005). It is therefore most surprising that the closest homologue has never been deeply investigated in the well-established model organism *C. elegans*.

This study provides a first foray into this area by addressing elementary questions regarding localization, expression pattern and interactions of MYS-2. It is currently premature to construct a detailed model of the MYS-2 function, but our findings suggest a function in global transcriptional regulation, presumably as a chromatin modifier. Loss of MYS-2 results in pleiotropic developmental defects, implying that a number of pathways are affected. It is furthermore essential, ubiquitously expressed, localized to chromatin and maternally provided to the egg. The finding that animals depleted for *mys-2* by deletion can be rescued to be phenotypical wild-type by maternal contribution indicate that the MYS-2 function is most important in early development. This is a time where transcriptional regulation is highly dynamic due to the plethora developmental programs, and even small alterations in precise

regulation are likely to have drastic consequences. These findings are consistent with reports on other chromatin modifiers in *C. elegans*. Interestingly, MOF null mutant mouse embryos lack H4K16Ac and arrest at the blastocyst stage, indicating an essential function for MOF in mammalian embryogenesis (Gupta et al. 2008).

However, still many questions about MYS-2 remain to be addressed. Most interesting would be the identification of additional subunits in a hypothesized MYS-2 containing complex. The clones identified in the yeast two-hybrid screen provide candidates that possibly interact with MYS-2. With further optimization, it might be possible to co-purify potential binding partners in immunoprecipitations using the α-MYS-2 antibodies. This would provide a basis for directed interaction studies using genetic, cytological and/or biochemical approaches. Genetic interaction studies might as well be useful, to reveal possible crosstalk between MYS-2 and other chromatin modifiers as for instances the HDACs HDA-1 or SIR-2.1. A deeper analysis of the localization of MYS-2, especially on the genomic level, can further narrow its impact on chromatin-mediated regulation. A corresponding approach using ChIP-Seq has already been initiated.

# 5. References


Ahringer (ed.) J. Reverse genetics. in *WormBook : the online review of C elegans biology* (ed. TCeR Community). WormBook.

Akhtar A, Becker PB. 2000. Activation of transcription through histone H4 acetylation by MOF, an acetyltransferase essential for dosage compensation in Drosophila. *Molecular cell* **5**: 367-375.

Akhtar A, Zink D, Becker PB. 2000. Chromodomains are protein-RNA interaction modules. *Nature* **407**: 405-409.

Alekseyenko AA, Peng S, Larschan E, Gorchakov AA, Lee OK, Kharchenko P, McGrath SD, Wang CI, Mardis ER, Park PJ et al. 2008. A sequence motif within chromatin entry sites directs MSL establishment on the Drosophila X chromosome. *Cell* **134**: 599-609.

Allard S, Utley RT, Savard J, Clarke A, Grant P, Brandl CJ, Pillus L, Workman JL, Cote J. 1999. NuA4, an essential transcription adaptor/histone H4 acetyltransferase complex containing Esa1p and the ATM-related cofactor Tra1p. *The EMBO journal* **18**: 5108-5119.

Allfrey VG, Faulkner R, Mirsky AE. 1964. Acetylation and Methylation of Histones and Their Possible Role in the Regulation of Rna Synthesis. *Proceedings of the National Academy of Sciences of the United States of America* **51**: 786-794.

Allis CD, Berger SL, Cote J, Dent S, Jenuwien T, Kouzarides T, Pillus L, Reinberg D, Shi Y, Shiekhattar R et al. 2007. New nomenclature for chromatin-modifying enzymes. *Cell* **131**: 633-636.

Andersen EC, Horvitz HR. 2007. Two C. elegans histone methyltransferases repress lin-3 EGF transcription to inhibit vulval development. *Development* **134**: 2991-2999.

Aparicio OM, Billington BL, Gottschling DE. 1991. Modifiers of position effect are shared between telomeric and silent mating-type loci in S. cerevisiae. *Cell* **66**: 1279-1287.

Barstead RJ, Kleiman L, Waterston RH. 1991. Cloning, sequencing, and mapping of an alpha-actinin gene from the nematode Caenorhabditis elegans. *Cell motility and the cytoskeleton* **20**: 69-78.

Berdichevsky A, Viswanathan M, Horvitz HR, Guarente L. 2006. C. elegans SIR-2.1 interacts with 14-3-3 proteins to activate DAF-16 and extend life span. *Cell* **125**: 1165-1177.

Bheda P, Swatkoski S, Fiedler KL, Boeke JD, Cotter RJ, Wolberger C. 2012. Biotinylation of lysine method identifies acetylated histone H3 lysine 79 in Saccharomyces cerevisiae as a substrate for Sir2. *Proceedings of the National Academy of Sciences of the United States of America* **109**: E916-925.

Blumenthal T. 2012. Trans-splicing and operons in C. elegans. *WormBook : the online review of C elegans biology*: 1-11.

Blumenthal T, Gleason KS. 2003. Caenorhabditis elegans operons: form and function. *Nature reviews Genetics* **4**: 112-120.

Bosher JM, Dufourcq P, Sookhareea S, Labouesse M. 1999. RNA interference can target pre-mRNA: consequences for gene expression in a Caenorhabditis elegans operon. *Genetics* **153**: 1245-1256.

Boudreault AA, Cronier D, Selleck W, Lacoste N, Utley RT, Allard S, Savard J, Lane WS, Tan S, Cote J. 2003. Yeast enhancer of polycomb defines global Esa1-dependent acetylation of chromatin. *Genes & development* **17**: 1415-1428.

Breeden L, Nasmyth K. 1985. Regulation of the yeast HO gene. *Cold Spring Harbor symposia on quantitative biology* **50**: 643-650.

Brenner S. 1974. The genetics of Caenorhabditis elegans. *Genetics* **77**: 71-94.

Celic I, Masumoto H, Griffith WP, Meluh P, Cotter RJ, Boeke JD, Verreault A. 2006. The sirtuins hst3 and Hst4p preserve genome integrity by controlling histone h3 lysine 56 deacetylation. *Current biology : CB* **16**: 1280-1289.

Ceol CJ, Horvitz HR. 2004. A new class of C. elegans synMuv genes implicates a Tip60/NuA4-like HAT complex as a negative regulator of Ras signaling. *Developmental cell* **6**: 563-576.

Clements A, Marmorstein R. 2003. Insights into structure and function of GCN5/PCAF and yEsa 1 histone acetyltransferase domains. *Methods in enzymology* **371**: 545-564.

Consortium CeS. 1998. Genome sequence of the nematode C. elegans: a platform for investigating biology. *Science* **282**: 2012-2018.

Crittenden SL, Troemel ER, Evans TC, Kimble J. 1994. GLP-1 is localized to the mitotic region of the C. elegans germ line. *Development* **120**: 2901-2911.

Cui M, Chen J, Myers TR, Hwang BJ, Sternberg PW, Greenwald I, Han M. 2006a. SynMuv genes redundantly inhibit lin-3/EGF expression to prevent inappropriate vulval induction in C. elegans. *Developmental cell* **10**: 667-672.

Cui M, Han M. Roles of chromatin factors in C. elegans development. in *WormBook : the online review of C elegans biology* (ed. TCeR Community). WormBook.

Cui M, Kim EB, Han M. 2006b. Diverse chromatin remodeling genes antagonize the Rb-involved SynMuv pathways in C. elegans. *PLoS genetics* **2**: e74.

Dekker J. 2008. Mapping in vivo chromatin interactions in yeast suggests an extended chromatin fiber with regional variation in compaction. *The Journal of biological chemistry* **283**: 34532-34540.

Deng X, Hiatt JB, Nguyen DK, Ercan S, Sturgill D, Hillier LW, Schlesinger F, Davis CA, Reinke VJ, Gingeras TR et al. 2011. Evidence for compensatory upregulation of expressed X-linked genes in mammals, Caenorhabditis elegans and Drosophila melanogaster. *Nature genetics* **43**: 1179-1185.

Desai A, Rybina S, Muller-Reichert T, Shevchenko A, Shevchenko A, Hyman A, Oegema K. 2003. KNL-1 directs assembly of the microtubule-binding interface of the kinetochore in C. elegans. *Genes & development* **17**: 2421-2435.

Do CB, Mahabhashyam MS, Brudno M, Batzoglou S. 2005. ProbCons: Probabilistic consistency-based multiple sequence alignment. *Genome Res* **15**: 330-340.

Dou Y, Milne TA, Tackett AJ, Smith ER, Fukuda A, Wysocka J, Allis CD, Chait BT, Hess JL, Roeder RG. 2005. Physical association and coordinate function of the H3 K4 methyltransferase MLL1 and the H4 K16 acetyltransferase MOF. *Cell* **121**: 873-885.

Duerr JS. Immunohistochemistry. in *WormBook : the online review of C elegans biology* (ed. TCeR Community). WormBook.

Duerr JS, Frisby DL, Gaskin J, Duke A, Asermely K, Huddleston D, Eiden LE, Rand JB. 1999. The cat-1 gene of Caenorhabditis elegans encodes a vesicular monoamine transporter required for specific monoamine-dependent behaviors. *The Journal of neuroscience : the official journal of the Society for Neuroscience* **19**: 72-84.

Dufourcq P, Victor M, Gay F, Calvo D, Hodgkin J, Shi Y. 2002. Functional requirement for histone deacetylase 1 in Caenorhabditis elegans gonadogenesis. *Molecular and cellular biology* **22**: 3024-3034.

Eastburn DJ, Han M. 2005. A gain-of-function allele of cbp-1, the Caenorhabditis elegans ortholog of the mammalian CBP/p300 gene, causes an increase in histone acetyltransferase activity and antagonism of activated Ras. *Molecular and cellular biology* **25**: 9427-9434.

Ehrenhofer-Murray AE, Rivier DH, Rine J. 1997. The role of Sas2, an acetyltransferase homologue of Saccharomyces cerevisiae, in silencing and ORC function. *Genetics* **145**: 923-934.

Ehrentraut S, Weber JM, Dybowski JN, Hoffmann D, Ehrenhofer-Murray AE. 2010. Rpd3-dependent boundary formation at telomeres by removal of Sir2 substrate. *Proceedings of the National Academy of Sciences of the United States of America* **107**: 5522-5527.

Eissenberg JC. 2012. Structural biology of the chromodomain: form and function. *Gene* **496**: 69-78.

Evans (ed.) TC. Transformation and microinjection. in *WormBook : the online review of C elegans biology* (ed. TCeR Community). WormBook.

Filippakopoulos P, Knapp S. 2012. The bromodomain interaction module. *FEBS letters* **586**: 2692-2704.

Finch JT, Klug A. 1976. Solenoidal model for superstructure in chromatin. *Proceedings of the National Academy of Sciences of the United States of America* **73**: 1897-1901.

Fire A, Xu S, Montgomery MK, Kostas SA, Driver SE, Mello CC. 1998. Potent and specific genetic interference by double-stranded RNA in Caenorhabditis elegans. *Nature* **391**: 806-811.

Fraga MF, Ballestar E, Villar-Garea A, Boix-Chornet M, Espada J, Schotta G, Bonaldi T, Haydon C, Ropero S, Petrie K et al. 2005. Loss of acetylation at Lys16 and trimethylation at Lys20 of histone H4 is a common hallmark of human cancer. *Nature genetics* **37**: 391-400.

Fussner E, Strauss M, Djuric U, Li R, Ahmed K, Hart M, Ellis J, Bazett-Jones DP. 2012. Open and closed domains in the mouse genome are configured as 10-nm chromatin fibres. *EMBO reports*.

Gerstein MB Lu ZJ Van Nostrand EL Cheng C Arshinoff BI Liu T Yip KY Robilotto R Rechtsteiner A Ikegami K et al. 2010. Integrative analysis of the Caenorhabditis elegans genome by the modENCODE project. *Science* **330**: 1775-1787.

Grant PA, Duggan L, Cote J, Roberts SM, Brownell JE, Candau R, Ohba R, Owen-Hughes T, Allis CD, Winston F et al. 1997. Yeast Gcn5 functions in two multisubunit complexes to acetylate nucleosomal histones: characterization of an Ada complex and the SAGA (Spt/Ada) complex. *Genes & development* **11**: 1640-1650.

Gu W, Szauter P, Lucchesi JC. 1998. Targeting of MOF, a putative histone acetyl transferase, to the X chromosome of Drosophila melanogaster. *Developmental genetics* **22**: 56-64.

Gupta A, Guerin-Peyrou TG, Sharma GG, Park C, Agarwal M, Ganju RK, Pandita S, Choi K, Sukumar S, Pandita RK et al. 2008. The mammalian ortholog of Drosophila MOF that acetylates histone H4 lysine 16 is essential for embryogenesis and oncogenesis. *Molecular and cellular biology* **28**: 397-409.

Gyuris J, Golemis E, Chertkov H, Brent R. 1993. Cdi1, a human G1 and S phase protein phosphatase that associates with Cdk2. *Cell* **75**: 791-803.

Hawkins NC, Garriga G, Beh CT. 2003. Creating precise GFP fusions in plasmids using yeast homologous recombination. *BioTechniques* **34**: 74-78, 80.

Heise F, Chung HR, Weber JM, Xu Z, Klein-Hitpass L, Steinmetz LM, Vingron M, Ehrenhofer-Murray AE. 2012. Genome-wide H4 K16 acetylation by SAS-I is deposited independently of transcription and histone exchange. *Nucleic acids research* **40**: 65-74.

Hengen PN. 1997. False positives from the yeast two-hybrid system. *Trends in biochemical sciences* **22**: 33-34.

Hilfiker A, Hilfiker-Kleiner D, Pannuti A, Lucchesi JC. 1997. mof, a putative acetyl transferase gene related to the Tip60 and MOZ human genes and to the SAS genes of yeast, is required for dosage compensation in Drosophila. *The EMBO journal* **16**: 2054-2060.

Hodgkin J. 1980. More sex-determination mutants of Caenorhabditis elegans. *Genetics* **96**: 649-664.

Huang P, Pleasance ED, Maydan JS, Hunt-Newbury R, O'Neil NJ, Mah A, Baillie DL, Marra MA, Moerman DG, Jones SJ. 2007. Identification and analysis of internal promoters in Caenorhabditis elegans operons. *Genome Res* **17**: 1478-1485.

Hubner MR, Eckersley-Maslin MA, Spector DL. 2012. Chromatin organization and transcriptional regulation. *Current opinion in genetics & development*.

Hunter S, Jones P, Mitchell A, Apweiler R, Attwood TK, Bateman A, Bernard T, Binns D, Bork P, Burge S et al. 2012. InterPro in 2011: new developments in the family and domain prediction database. *Nucleic acids research* **40**: D306-312.

Kamath RS, Fraser AG, Dong Y, Poulin G, Durbin R, Gotta M, Kanapin A, Le Bot N, Moreno S, Sohrmann M et al. 2003. Systematic functional analysis of the Caenorhabditis elegans genome using RNAi. *Nature* **421**: 231-237.

Kamath RS, Martinez-Campos M, Zipperlen P, Fraser AG, Ahringer J. 2001. Effectiveness of specific RNA-mediated interference through ingested double-stranded RNA in Caenorhabditis elegans. *Genome biology* **2**: RESEARCH0002.

Kelley RL, Kuroda MI. 1995. Equality for X chromosomes. *Science* **270**: 1607-1610.

Kelley RL, Meller VH, Gordadze PR, Roman G, Davis RL, Kuroda MI. 1999. Epigenetic spreading of the Drosophila dosage compensation complex from roX RNA genes into flanking chromatin. *Cell* **98**: 513-522.

Kelly WG, Fire A. 1998. Chromatin silencing and the maintenance of a functional germline in Caenorhabditis elegans. *Development* **125**: 2451-2456.

Kelly WG, Xu S, Montgomery MK, Fire A. 1997. Distinct requirements for somatic and germline expression of a generally expressed Caernorhabditis elegans gene. *Genetics* **146**: 227-238.

Kimura A, Umehara T, Horikoshi M. 2002. Chromosomal gradient of histone acetylation established by Sas2p and Sir2p functions as a shield against gene silencing. *Nature genetics* **32**: 370-377.

Kind J, Vaquerizas JM, Gebhardt P, Gentzel M, Luscombe NM, Bertone P, Akhtar A. 2008. Genome-wide analysis reveals MOF as a key regulator of dosage compensation and gene expression in Drosophila. *Cell* **133**: 813-828.

Kohlmaier A, Savarese F, Lachner M, Martens J, Jenuwein T, Wutz A. 2004. A chromosomal memory triggered by Xist regulates histone methylation in X inactivation. *PLoS biology* **2**: E171.

Laemmli UK. 1970. Cleavage of structural proteins during the assembly of the head of bacteriophage T4. *Nature* **227**: 680-685.

Lam KC, Muhlpfordt F, Vaquerizas JM, Raja SJ, Holz H, Luscombe NM, Manke T, Akhtar A. 2012. The NSL complex regulates housekeeping genes in Drosophila. *PLoS genetics* **8**: e1002736.

Lander ES Linton LM Birren B Nusbaum C Zody MC Baldwin J Devon K Dewar K Doyle M FitzHugh W et al. 2001. Initial sequencing and analysis of the human genome. *Nature* **409**: 860-921.

Laverty C, Lucci J, Akhtar A. 2010. The MSL complex: X chromosome and beyond. *Current opinion in genetics & development* **20**: 171-178.

Levin M, Hashimshony T, Wagner F, Yanai I. 2012. Developmental milestones punctuate gene expression in the Caenorhabditis embryo. *Developmental cell* **22**: 1101-1108.

Lewis JA, Fleming JT. 1995. Basic culture methods. *Methods in cell biology* **48**: 3-29.

Li XZ, Wu LP, Corsa CAS, Kunkel S, Dou YL. 2009. Two Mammalian MOF Complexes Regulate Transcription Activation by Distinct Mechanisms. *Molecular cell* **36**: 290-301.

Lieberman-Aiden E, van Berkum NL, Williams L, Imakaev M, Ragoczy T, Telling A, Amit I, Lajoie BR, Sabo PJ, Dorschner MO et al. 2009. Comprehensive mapping of long-

range interactions reveals folding principles of the human genome. *Science* **326**: 289-293.

Liu T, Rechtsteiner A, Egelhofer TA, Vielle A, Latorre I, Cheung MS, Ercan S, Ikegami K, Jensen M, Kolasinska-Zwierz P et al. 2011. Broad chromosomal domains of histone modification patterns in C. elegans. *Genome Res* **21**: 227-236.

Lu L, Li L, Lv X, Wu XS, Liu DP, Liang CC. 2011. Modulations of hMOF autoacetylation by SIRT1 regulate hMOF recruitment and activities on the chromatin. *Cell research* **21**: 1182-1195.

Lu X, Horvitz HR. 1998. lin-35 and lin-53, two genes that antagonize a C. elegans Ras pathway, encode proteins similar to Rb and its binding protein RbAp48. *Cell* **95**: 981-991.

Luger K, Mader AW, Richmond RK, Sargent DF, Richmond TJ. 1997. Crystal structure of the nucleosome core particle at 2.8 A resolution. *Nature* **389**: 251-260.

Maeshima K, Hihara S, Eltsov M. 2010. Chromatin structure: does the 30-nm fibre exist in vivo? *Current opinion in cell biology* **22**: 291-297.

Marin I. 2003. Evolution of chromatin-remodeling complexes: comparative genomics reveals the ancient origin of "novel" compensasome genes. *Journal of molecular evolution* **56**: 527-539.

Marushige K. 1976. Activation of chromatin by acetylation of histone side chains. *Proceedings of the National Academy of Sciences of the United States of America* **73**: 3937-3941.

Meijsing SH, Ehrenhofer-Murray AE. 2001. The silencing complex SAS-I links histone acetylation to the assembly of repressed chromatin by CAF-I and Asf1 in Saccharomyces cerevisiae. *Genes & development* **15**: 3169-3182.

Mello C, Fire A. 1995. DNA transformation. *Methods in cell biology* **48**: 451-482.

Mello CC, Kramer JM, Stinchcomb D, Ambros V. 1991. Efficient gene transfer in C.elegans: extrachromosomal maintenance and integration of transforming sequences. *The EMBO journal* **10**: 3959-3970.

Meyer BJ. 2010. Targeting X chromosomes for repression. *Current opinion in genetics & development* **20**: 179-189.

Milne T, Briggs S, Brock H, Gibbs D, Allis CD, Hess JL. 2002. The mixed lineage leukemia protein (MLL) targets SET domain methyltransferase activity to Hox gene promoters. *Blood* **100**: 137A-137A.

Moresco JJ, Carvalho PC, Yates JR, 3rd. 2010. Identifying components of protein complexes in C. elegans using co-immunoprecipitation and mass spectrometry. *Journal of proteomics* **73**: 2198-2204.

Musselman CA, Kutateladze TG. 2009. PHD fingers: epigenetic effectors and potential drug targets. *Molecular interventions* **9**: 314-323.

Naidoo N, Pawitan Y, Soong R, Cooper DN, Ku CS. 2011. Human genetics and genomics a decade after the release of the draft sequence of the human genome. *Human genomics* **5**: 577-622.

Neal KC, Pannuti A, Smith ER, Lucchesi JC. 2000. A new human member of the MYST family of histone acetyl transferases with high sequence similarity to Drosophila MOF. *Biochimica et biophysica acta* **1490**: 170-174.

Nielsen SJ, Schneider R, Bauer UM, Bannister AJ, Morrison A, O'Carroll D, Firestein R, Cleary M, Jenuwein T, Herrera RE et al. 2001. Rb targets histone H3 methylation and HP1 to promoters. *Nature* **412**: 561-565.

O'Meara MM, Zhang F, Hobert O. 2010. Maintenance of neuronal laterality in Caenorhabditis elegans through MYST histone acetyltransferase complex components LSY-12, LSY-13 and LIN-49. *Genetics* **186**: 1497-1502.

Osada S, Sutton A, Muster N, Brown CE, Yates JR, 3rd, Sternglanz R, Workman JL. 2001. The yeast SAS (something about silencing) protein complex contains a MYST-type putative acetyltransferase and functions with chromatin assembly factor ASF1. *Genes & development* **15**: 3155-3168.

Pesole G. 2008. What is a gene? An updated operational definition. *Gene* **417**: 1-4.

Peterson KR. 2007. Preparation of intact yeast artificial chromosome DNA for transgenesis of mice. *Nature protocols* **2**: 3009-3015.

Petrella LN, Wang W, Spike CA, Rechtsteiner A, Reinke V, Strome S. 2011. synMuv B proteins antagonize germline fate in the intestine and ensure C. elegans survival. *Development* **138**: 1069-1079.

Piano F, Schetter AJ, Morton DG, Gunsalus KC, Reinke V, Kim SK, Kemphues KJ. 2002. Gene clustering based on RNAi phenotypes of ovary-enriched genes in C. elegans. *Current biology : CB* **12**: 1959-1964.

Poux AN, Marmorstein R. 2003. Molecular basis for Gcn5/PCAF histone acetyltransferase selectivity for histone and nonhistone substrates. *Biochemistry* **42**: 14366-14374.

Raja SJ, Charapitsa I, Conrad T, Vaquerizas JM, Gebhardt P, Holz H, Kadlec J, Fraterman S, Luscombe NM, Akhtar A. 2010. The nonspecific lethal complex is a transcriptional regulator in Drosophila. *Molecular cell* **38**: 827-841.

Razin SV, Borunova VV, Maksimenko OG, Kantidze OL. 2012. Cys2His2 zinc finger protein family: classification, functions, and major members. *Biochemistry Biokhimiia* **77**: 217-226.

Rechtsteiner A, Ercan S, Takasaki T, Phippen TM, Egelhofer TA, Wang W, Kimura H, Lieb JD, Strome S. 2010. The histone H3K36 methyltransferase MES-4 acts epigenetically to transmit the memory of germline gene expression to progeny. *PLoS genetics* **6**.

Reifsnyder C, Lowell J, Clarke A, Pillus L. 1996. Yeast SAS silencing genes and human genes associated with AML and HIV-1 Tat interactions are homologous with acetyltransferases. *Nature genetics* **14**: 42-49.

Rojas JR, Trievel RC, Zhou J, Mo Y, Li X, Berger SL, Allis CD, Marmorstein R. 1999. Structure of Tetrahymena GCN5 bound to coenzyme A and a histone H3 peptide. *Nature* **401**: 93-98.

Sambrook J, Fritsch EF, Maniatis T. 1989. *Molecular cloning : a laboratory manual*. Cold Spring Harbor Laboratory, Cold Spring Harbor, N.Y.

Sanjuan R, Marin I. 2001. Tracing the origin of the compensasome: evolutionary history of DEAH helicase and MYST acetyltransferase gene families. *Molecular biology and evolution* **18**: 330-343.

Sapountzi V, Cote J. 2011. MYST-family histone acetyltransferases: beyond chromatin. *Cellular and molecular life sciences : CMLS* **68**: 1147-1156.

Schalch T, Duda S, Sargent DF, Richmond TJ. 2005. X-ray structure of a tetranucleosome and its implications for the chromatin fibre. *Nature* **436**: 138-141.

Schuettengruber B, Chourrout D, Vervoort M, Leblanc B, Cavalli G. 2007. Genome regulation by polycomb and trithorax proteins. *Cell* **128**: 735-745.

Scott MJ, Pan LL, Cleland SB, Knox AL, Heinrich J. 2000. MSL1 plays a central role in assembly of the MSL complex, essential for dosage compensation in Drosophila. *The EMBO journal* **19**: 144-155.

Seitz S. 2004. Connecting the histone acetyltransferase complex SAS-I to the centromere in S. cerevisiae. in *Mathematisch-Naturwissenschaftliche Fakultät I*. Humboldt-Universität zu Berlin.

Seydoux G, Dunn MA. 1997. Transcriptionally repressed germ cells lack a subpopulation of phosphorylated RNA polymerase II in early embryos of Caenorhabditis elegans and Drosophila melanogaster. *Development* **124**: 2191-2201.

Shaham (ed.) S. Methods in cell biology. in *WormBook : the online review of C elegans biology* (ed. TCeR Community). WormBook.

Sherman F. 1991. Getting started with yeast. *Methods in enzymology* **194**: 3-21.

Shi Y, Mello C. 1998. A CBP/p300 homolog specifies multiple differentiation pathways in Caenorhabditis elegans. *Genes & development* **12**: 943-955.

Shibata Y, Takeshita H, Sasakawa N, Sawa H. 2010. Double bromodomain protein BET-1 and MYST HATs establish and maintain stable cell fates in C. elegans. *Development* **137**: 1045-1053.

Shogren-Knaak M, Ishii H, Sun JM, Pazin MJ, Davie JR, Peterson CL. 2006. Histone H4-K16 acetylation controls chromatin structure and protein interactions. *Science* **311**: 844-847.

Simmer F, Tijsterman M, Parrish S, Koushika SP, Nonet ML, Fire A, Ahringer J, Plasterk RH. 2002. Loss of the putative RNA-directed RNA polymerase RRF-3 makes C. elegans hypersensitive to RNAi. *Current biology : CB* **12**: 1317-1319.

Simonet T, Dulermo R, Schott S, Palladino F. 2007. Antagonistic functions of SET-2/SET1 and HPL/HP1 proteins in C. elegans development. *Developmental biology* **312**: 367-383.

Smith DE, Fisher PA. 1984. Identification, developmental regulation, and response to heat shock of two antigenically related forms of a major nuclear envelope protein in Drosophila embryos: application of an improved method for affinity purification of antibodies using polypeptides immobilized on nitrocellulose blots. *The Journal of cell biology* **99**: 20-28.

Smith ER, Cayrou C, Huang R, Lane WS, Cote J, Lucchesi JC. 2005. A human protein complex homologous to the Drosophila MSL complex is responsible for the majority of histone H4 acetylation at lysine 16. *Molecular and cellular biology* **25**: 9175-9188.

Smith ER, Pannuti A, Gu W, Steurnagel A, Cook RG, Allis CD, Lucchesi JC. 2000. The drosophila MSL complex acetylates histone H4 at lysine 16, a chromatin modification linked to dosage compensation. *Molecular and cellular biology* **20**: 312-318.

Squatrito M, Gorrini C, Amati B. 2006. Tip60 in DNA damage response and growth control: many tricks in one HAT. *Trends in cell biology* **16**: 433-442.

Sternberg PW, Horvitz HR. 1991. Signal transduction during C. elegans vulval induction. *Trends in genetics : TIG* **7**: 366-371.

Stinchcomb DT, Shaw JE, Carr SH, Hirsh D. 1985. Extrachromosomal DNA transformation of Caenorhabditis elegans. *Molecular and cellular biology* **5**: 3484-3496.

Strome S. 2005. Specification of the germ line. *WormBook : the online review of C elegans biology*: 1-10.

Suka N, Luo K, Grunstein M. 2002. Sir2p and Sas2p opposingly regulate acetylation of yeast histone H4 lysine16 and spreading of heterochromatin. *Nature genetics* **32**: 378-383.

Sutton A, Shia WJ, Band D, Kaufman PD, Osada S, Workman JL, Sternglanz R. 2003. Sas4 and Sas5 are required for the histone acetyltransferase activity of Sas2 in the SAS complex. *The Journal of biological chemistry* **278**: 16887-16892.

Sykes SM, Mellert HS, Holbert MA, Li K, Marmorstein R, Lane WS, McMahon SB. 2006. Acetylation of the p53 DNA-binding domain regulates apoptosis induction. *Molecular cell* **24**: 841-851.

Taipale M, Rea S, Richter K, Vilar A, Lichter P, Imhof A, Akhtar A. 2005. hMOF histone acetyltransferase is required for histone H4 lysine 16 acetylation in mammalian cells. *Molecular and cellular biology* **25**: 6798-6810.

Timmons L, Fire A. 1998. Specific interference by ingested dsRNA. *Nature* **395**: 854.

Towbin BD, Meister P, Pike BL, Gasser SM. 2010. Repetitive transgenes in C. elegans accumulate heterochromatic marks and are sequestered at the nuclear envelope in a

copy-number- and lamin-dependent manner. *Cold Spring Harbor symposia on quantitative biology* **75**: 555-565.

Tsang WY, Lemire BD. 2003. The role of mitochondria in the life of the nematode, Caenorhabditis elegans. *Biochimica et biophysica acta* **1638**: 91-105.

Updike DL, Mango SE. 2006. Temporal regulation of foregut development by HTZ-1/H2A.Z and PHA-4/FoxA. *PLoS genetics* **2**: e161.

Vanfleteren JR, Van Bun SM, Delcambe LL, Van Beeumen JJ. 1986. Multiple forms of histone H2B from the nematode Caenorhabditis elegans. *The Biochemical journal* **235**: 769-773.

Vanfleteren JR, Van Bun SM, Van Beeumen JJ. 1987a. The primary structure of histone H2A from the nematode Caenorhabditis elegans. *The Biochemical journal* **243**: 297-300.

-. 1987b. The primary structure of histone H3 from the nematode Caenorhabditis elegans. *FEBS letters* **211**: 59-63.

-. 1987c. The primary structure of histone H4 from the nematode Caenorhabditis elegans. *Comparative biochemistry and physiology B, Comparative biochemistry* **87**: 847-849.

-. 1989. The histones of Caenorhabditis elegans: no evidence of stage-specific isoforms. An overview. *FEBS letters* **257**: 233-237.

Vastenhouw NL, Brunschwig K, Okihara KL, Muller F, Tijsterman M, Plasterk RH. 2006. Gene expression: long-term gene silencing by RNAi. *Nature* **442**: 882.

Wach A, Brachat A, Pohlmann R, Philippsen P. 1994. New heterologous modules for classical or PCR-based gene disruptions in Saccharomyces cerevisiae. *Yeast* **10**: 1793-1808.

Wang D, Kennedy S, Conte D, Jr., Kim JK, Gabel HW, Kamath RS, Mello CC, Ruvkun G. 2005. Somatic misexpression of germline P granules and enhanced RNA interference in retinoblastoma pathway mutants. *Nature* **436**: 593-597.

Wells MB, Snyder MJ, Custer LM, Csankovszki G. 2012. Caenorhabditis elegans dosage compensation regulates histone H4 chromatin state on X chromosomes. *Molecular and cellular biology* **32**: 1710-1719.

Wenzel D, Palladino F, Jedrusik-Bode M. 2011. Epigenetics in C. elegans: facts and challenges. *Genesis* **49**: 647-661.

Whetstine JR, Ceron J, Ladd B, Dufourcq P, Reinke V, Shi Y. 2005. Regulation of tissue-specific and extracellular matrix-related genes by a class I histone deacetylase. *Molecular cell* **18**: 483-490.

Whittle CM, McClinic KN, Ercan S, Zhang X, Green RD, Kelly WG, Lieb JD. 2008. The genomic distribution and function of histone variant HTZ-1 during C. elegans embryogenesis. *PLoS genetics* **4**: e1000187.

Williams BD, Schrank B, Huynh C, Shownkeen R, Waterston RH. 1992. A genetic mapping system in Caenorhabditis elegans based on polymorphic sequence-tagged sites. *Genetics* **131**: 609-624.

Wirth M, Paap F, Fischle W, Wenzel D, Agafonov DE, Samatov TR, Wisniewski JR, Jedrusik-Bode M. 2009. HIS-24 linker histone and SIR-2.1 deacetylase induce H3K27me3 in the Caenorhabditis elegans germ line. *Molecular and cellular biology* **29**: 3700-3709.

Wu H, Moshkina N, Min J, Zeng H, Joshua J, Zhou MM, Plotnikov AN. 2012a. Structural basis for substrate specificity and catalysis of human histone acetyltransferase 1. *Proceedings of the National Academy of Sciences of the United States of America* **109**: 8925-8930.

Wu X, Shi Z, Cui M, Han M, Ruvkun G. 2012b. Repression of germline RNAi pathways in somatic cells by retinoblastoma pathway chromatin complexes. *PLoS genetics* **8**: e1002542.

Xu F, Zhang K, Grunstein M. 2005. Acetylation in histone H3 globular domain regulates gene expression in yeast. *Cell* **121**: 375-385.

Yang XJ. 2004. The diverse superfamily of lysine acetyltransferases and their roles in leukemia and other diseases. *Nucleic acids research* **32**: 959-976.

Yuan H, Marmorstein R. 2013. Histone acetyltransferases: Rising ancient counterparts to protein kinases. *Biopolymers* **99**: 98-111.

Zinovyeva AY, Graham SM, Cloud VJ, Forrester WC. 2006. The C. elegans histone deacetylase HDA-1 is required for cell migration and axon pathfinding. *Developmental biology* **289**: 229-242.

Zipperlen P, Fraser AG, Kamath RS, Martinez-Campos M, Ahringer J. 2001. Roles for 147 embryonic lethal genes on C.elegans chromosome I identified by RNA interference and video microscopy. *The EMBO journal* **20**: 3984-3992.

# 6. Danksagung

Mein besonderer Dank gilt Prof. Dr. Ann Ehrenhofer-Murray für die Möglichkeit, an diesem sehr interessanten Thema arbeiten zu können, sowie für ihre stetige Anteilnahme und hilfreiche Unterstützung für die Erstellung meiner Doktorarbeit.

Ich bedanke mich bei Prof. Dr. Iliakis und den Mitarbeitern des Instituts für medizinische Strahlenbiologie des Universitätsklinikums Essen, insbesondere bei Maria Siemann und Dr. Mario Moscariello für die kompetente Hilfe bei der Durchführung der Pulsed Field Gel Elektrophorese sowie für die Durchführung des radioaktiven Labellings für den Southern Blot.

Bei Prof. Dr. Ralf Schnabel von der TU Braunschweig bedanke ich mich für die freundliche Anleitung und Einarbeitung in das Immunfärben von Embryonen sowie für produktive Diskussionen zum aktuellen Stand der Wissenschaft und interessante Einblicke in die Entwicklungsbiologie von *C. elegans*.

Ein großer Dank geht an alle ehemaligen und derzeitigen Mitarbeiter der Arbeitsgruppe Genetik, insbesondere Rita für tatkräftige Unterstützung und aufbauende Worte während meiner Arbeit. Bei Karolin und Martina bedanke ich mich für die stetige Bereitstellung von Materialien und die gute Organisation im Labor. Jan und Stefan danke ich für die unterhaltsamen und sportbegeisterten Gespräche und Anke, Juliane und Christian für die mittäglichen Diskussionen in der Mensa. Weiterhin bedanke ich mich bei Maria, Tanja und Gesine und allen anderen Kollegen für das angenehme Arbeitsklima in der Abteilung.

Abschließend möchte ich mich noch bei meiner Familie und Freunden für die moralische Unterstützung und den Rückhalt bedanken. Und, zu guter Letzt, danke ich Christiane für ihre ständige Unterstützung und Hilfe in allen Lebenslagen.

## Lebenslauf

Der Lebenslauf ist in der Online-Version aus Gründen des Datenschutzes nicht enthalten.

## Erklärung:

Hiermit erkläre ich, gem. § 6 Abs. (2) f) der Promotionsordnung der Fakultäten für Biologie, Chemie und Mathematik zur Erlangung der Dr. rer. nat., dass ich das Arbeitgebiet, dem das Thema „Characterization of the MYST histone acetyltransferase MYS-2 in *Caenorhabditis elegans*“ zuzuordnen ist, in Forschung und Lehre vertrete und den Antrag von Martin Müller befürworte und die Betreuung auch im Falle eines Weggangs, wenn nicht wichtige Gründe dem entgegenstehen, weiterführen werde.

Essen, den _____

## Erklärung:

Hiermit erkläre ich, gem. § 7 Abs. (2) c) + e) der Promotionsordnung Fakultäten für Biologie, Chemie und Mathematik zur Erlangung des Dr. rer. nat., dass ich die vorliegende Dissertation selbständig verfasst und mich keiner anderen als der angegebenen Hilfsmittel bedient habe.

Essen, den _____

## Erklärung:

Hiermit erkläre ich, gem. § 7 Abs. (2) d) + f) der Promotionsordnung der Fakultäten für Biologie, Chemie und Mathematik zur Erlangung des Dr. rer. nat., dass ich keine anderen Promotionen bzw. Promotionsversuche in der Vergangenheit durchgeführt habe und dass diese Arbeit von keiner anderen Fakultät/Fachbereich abgelehnt worden ist.

Essen, den _____